


Max-Planck-Institut
für chemische Ökologie



Department of Evolutionary
Neuroethology

Processing of Complex Host Blends in the Moth Antennal Lobe

A Dissertation

Submitted to the Faculty of Biology and Pharmacy of the
Friedrich-Schiller-University Jena

For the degree of

doctor rerum naturalium (Dr. rer. nat.)

Linda Sara Kübler

born Oktober 19, 1979 in Füssen, Germany

Written assessments by:

Prof Dr Jürgen Bolz, Friedrich-Schiller-University, Jena, Germany.

Prof Dr Bill Hansson, MPI for Chemical Ecology, Jena, Germany.

PD Dr Mattias Larsson, SLU Alnarp, Sweden.

Date of public defense:

June 24, 2011

“Mein Genie ist in meinen Nüstern”

Friedrich Nietzsche

Ecce Homo; kritische Studienausgabe (KSA) Bd.6, München:dtv Berlin, New York: Walter de Gruyter 1988, 366.

TABLE OF CONTENTS

TABLE OF CONTENTS	5
INTRODUCTION	7
The sense of smell	7
The scent of an odor.....	9
The olfactory pathway in insects.....	10
Blend processing	12
Overview of Manuscripts	17
CHAPTER I.....	21
The antennal transcriptome of <i>Manduca sexta</i>	
CHAPTER II.....	43
A novel multicomponent stimulus device for use in olfactory experiments	
CHAPTER III.....	63
Neuronal processing of complex mixtures establishes a unique odor representation in the moth antennal lobe	
CHAPTER IV.....	89
Novel blend patterns: simultaneous optophysiological studies at multiple levels of the moth AL	
GENERAL DISCUSSION	111
SUMMARY	119
ZUSAMMENFASSUNG.....	121
REFERENCES	124
Declaration of Independent Assignment.....	137
ACKNOWLEDGEMENTS	138



INTRODUCTION

The present thesis elucidates basic principles of odor processing and provides exciting new insights into how the moth brain performs host blend coding at the primary level, the antennal lobe. In particular, this study reveals significant non-linear coding of host-associated blends, indicating high levels of across-fiber patterning that establish a novel “blend code” separate from individual component identities.

The results are thoroughly discussed against the current state of olfactory research; they provide a novel foundation for future studies on complex blend processing. Thus, this study is of broad interest not only to the world of invertebrate neuroscience, but also to those generally interested in information processing.

The sense of smell

The chemical senses (taste & smell) are perhaps the most prevalent sense across the animal kingdom. Even the simplest organisms, such as paramecia or slime molds are capable of detecting chemical signals, and utilize chemical signals to gain information about their environment (Sasner and Houten, 1989; Maeda et al., 2009). For most organisms, the ability to detect odor molecules is strongly connected to survival and reproduction, leading to a highly developed olfactory system. Diverse, highly sensitive olfactory organs have evolved across almost all animal phyla (Hildebrand and Shepherd, 1997a). Despite its biological importance, the historical significance of olfaction has greatly fluctuated over the centuries.

During the early 20th century, the sense of smell gained a doubtful reputation and received little scientific attention. Kant described the sense of smell itself as animalistic, underdeveloped, and therefore the most dispensable sense of all:

"Welcher Organsinn ist der undankbarste und scheint auch der entbehrlichste zu sein? Der des Geruchs" (Kant, 1917).

Indeed, compared to other senses, scientific investigations on olfaction played only a minor role and proceeded slowly. Although Fabre hypothesized in the late 19th century that the female moth releases an odor that powerfully attracts the opposite sex of her species, it almost took another century before the first insect pheromone was successfully characterized. In 1959, Nobel Prize

INTRODUCTION

winner, Adolph Butenandt, who also discovered the human sex hormones estrone, testosterone, and progesterone, elucidated bombykol, named after the moth's Latin name, *Bombyx mori* (Butenandt et al., 1961). That same year Peter Karlson and Martin Lüscher introduced the term "pheromone" (greek: "pherein" carry, mediate; Karlson and Luscher, 1959). From then on, technical improvements such as gas chromatography and mass spectrometry used in combination with electrophysiology (EAGs, Roelofs et al., 1971 & 1971b) dramatically increased the pace and productivity of olfactory research. Moreover, in recent years olfaction in general has increasingly gained focus for scientific research. Molecular cloning of olfactory receptor genes in vertebrates and insects (see e.g. Buck and Axel, 1991; Mombaerts, 1999, Vosshall, 2000; Touhara, 2007; Zhao and Firestein, 1999) as well as the establishment of optophysiological techniques visualizing neural representations of odors in the brain in real time (reviewed by Masse et al., 2009; Galizia and Menzel, 2001; Kauer and White, 2001) boosted the field. In 2004, the Nobel Prize in medicine was awarded jointly to Richard Axel and Linda B. Buck "for their discoveries of odorant receptors and the organization of the olfactory system". Several research departments worldwide are currently working in the field of olfaction within a wide scope spanning molecular biology, physiology, psychology, neuroengineering, and many other fields.



Figure 1: Female hawkmoth. *Manduca sexta* (Lepidoptera, Sphingidae) is present through much of the American continents. Commonly known as the tobacco hornworm, *Manduca* is a model organism in insect olfaction.

Moths, one of the key insect models of olfaction, are known for their highly specific and sensitive olfactory sense and offer extraordinarily complex chemosensory

behavior (Anderson et al., 1995; Schneider, 1962; Baker, 1989; Hansson, 1995; Raguso et al., 2005). Odor processing has been extensively studied for pheromone receptive neurons among several moth species (Christensen and Hildebrand, 1987; Christensen et al., 1995; Anton et al., 1997; Barrozo et al., 2010). Nevertheless, the nature of complex host blend processing and the mechanisms by which neurons generate a unique blend percept in the olfactory system remains largely unclear. I have focused my study on the olfactory system of *Manduca sexta*, the giant sphinx

INTRODUCTION

moth; which has emerged as one of the most extensively investigated insect species over the last 45 years (Figure 1; Christensen and Sorensen, 1996). Its prominent size and durability, and the stereotypic organization of the olfactory system makes it an ideal physiological model to analyze odor processing (Eisthen, 2002). Additionally, while hawkmoths forage opportunistically on a variety of flowers, females oviposit almost exclusively on Solanaceous plants, which they recognize on the basis of olfactory cues (Reisenman et al., 2009). This multifaceted lifestyle and respective perceptual bandwidth make *Manduca* an interesting model for investigating neuronal mechanisms of olfactory blend processing.

The scent of an odor



Strawberry	Onion
  BUTYL CINNAMATE ETHYL ACETATE ETHYL ISOBUTYRATE ETHYL 2-METHYLBUTYRATE ETHYL ISOVALERATE 3-(2-FURYL) ACROLEIN trans-2-HEXENAL trans-2-HEXEN-1-OL 2-METHOXY-4-METHYLPHENOL (CREOSOL) 2-METHOXY-4-VINYLPHENOL 2-METHOXY-4-VINYLPHENOL 10% IN PG NAT 2-METHOXY-4-VINYLPHENOL 1% IN PG METHYL p-TERTBUTYLPHENYLACETATE 2-METHYLBUTYRIC ACID NATURAL METHYL CINNAMATE METHYL 2-METHYLBUTYRATE NATURAL HYDROXY DIMETHYL FURANONE HYDROXY DIMETHYL FURANONE 10% IN PG METHYL THIOBUTYRATE -BUTYL 2-METHYLBUTYRATE cis-3-HEXENYL HEXANOATE ETHYL trans-2-BUTENOATE ISOPROPYL 2-METHYLBUTYRATE ACETOXY DIMETHYL FURANONE METHYL (3-METHYL)THIOBUTYRATE BUTYL BENZOATE	ALLYL DISULPHIDE ALLYL MERCAPTAN ALLYL METHYL DISULPHIDE METHYL PROPYL DISULPHIDE PROPYL DISULPHIDE 2,2-(THIODIMETHYLENE)DIFURAN ALLYL METHYL TRISULPHIDE DIALLYL TRISULPHIDE 35-40% DIMETHYL TRISULPHIDE DIPROPYL TRISULPHIDE METHYL PROPYL TRISULPHIDE 1-OCTEN-3-ONE DIALLYL POLYSULPHIDE DIMETHYL DISULPHIDE ETHYL 3-(FURFURYLTHIO)PROPIONATE TETRAHYDRO-2-METHYLFURAN-3-THIOL ALLYL PROPYL DISULPHIDE DIPROPYL SULPHIDE METHYL PROPYL SULPHIDE ONION OIL EXTENDER ALLYL PROPYL SULPHIDE 2,5-DIMETHYLTHIOPHENE ALLYL PROPYL TRISULPHIDE DIMETHYL TETRASULPHIDE ALLYL METHYL SULPHIDE http://www.oxfordchemicals.com

Figure 2: Excerpt of volatiles emitted by the odorant bouquet of strawberry and onion.

The world is a cacophony of scent creating a highly dynamic olfactory environment. What we might perceive as a “single scent” is often several compounds acting in concert to form an odor blend. A single strawberry emits up to 360 volatile components (compare Figure 2) and in contrast to many insect pheromones (Roelofs, 1995), few behaviorally relevant host odors are single compounds (Olsson et al., 2009; Reisenman et al., 2009; Raguso et al., 2005). The olfactory system is at any moment bombarded with hundreds of volatile compounds. It must therefore be capable of handling an enormous number of diverse odorant molecules, varying in chemical structure, molecular weight and other electrochemical properties. Moreover exogenous factors can alter the bouquet and the scent; e.g. a rose may smell differently depending on daytime, weather conditions and physiological

state of the plant. Nevertheless, the brain is able to assign the green whiff of a dog rose in the backyard on a rainy day; the oriental scent of a damascene rose as well as the artificial, sleazy pink hand wash from the supermarket to the quality “rose”. Thus, the olfactory system seems to accommodate the unpredictability of the olfactory world (Laurent, 1999). This exciting configural (Chandra and Smith, 1998) property of olfaction, where a specific quality is assigned to random components, separates olfaction from the visual and auditory system, and challenges its investigation.

Insects have a remarkable capacity to recognize and discriminate odor blends even at extremely low odor concentrations. When a female moth searches for a nectar-rich flower or a suitable oviposition substrate, her olfactory system has to extract information from a broad palette of components. Therefore, rather than determining the molecular composition of an odor, the moth may identify an odor blend as a specific object with particular relevance. The underlying processing codes in the brain should reflect such perceptual biases (Laurent, 1999). Yet, how does the insect’s olfactory system identify these complex blends?

The olfactory pathway in insects

In insects, odorant molecules are detected by peripheral sensory neurons (OSNs) on the antenna, and transduced into electrical potentials that transfer information about the odorant molecule to the brain. Each receptor encodes a seven-transmembrane domain protein that is generally expressed by only a single OSN type (Mombaerts, 1996). Whereas mice express roughly 1000 different receptor types (Zhang and Firestein, 2002; Godfrey et al., 2004) and humans about 300 (Malnic et al., 2004) insects, e.g. *Drosophila*, only possess around 60 different odorant receptors (de Bruyne et al., 1999; Vosshall et al., 1999). In *Manduca sexta*, we identified 54 receptor fragments from our antennal transcriptomic data set (see ChapterII for a review on olfactory receptors). The small number of receptor genes reported (ChapterI) appears contradictory when compared to the enormous array of odorant molecules in the moth’s environment. But the olfactory system has obviously developed a strategy where a minimum subset of receptors with varying selectivity is capable of detecting a variety of complex blends (c.f. *Drosophila*, Hallem and Carlson, 2006).

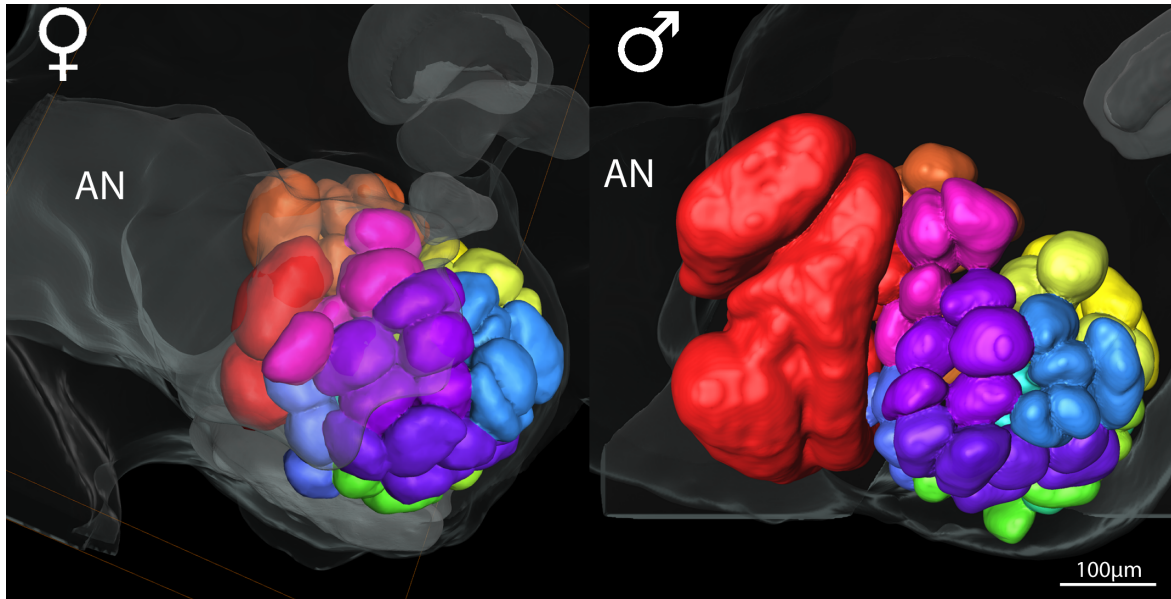


Figure 3: 3D reconstruction of the antennal lobe of *Manduca sexta* (female and male respectively). The first olfactory neuropil is a conglomeration of spherical subunits of neuropil known as glomeruli (around 70 in *Manduca*). Gender-specific glomeruli at the entrance of the antennal nerve (AN) are depicted in red in both sexes.

The antennal lobe (AL, Figure 3), the insect analog of the olfactory bulb, is a conglomeration of anatomically discrete subunits of neuropil known as glomeruli. OSN populations expressing the same receptor innervate the same glomerulus in the antennal lobe (Mombaerts, 1999; Ressler et al., 1994; Vosshall, 2000). The total number of glomeruli in the AL is thus related to the total number of functionally distinct OSN populations and receptor genes (de Bruyne and Baker, 2008). As a consequence of OSN targeting, odors are represented as stable, spatial patterns of neuronal activity in the CNS of both vertebrates (Friedrich and Korsching, 1997; Friedrich and Korsching, 1998; Fried et al., 2002; Meister and Bonhoeffer, 2001; Rubin and Katz, 1999; Uchida et al., 2000) and insects (Joerges et al., 1997; Galizia et al., 1999; Wang et al., 2003; Skiri et al., 2004; Carlsson et al., 2005; Sachse and Galizia, 2002; Silbering and Galizia, 2007). In the moth AL, the massive afferent input of roughly 250000 OSNs converges onto two categories of AL neurons: roughly 900 projection neurons (PNs) and 360 local interneurons (LNs; compare Figure 4; Homberg et al., 1989). LNs exclusively branch within the AL, interconnecting glomeruli and modifying information from input (OSNs) to output (PNs) levels via mostly inhibitory connections (for reviews see de Bruyne and Baker, 2008; Hansson and Anton, 2000; Hildebrand and Shepherd, 1997b; Homberg et al., 1989). PNs subsequently relay AL output to higher brain centers including the mushroom bodies (MB), known to play a significant role in learning in memory, and the lateral horn (LH) in the protocerebrum, for which the concrete function is still generally unknown. The antennal lobe and its glomeruli thus serve as the primary processing center for blend information in the insect brain. Glomeruli have

been described as one of the most distinctive structures in the brain (Shipley and Ennis, 1996), and the numbers of glomeruli across animals range from 43 in *Drosophila* (Laissue et al., 1999; Laissue and Vosshall, 2008), 70 in *Manduca* (see Figure 2 in introduction, Chapter I, Große-Wilde et al., 2011), 160 in honeybees (Flanagan and Mercer, 1989) to around 2000 - 3000 in mice and rats (reviewed by Shipley and Ennis, 1996).

Blend processing

The insect brain may process odor blends either through elementary or combinatorial coding (Rescorla, 1972). Elementary coding results from a linear summation of blend components, while combinatorial (non-linear) coding necessitates across-fiber processing in the AL network, supposedly facilitated by inhibitory local neurons. Thus, the resultant neuronal representation of an odor mixture may either retain the monomolecular information of single blend components, or reveal non-linear interactions different from the sum due to processing in the AL network. Duchamp-Viret et al. developed a series of definitions for such non-linear interactions, defined as synergism, suppression, and hypoadditivity (discussed in Chapter III&IV; Duchamp-Viret et al., 2003). In vertebrates, non-linear processing has been observed both at the periphery (Duchamp-Viret et al., 2003) and in the central nervous system (Giraudet et al., 2002; Tabor et al., 2004; Laissue et al., 1999; Lei et al., 2006; Lin et al., 2006; Davison and Katz, 2007; Johnson et al., 2010). But considering insects, mixture interactions have been witnessed mainly in the CNS (but see Ochieng et al., 2002; Hillier and Vickers, 2011) within a variety of species (for review see Lei and Vickers, 2008). Although extensively studied among pheromone components (Christensen and Hildebrand, 1987; Homberg et al., 1989; Christensen et al., 1995; Wu et al., 1996; Anton et al., 1997; Hartlieb et al., 1999; Barrozo et al., 2010) the processing of plant-related mixtures in moths has been largely overlooked.

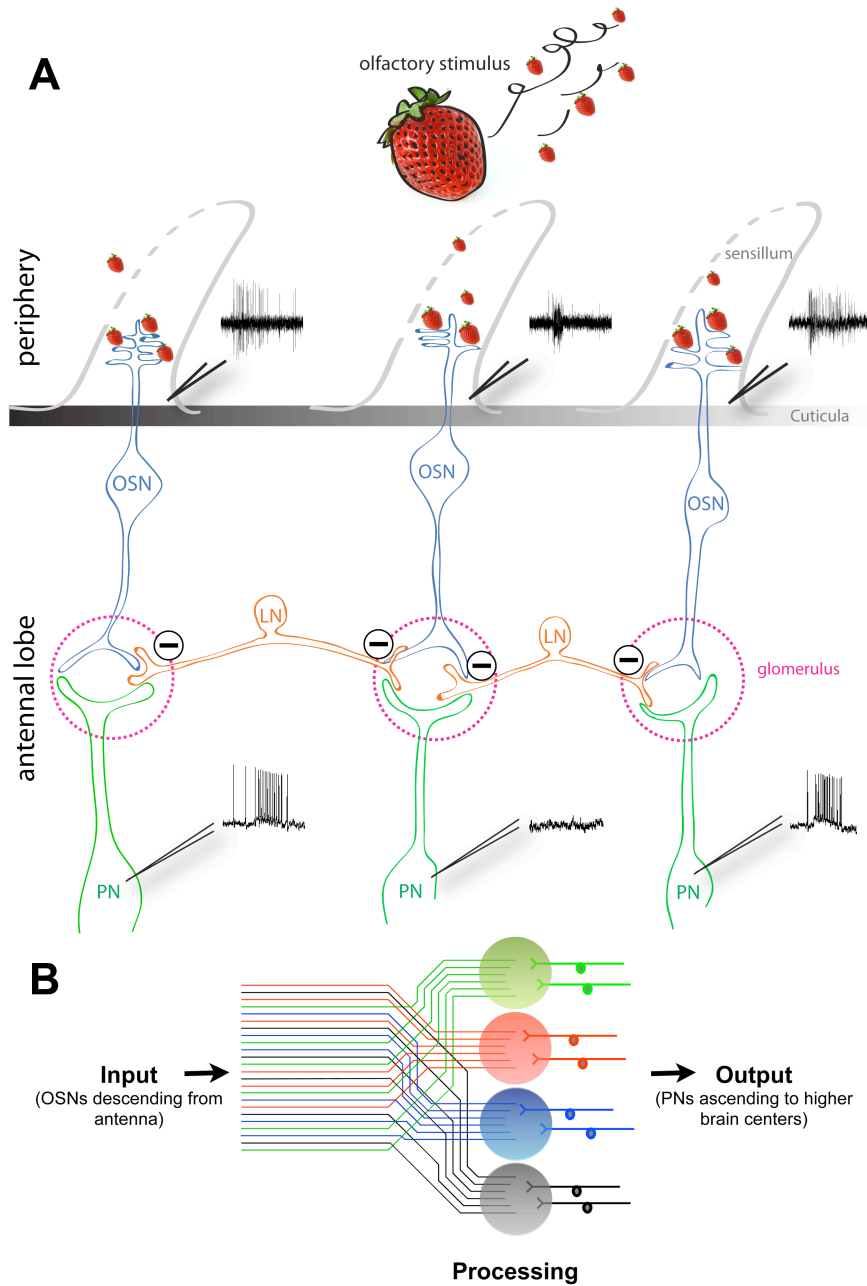


Figure 4: General model of Olfactory Processing in Insects

Olfactory stimuli activate multiple classes of olfactory sensory neurons (OSNs, blue), each expressing a single receptor protein subtype (OR). Each olfactory stimulus can activate many different classes of receptor cells (A). The OSNs send their unbranched axons to spherical targets in the antennal lobe (AL) known as glomeruli (magenta): Each receptor subset sends its axons to its respective glomerulus (B). As a consequence of OSN targeting, odors are represented as stable, spatial patterns of neuronal activity in the AL. Output neurons (projection neuron, PN, green) project their axons to higher-level processing areas (not shown). Local interneurons (LN, orange) interconnect glomeruli, mediating mostly inhibitory actions. Presynaptic lateral inhibition modulates signals from Input (OSN) to Output (PN), resulting in suppression in downstream PNs (PN middle). Inhibitory effects may serve as a gain control, enhancing the contrast of odor representation and prevent adaptation (B modified after C. Kleineidam).

INTRODUCTION

Recent optophysiological recordings in the insect AL show that responses to an odor mixture could generally be predicted from the single component responses at input- but not output levels (Silbering et al., 2008). In accordance with this finding, our single cell recordings show that blend patterns in the *Manduca* AL are highly non-linear and strong interactions, such as suppression and synergism emerged (Chapter III). The electrophysiological method of sharp recordings provides high temporal resolution, but only shows the response properties of one neuron at a time. To investigate blend coding across the AL, we applied optophysiological techniques, visualizing the global neural representations of odor mixtures in the brain (Chapter IV). In Chapter IV, we show that the mechanisms of blend processing revealed on the single neuron level (Chapter III) were maintained across the glomerular array: Simultaneously measuring OSN network input in concert with PN output showed that at the input level the pattern of blend representation in the moth antennal lobe (AL) was reassembled by the representation of the single components. In contrast, at the output level strong mixture interactions occurred. Hence, like in *Drosophila*, the output odor pattern of a blend response could not simply be predicted from its single component patterns. The high levels of interactions reported indicate that the local network (LNs) modulates PN output to generate a unique blend percept as early in the olfactory pathway as the first processing stage, the AL.

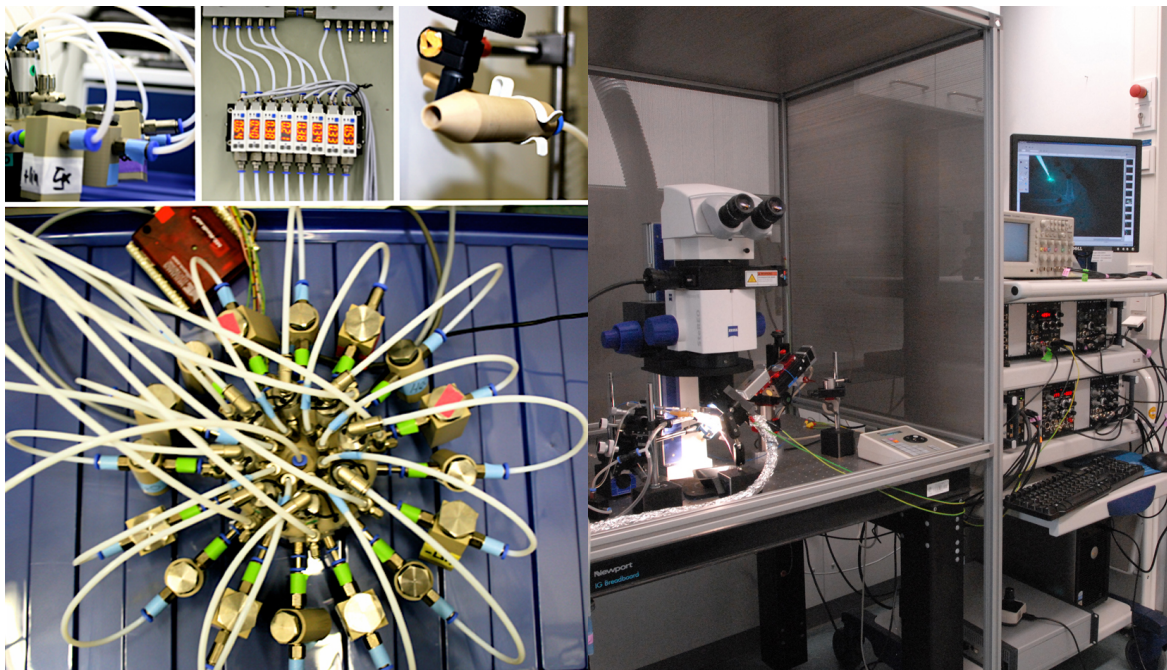


Figure 5: Electrophysiological setup with custom made multicomponent stimulus device for olfactory experiments

INTRODUCTION

This dissertation evaluates blend processing of host plant odorants using several techniques at different processing levels in order to increase understanding of complex mixture coding in the moth olfactory system. Using a novel multicomponent stimulus system (Figure 5, ChapterII) together with a combined physiological approach (ChapterIII&IV) enabled us to push our understanding of olfactory processing beyond the receptor level (ChapterI), and directly measure how the cellular network of the AL shapes the representation of odor blends relayed by the receptor neurons (OSNs). Response patterns in the moth AL result in a unique blend percept as early in the olfactory pathway as the first processing stage, the AL. My dissertation shows that host blend processing in *Manduca* does not follow a simple model explained by the elementary composition of odor mixtures. Moreover, analysis of blend input from OSNs cannot unambiguously predict AL output on any spatial or temporal scale. Shaped by the AL network, blend coding involves high levels of non-linear responses by AL neurons, each utilizing a variety of parameters to produce the novel, unique signal representing the entire blend.





Overview of Manuscripts

CHAPTER I

The antennal transcriptome of *Manduca sexta*

Ewald Grosse-Wilde, Linda S. Kuebler, Sascha Bucks, Heiko Vogel, Dieter Wicher & Bill S. Hansson

PNAS (2011) 108, 7449-7454.

The first chapter presents the use of transcriptomic and microarray data to identify transcripts from the main olfactory gene families of *Manduca sexta*. In order to assess the quality of the data, we compared the architecture of the first olfactory neuropil, the antennal lobe (AL), of female and male moths. The anatomical study revealed that the AL of *Manduca sexta* comprises a total of 70±1 glomeruli in females, and 68 glomeruli in male moths. This morphological data correlates closely to our information on expressed receptor genes. Finally, we compare the expression of the near-complete transcript sets in male and female antennae.

Built on an idea conceived by all authors. E. Große Wilde, L. Kuebler, D. Wicher and B.S. Hansson designed the experiments. L. Kuebler supervised 3D visualizations and conducted neuromorphological experiments. S. Bucks carried out RACE PCR. H. Vogel performed GO Annotation and cDNA normalization. E. Große Wilde, B. Hansson, D. Wicher & L. Kuebler wrote the manuscript.

CHAPTER II

A novel multicomponent stimulus device for use in olfactory experiments

Shannon B. Olsson^{*}, Linda S. Kuebler^{*}, Daniel Veit, Kathrin Steck, Alexandra Schmidt, Markus Knaden
& Bill S. Hansson

^{*}These authors contributed equally to this work

Journal of Neuroscience Methods (2010) 195, 1-9.

In the second chapter, we present a novel, multicomponent stimulus system for use in olfactory experiments that is capable of presenting up to 8 different odorants simultaneously or in sequence at defined concentrations and time scales. This device provides a unique method for introducing complex volatile mixtures for olfactory studies, and allows for accurate control of odor intensities in both time and space.

Built on an idea conceived by all authors. L. Kuebler & S. Olsson designed the device. L. Kuebler, K. Steck & Alexandra Schmidt conducted the experiments. D. Veit engineered the device. S. Olsson, M. Knaden & B. Hansson wrote the manuscript.

CHAPTER III

Neuronal processing of complex mixtures establishes a unique odor representation in the moth antennal lobe

Linda S. Kuebler, Shannon B. Olsson, Richard Weniger & Bill S. Hansson

Frontiers in neural circuits (2011) 5(7), 1-16.

Insects are never exposed to monomolecular olfactory stimuli in nature. When a female moth searches for a nectar-rich flower or a suitable oviposition substrate, the olfactory system has to extract information from rich blends of components. Relevant components are often detected by different types of olfactory sensory neurons (ChapterI) and information thus reaches the brain via separate channels. The third chapter of the thesis provides new insights into how the moth brain performs host blend coding at cellular levels of the first olfactory processing center of the brain, the antennal lobe. Using a novel multicomponent stimulus system (ChapterII), the study reveals significant non-linear coding of host associated blends, indicating high levels of across-fiber patterning that establish a novel “blend code” separate from individual component identities. Olfactory blends appear to be coded cellularly by the rate, latency, temporal patterning, and spatial location of the response. To our knowledge, this is the first paper that thoroughly addresses the question of host blend processing in insects from the perspective of individual neurons.

Built on an idea conceived by all authors, who also designed the experiments. L. Kuebler conducted the experiments. L. Kuebler and S. Olsson performed the data analysis. R. Weniger generated 3D visualizations. L. Kuebler, S. Olsson & B. Hansson wrote the manuscript.

CHAPTER IV

Novel blend patterns: simultaneous optophysiological studies at multiple levels of the moth AL

Linda S. Kuebler, Marco Schubert, Shannon B. Olsson & Bill S. Hansson

To be submitted in 2011/ in Vorbereitung

In the fourth chapter, we show that the mechanisms of blend processing revealed on the single neuron level (Chapter III) were maintained across the glomerular array. Using optophysiological (Calcium Imaging) techniques, we simultaneously measured OSN network input in concert with PN output across the glomerular array. By comparing patterns and intensity of activation between input and output levels, we directly determined the degree of AL network processing within a single animal. Our combined physiological approach revealed that although the input pattern of the blend in the antennal lobe spatially resembled the single component patterns, the output odor pattern of a blend response could not be predicted from its single component patterns. Generation of a novel pattern thus creates a unique blend percept as early as in the initial olfactory processing center in the brain, the AL.

Built on an idea conceived by all authors. L. Kuebler designed and carried out the experiment. L. Kuebler, M. Schubert, and S. Olsson analyzed the dataset. L. Kuebler wrote the manuscript. S. Olsson, M. Schubert & B. Hansson edited the manuscript.

CHAPTER I

The antennal transcriptome of *Manduca sexta*

Ewald Grosse-Wilde, Linda S. Kuebler, Sascha Bucks, Heiko Vogel, Dieter Wicher & Bill S. Hansson

Abstract

In recent years considerable progress has been made in understanding the molecular mechanisms underlying olfaction in insects. Because of the diverse nature of the gene families involved, this progress has largely relied on genomic data. As a consequence, progress has been limited to a small subset of species with extensive genomic information. For Lepidoptera, a large order historically crucial to olfactory research, this has mostly limited advances to the domesticated species *Bombyx mori*, with some progress in the noctuid *Heliothis virescens* based on a non-public partial genome database. Due to the limited behavioral repertoire and non-existent ecological importance of *Bombyx*, molecular data on the tobacco hornworm *Manduca sexta* is of utmost importance, especially with regards to its position as a classical olfactory model and its complex natural behavior. Here we present the use of transcriptomic and microarray data to identify members of the main olfactory gene families of *Manduca*. To assess the quality of our data, we correlate information on expressed receptor genes with new detailed morphological data on the antennal lobe. Finally, we compare the expression of the near-complete transcript sets in male and female antennae.

Introduction

Sensory assessment of the environment is crucial to survival and reproduction, and therefore directly affects the fitness of animals. In insects, receptors for sensory modalities such as olfaction, taste, mechanosensation and thermo- and hygrosensation are situated in the antenna. The antennal olfactory sense is of special importance to insects as it provides information on the chemical quality of e.g. food sources or oviposition sites, and is also employed in intraspecific communication via pheromones. Due to their highly specific and sensitive olfactory sense and extraordinarily complex chemosensory behavior, lepidopteran species have been widely utilized in the field of insect olfaction. For example, the first identified pheromone, bombykol, is the main pheromone

component of the silk moth, *Bombyx mori*. Moths also played an important role in physiological studies, both at the olfactory periphery and the central nervous level (Mustaparta, 1990;Hildebrand, 1995). Since the tobacco hornworm *Manduca sexta*, reflective of natural ecosystems shows far more complex behavior compared to the domesticated *Bombyx*, it was the focus of many studies and led to important advances in the field (e.g. Lee and Strausfeld, 1990;Hansson et al., 2003;Riffell et al., 2009).

In our effort to analyse the antennal transcriptome of *M. sexta*, we focussed on gene families that have been implicated in olfaction: OBPs, CSPs, SNMPs, ODEs, ORs, GRs and IRs (Angeli et al., 1999;Vogt, 2003;de Bruyne and Baker, 2008;Benton et al., 2009). The key players are the odorant receptor proteins (ORs; Vosshall et al., 1999). ORs are embedded in the dendrites of olfactory sensory neurons (OSN) in the antennae and – to a lesser extent - the maxillary palps. ORs are seven transmembrane domain receptors with inverted membrane topology in comparison to other G-protein coupled receptors (Benton et al., 2006). Insect ORs are not related to vertebrate ORs (Benton et al., 2006). ORs apparently share a common ancestor with gustatory receptors (GRs) (Robertson et al., 2003), which can also be expressed in neurons in the insect antennae (Scott et al., 2001;Jones et al., 2007). ORs supposedly function as dimers (Neuhaus et al., 2005;Benton et al., 2006), with a conserved protein acting as an ion channel (originally called DOr83b in *Drosophila* but now with the universal name ORCO) (Sato et al., 2008;Wicher et al., 2008), and a variable partner (OrX) that apparently determines ligand specificity (Hallem et al., 2004). Beside OR-based detection of odorants, recent discoveries have implicated ionotropic receptors (IR) as being involved in odor detection as well (Benton et al., 2009). IRs are relatives of ionotropic glutamate receptors (iGluR) with atypical binding domains that are conserved across protostome lineages and therefore far more ancient than ORs (Croset et al., 2010). The IR family contains a conserved subgroup, the “antennal”, presumably olfactory IRs (Croset et al., 2010). Both IR- and OR-expressing OSN populations expressing the same receptor innervate the same spherical structures, so called glomeruli, in the antennal lobe (AL), the first olfactory neuropil of the insect brain. All neurons expressing the same receptor target the same glomerulus (Stocker et al., 1983;Hansson et al., 1992;Couto et al., 2005;Fishilevich and Vosshall, 2005;Benton et al., 2009). The total number of glomeruli in the AL is thus related to the total number of functionally distinct OSN populations and therefore to the number of receptor genes (de Bruyne and Baker, 2008).

Because of the large sequence diversity exhibited by olfaction-related genes across insects, (Vosshall et al., 1999;Krieger et al., 2004;Robertson and Wanner, 2006;Engsontia et al., 2008;Tanaka et al.,

2009), identification by purely homology-based methods has been of limited use. Therefore, research in the molecular field of moth olfaction has largely been restricted to *Bombyx* due to the availability of genomic data (Sakurai et al., 2004; Krieger et al., 2005; Nakagawa et al., 2005; Wanner et al., 2007b; 2008; Tanaka et al., 2009).

Here we report the analysis of an antennal transcriptome of *Manduca*. Assessment of the data based on Gene Ontology (GO) indicated enrichment not only in signal detection and transduction, but also in enzymatic activity. Additionally, we identified extensive sets of representatives of all gene families involved in olfaction. Using the correlation between the total number of antennal receptor genes and olfactory glomeruli, we estimate the success of our approach by comparison with a newly constructed AL map. Furthermore, we analyzed sexually dimorphic gene expression using microarrays to identify genes potentially involved in sex-specific behavior, such as oviposition or pheromone detection. Our results demonstrate the feasibility of the approach and provide the basis for a deeper understanding of lepidopteran olfaction in the context of complex behavior.

Results

Initial sequencing

Transcriptomic sequence data was generated using a normalized antennal cDNA library and GS/FLX 454 technology. In total, we acquired 66 Mio. bases of sequence data in 275949 ESTs. After assembly, resulting in 22934 contigs, GO annotation was employed for an initial assessment of the transcriptome (Figure 1). GO annotation associates analyzed transcripts with terms from hierarchical vocabularies describing e.g. molecular function to allow meta-analyses of gene populations (Ashburner et al., 2000). Beside basic cell functions, GO terms connected to olfaction (e.g. “odorant binding”) and signal transduction (e.g. “response to stimulus”, “signal transducer activity”) were well represented. Additionally we found strong representation of terms connected to enzymatic activity (for example “hydrolase activity” 12%, “transferase activity” 9%). It should be noted that in comparison with other tissues, an inordinate number of transcripts (*Manduca* midgut transcriptome with 49% of the data without BLAST hit) have no associated GO terms (15803 out of 22934 contigs, ca. 69%), potentially representing orphan genes.

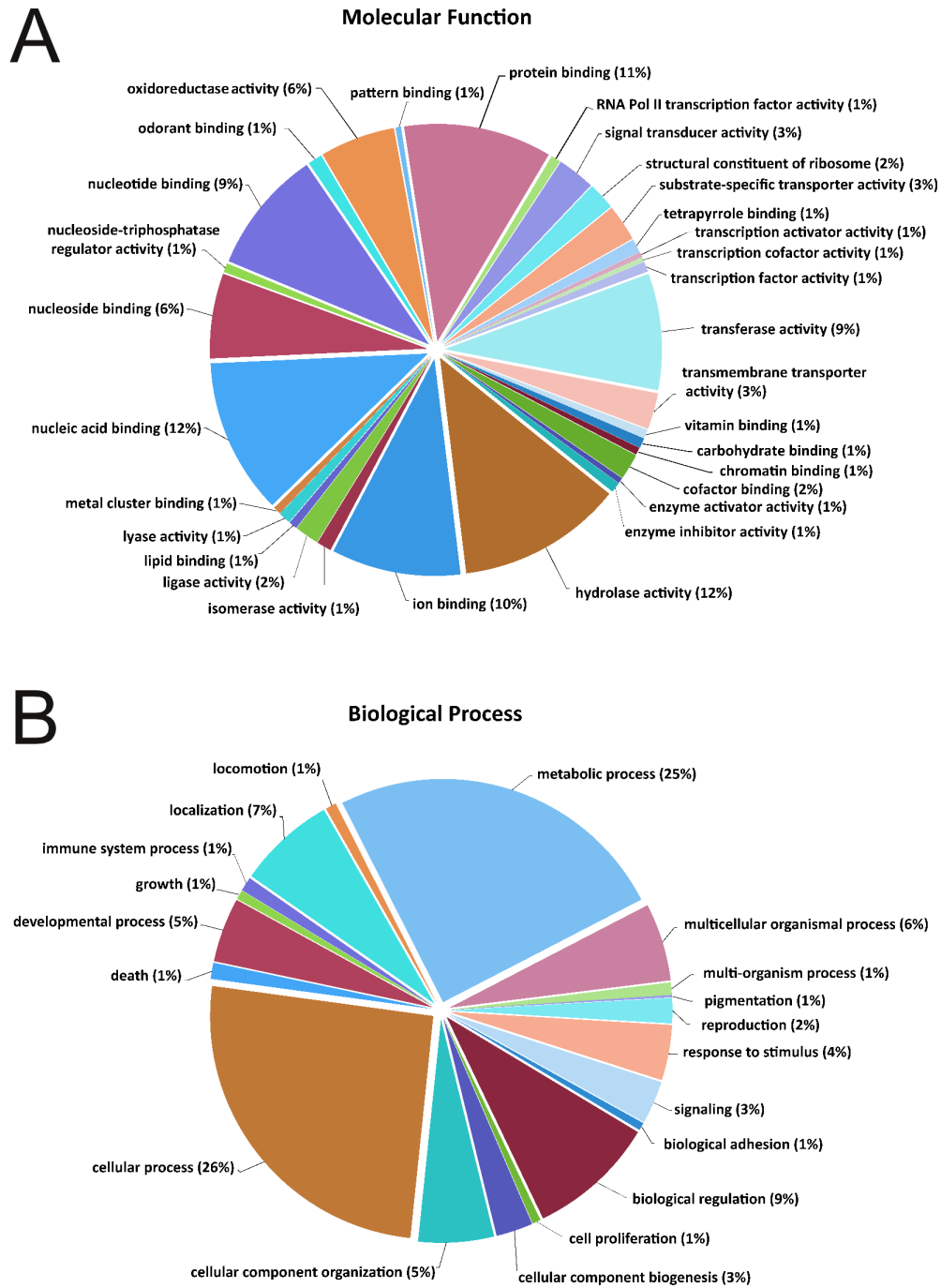


Figure 1: Gene ontology (GO) analyses of *Manduca* antennal transcriptome data. GO analysis of *Manduca* sequences corresponding to 7131 contigs, as predicted for their involvement in (A) molecular functions and (B) biological processes. Data is presented as level 3 GO categorization for molecular function and level 2 GO categorization for biological process. Classified gene objects are depicted as percentages (in brackets) of the total number of gene objects with GO assignments.

Non-receptor olfactory gene families

For a more detailed analysis of the transcriptome, we focused on putative members of olfactory gene families, starting with OBP-coding genes. OBPs are small, globular proteins comprised of 140-

220 amino acids (Vogt and Riddiford, 1981; Vogt, 2003) that are characterized by a pattern of six conserved cysteines (Leal et al., 1999; Scaloni et al., 1999). In addition to the 12 OBPs reported previously for *Manduca* (Gyorgyi et al., 1988; Vogt et al., 1991; Robertson et al., 1999; Vogt et al., 2002) we were able to identify six new putative OBP-coding transcripts (Figure S1), three of which seemingly include the full coding sequence. All non-full-length transcripts encode overlapping but distinct OBP domains, establishing them as parts of independent genes. The total amount of putative OBP-coding genes in *Manduca* is 18, compared to 17 reported for *Bombyx*.

A second group of proteins present in the sensillum lymph are the chemosensory proteins (CSP) (Angeli et al., 1999). While they exhibit a similar expression in the antenna to OBPs, CSPs are not related. They are generally more conserved and differ in tertiary structure, with four cysteines forming two disulphide bridges in a configuration distinct from OBPs (Angeli et al., 1999). So far, 5 CSPs have been reported for *Manduca* (Robertson et al., 1999). We identified a total of 14 additional CSP-coding gene fragments in the antennal transcriptome, four of which encode full-length proteins (Figure S2). The total number (21 CSPs) exceeds the number reported for *Bombyx* (16 CSPs; Gong et al., 2007).

A third class of non-receptor proteins described in *M. sexta* are sensory marker neuron proteins, CD36-class proteins expressed in the antenna (SNMPs, Vogt, 2003). While SNMP-1 is expressed in pheromone sensitive OSNs and necessary for pheromone detection (Benton et al., 2007), SNMP-2 is expressed by the support cells surrounding these neurons (Forstner et al., 2008). Both previously described *Manduca* SNMPs (Rogers et al., 2001) were represented in our data.

Receptor coding transcripts

The third protein family of interest is the family of ionotropic receptors (IRs). IRs show extended sequence variability in comparison to other gene families, but share a distinct structure (Benton et al., 2009). Generally, IRs are subdivided into diverse, antennal and the IR25a/8a subgroup, with the latter two involved in olfaction in the antenna (Croset et al., 2010). In the genome of *Bombyx* 11 putative antennal IRs and two pseudogenes have been identified (Croset et al., 2010). Additionally, 12 homologous IRs have been identified from an antennal EST database of the noctuid *Spodoptera littoralis* (Olivier et al., 2010). We were able to identify 6 transcripts encoding homologous receptors in *Manduca*. All of them show clear homology to antennal IRs in *Bombyx* (Figure S3).

Central to odorant detection are odorant receptors (ORs). Due to their high sequence variability, the most common method to identify OR-coding genes is to analyze genomic sequence databases. For *Manduca*, the coreceptor (MsexOR-2) and 5 OR-coding genes have been identified previously (Patch

et al., 2009; Grosse-Wilde et al., 2010). Transcripts for all except MsexOR-3 were present in our data; MsexOR-2 and MsexOR-6 could also be extended to full-length. Using RACE-PCR we were able to verify 47 OR genes as unigenes (Figure 2, MsexOR-2 excluded), as well as one GR. Full-length OR-coding sequences seem to be present in 27 cases.

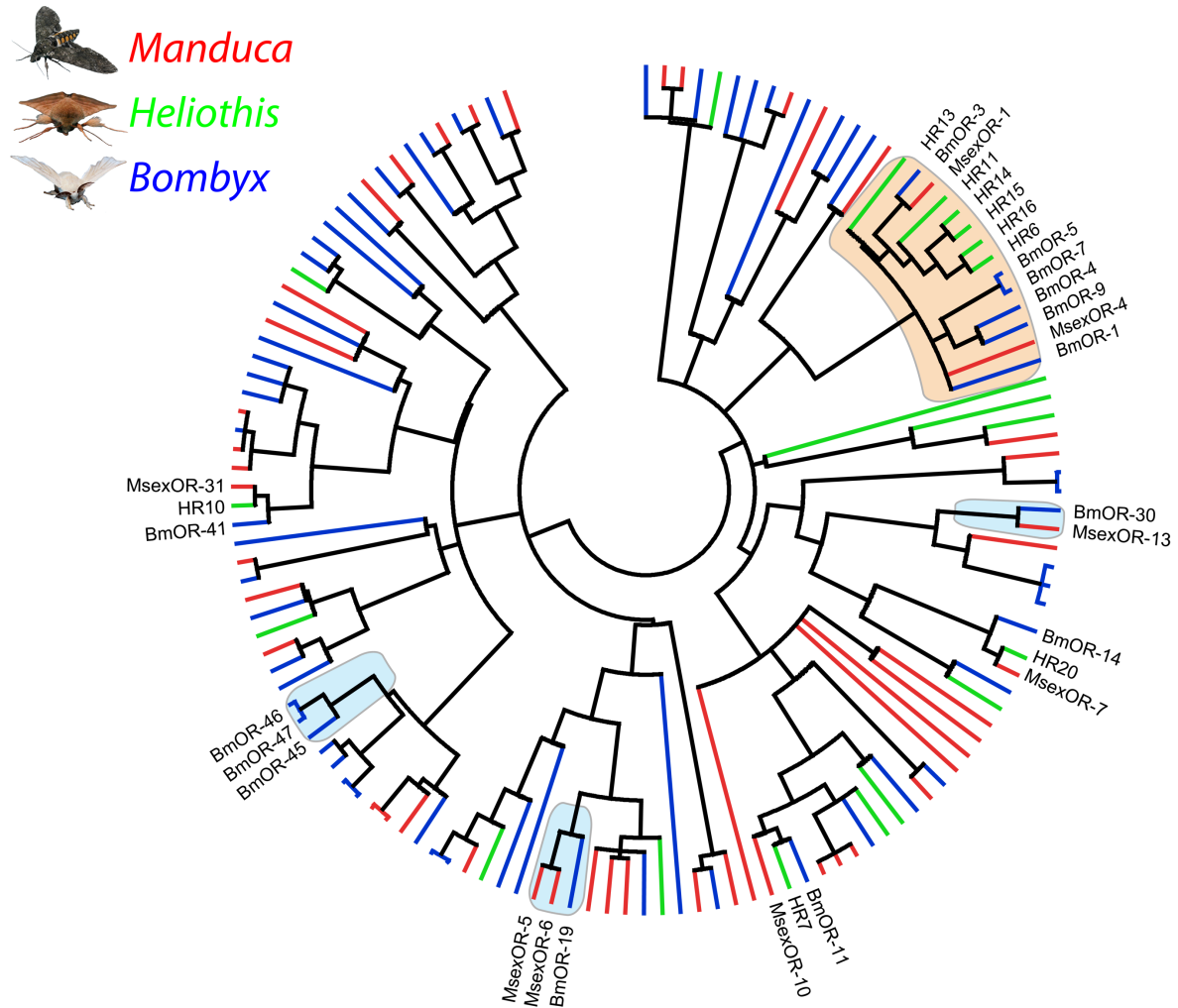


Figure 2: Aligned putative odorant receptor protein sequences of *Manduca* (red), *Bombyx* (blue) and *Heliothis* (green). The identified receptor candidates of *Manduca* are spread evenly inside the family. Two candidates belonging to the subgroup of male pheromone receptors (orange) have been identified. Additionally, female-specific ORs of *Bombyx* have been marked (blue). Two female-specific receptor groups also include receptor candidates of *Manduca*. Additional instances with clear homologues in all three species have been indicated by name. Coreceptors (MsexOR-2, BmorOR-2 and HR2) have been excluded.

Comparison with OR genes from *Bombyx* (Sakurai et al., 2004; Krieger et al., 2005; Nakagawa et al., 2005; Wanner et al., 2007a; Tanaka et al., 2009) and *Heliothis* (Krieger et al., 2002; Krieger et al., 2004; Figure 2) allowed several observations. In Lepidoptera, several sex-specific ORs have been identified, including a subgroup containing male-specific pheromone receptors (Krieger et al., 2004;

Krieger et al., 2005; Nakagawa et al., 2005; Miura et al., 2009; Wanner et al., 2010, labelled 1 in Figure 1). Beside the previously reported MsexOR-1 and -4 we were not able to identify further members of this group. In addition to male-specific ORs, female-specific receptors with known function have been reported for *Bombyx* (Anderson et al., 2009, labelled 2-4 in Figure 2). The comparison allowed us to ascertain the presence of putative homologues for BmOR-19 and BmOR-30. Interestingly, while BmOR-30 has exactly one homologue in *Manduca* (MsexOR-13), two homologues for the linalool-detecting BmOR-19 seem to be present (MsexOR-5 and -6).

We found several instances with conservation of OR-coding genes across the three analyzed species (Figure 2, black arrows). In all three instances, one homologue per species exists, the coding gene seems comparatively conserved, and no specific expression pattern or function has been reported.

Antennal lobe

The number of glomeruli within the antennal lobe of most insects is correlated with the number of distinct functional populations of OSNs in the antenna and in the maxillary palp (12% in *Drosophila*, Couto et al., 2005; Fishilevich and Vosshall, 2005; de Bruyne and Baker, 2008). As the number of distinct functional groups of neurons is associated with the total number of functional ORs, GRs (Couto et al., 2005; Fishilevich and Vosshall, 2005; de Bruyne and Baker, 2008) and IRs (Benton et al., 2009) on the antenna, we could estimate a total number of antennally expressed receptor genes based on the total number of glomeruli. For *Manduca*, this number has been determined previously as 63 ± 1 (Rospars and Hildebrand, 1992; 2000; Huetteroth and Schachtner, 2005). We recreated the previous analysis using a non-histochemical approach based on confocal laser scanning microscopy followed by computer-assisted 3D reconstruction for both male and female animals (Figure 3, Figure S6 & S7, Movie S1 & S2). A detailed analysis revealed the presence of a total of 70 ± 1 glomeruli in *Manduca* females and 68 glomeruli in males. Using landmarks, all glomeruli could be identified individually in both sexes ($n = 3$ each for males and females) and were designated according to *Drosophila* nomenclature (see Movies S1 & S2; Laissue et al., 1999). The male-specific macroglomerular complex (MGC) (Hansson et al., 1991; Heinbockel and Hildebrand, 1998) and the two female specific glomeruli (mLFG and ILFG) as described by Rössler et al. (Rössler et al., 1998) were easy to determine. Comparison of general AL architecture in terms of number of glomeruli and discounting MFG and LFGs revealed a small sexual dimorphism, with three non-LFG glomeruli (P5, VN3, VA4) present in females but not in males.

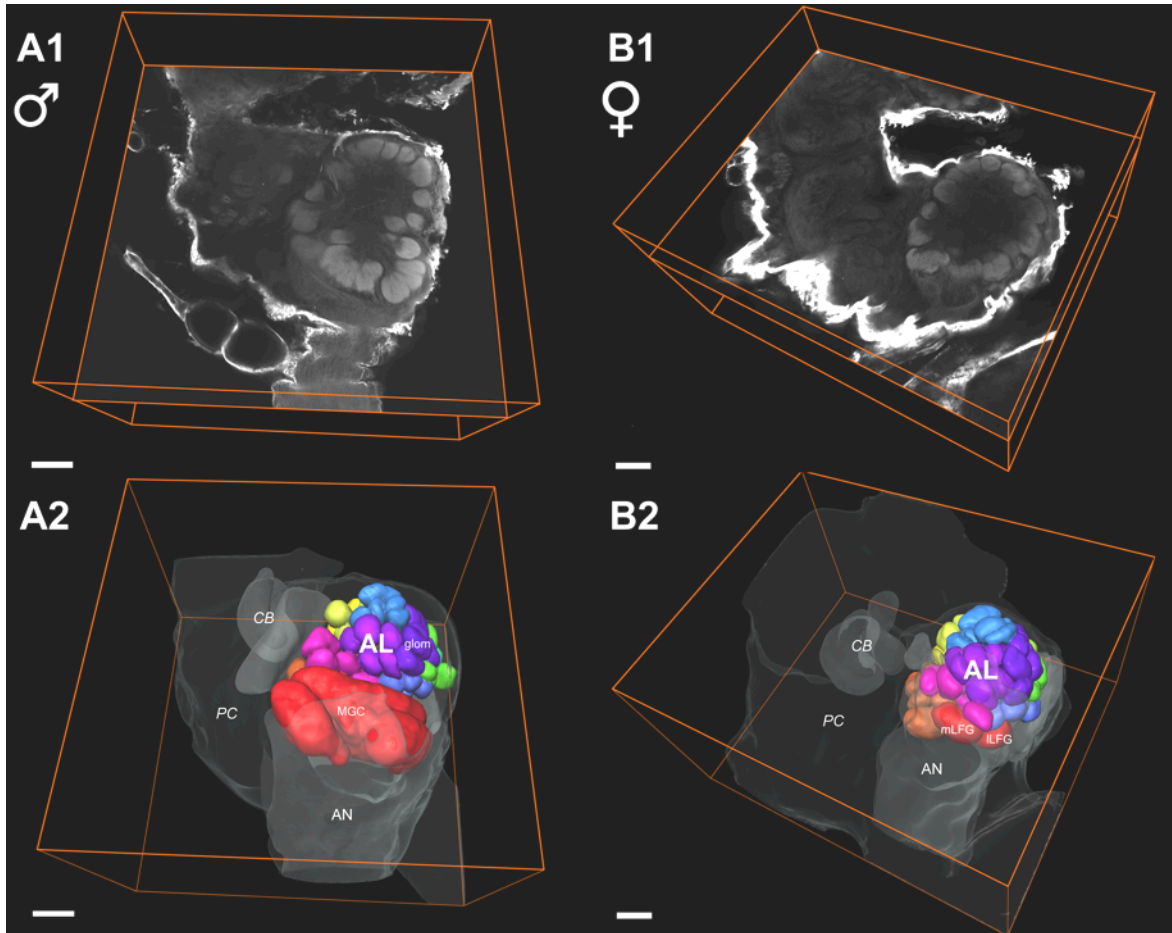


Figure 3: Example of the right hemisphere of the *Manduca* brain with focus on the antennal lobe (AL) and its innervation by antennal nerve fibres (AN).

A: Confocal micrographs extracting one single optical orthogonal slice from the 3D data set of one male (A1) and one female antennal lobe (A2).

B: 3D reconstructions of the AL of both sexes depicting a ventral view of reconstructed glomeruli (B1: males, n=68, B2: females n=70+/-1,) corresponding to optical slices in A. ALs display typical moth glomerular architecture: the striking sex-specific glomeruli; the male-specific macrogglomerular complex (MGC) and the medial large (mLFG) and lateral large female glomeruli (ILFG) are situated at the entrance of the antennal nerve and are illustrated in red. Brain outlines of adjacent neuropil areas serve as orientation guidelines. CB central body, PC protocerebrum, OL optic lobe, AN antennal nerve, glom glomerulus, scale bars = 100 μ m.

Sex-specific gene expression

Based on the transcriptomic data from the present study, the larval midgut (Pauchet et al., 2010) as well as data present in NCBI databases we constructed microarrays to scrutinize differential gene expression, using both male and female antenna. For analysis, differentially expressed genes were associated with GO terms (Figure S4 and S5). In comparison to larval midgut expression, a somewhat small amount of gene objects were limited to male and female antennae (383 and 417, respectively, Figure S4). In comparison, >8000 genes present in the midgut were not detected in the antenna. However, the depleted antennal data sets were heavily enriched in terms associated with olfaction. Additionally, while the total number of transcripts appeared decreased, a surprisingly high percentage of terms signifying enzymes present in the data remained. Comparing male and female

antennae, the most obvious difference was the higher complexity of the female antenna. In terms of number of transcripts, 729 were present in the female, while only 348 were found in the male. This is further supported by the associated GO terms with the reduced data sets (Figure S5). In female antennae the number of terms appearing for biological process and molecular function is roughly twice the number as for male antennae.

Discussion

We used next generation sequencing to analyze the antennal transcriptome of the tobacco hornworm *Manduca sexta*. The sequence data (ca. 22000 contigs with an average size of 460 bases) allows an estimation of tissue complexity in terms of gene expression. Using the mean CDS size of 1.1-1.2 kb in the *Bombyx* genome as reference (2008), we can estimate the total number of genes expressed to be around 7000-8000. Compared to the microarray data, the larval midgut exhibited more than 8000 unique gene calls, while less than 1000 were limited to the antenna (Figure S4). Overall, the data indicates a low complexity of antennal gene expression.

Another intriguing result of our study is the large amount of transcripts of unknown function in the transcriptome. While our knowledge regarding the function of genes in general is limited, especially in species that are not genetic models, a failure to associate GO terms for ca. 69% of the transcripts is remarkable, indicated high levels of unknown processes in this tissue. It seems possible that the non-annotated contigs are untranslated. However, comparison with the larval midgut data that has been generated using the same methods and does not exhibit the same percentage apparently indicated that this is not the case. While a large portion of the non-annotated transcripts are common to both tissues, some are only present in the antennal data. Due to the specialized nature of the antenna, it is possible that these transcripts are involved in processes that are directly or indirectly connected to sensory perception.

Nonetheless, the annotated transcripts allow us to draw some conclusions. Surprisingly, we found an enrichment of terms connected to enzymatic activity. While ODEs seem to be involved in removing active odor molecules from the sensillum lymph, possibly playing a crucial role in the retention of sensitivity, only a small number of enzyme families have been identified as containing ODE candidates (reviewed in Vogt, 2003). For example for the noctuid *Spodoptera littoralis* 16 antennal esterases have been reported, with recent work indicating a role as ODEs (Durand et al., 2010). It is possible that a majority of ODEs from different enzyme families are still unidentified. Therefore it seems likely that many of the transcripts coding for enzymes are indeed ODEs. Additionally, we noticed a large amount of regulatory transcripts in the data set. This might indicate

epigenetic plasticity in the antenna, especially in light of studies demonstrating circadian changes in the pheromone sensitivity of *Manduca* (Flecke et al., 2006; Schuckel et al., 2007; Flecke and Stengl, 2009). Indeed, post-developmental regulation of OR gene expression has been demonstrated previously in one other species (Fox et al., 2001).

As an indicator of our success in identifying antennally expressed receptors involved in olfaction as well as the completeness of our transcriptome, we used morphological data from the AL. We identified 54 receptor fragments from our transcriptomic data set, compared to 73 unique glomeruli. However, we must consider that some neuron populations innervating glomeruli in *Manduca* may be derived from the maxillary palp (Kent et al., 1986; Guerenstein et al., 2004; Couto et al., 2005; Fishilevich and Vosshall, 2005). With current knowledge on antennal physiology we suspect the missing transcripts are expressed in very few cells, resulting in very low overall expression levels. A low representation of transcripts means a higher likelihood of either elimination in the normalization, or to be missed during random sequencing. However, it is possible to derive information on the identity of the missing receptors by comparison with other species. Assuming a similar organization in both *Manduca* and *Bombyx*, we missed five antennal IR transcripts out of eleven (Croset et al., 2010), with possibly functional homologues for at least one pseudogene in *Bombyx* (IR68a). Since IRs are expressed in OSNs associated with comparatively rare coeloconic sensilla (Benton et al., 2009), this supports the hypothesis that our unsuccessful identification was due to low expression levels. Similarly, further comparison to two moth species with extensive reported OR gene sets (*Bombyx* and *Heliothis*) also indicates the identity of missed OR genes. The best described OR subgroup in Lepidoptera contains a number of male-specific receptors detecting active pheromone compounds in both *Heliothis* and *Bombyx* (Sakurai et al., 2004; Nakagawa et al., 2005; Grosse-Wilde et al., 2006; Grosse-Wilde et al., 2007). Published expression data for MsexOR-1 and MsexOR-4 indicates a role in the detection of the major pheromone component bombykal as well as the minor component E10,E12,Z14-16:Al. However, a third pheromone component (E10,E12,E14-16:Al) is detected by a small, distinct neuron population (Kaissling et al., 1989; Hansson et al., 1991; Kalinova et al., 2001). This indicates that a third male-specific receptor eluded us. Additionally, the pheromone receptor group also contains non-sex-specific members not involved in pheromone communication (four in *Bombyx*) that seem to be expressed in very few cells and possibly detect plant odors (Jordan et al., 2009). Again, we did not identify any homologues in *Manduca*. Similarly, we are lacking homologues for two female specific receptors of *Bombyx* (BmOR-45 and -47). Since their function (Anderson et al., 2009) is of high importance to *Manduca* (Riffell et

al., 2009) it seems apparent that their homologues are still elusive. In total, we can predict the identity of 12 missing receptor genes, all of which seem to be expressed in low levels and with predicted functions. The presented data therefore will allow extensive analysis of the receptor population of a complex behaving moth.

Comparison with morphological data also allows us to draw additional conclusions from the microarray expression data. According to the AL data, five glomeruli are female-specific and three are male-specific. This correlates with five female- and three male-specific OR genes. While the identity of the male-specific receptor genes seems obvious (the three putative pheromone receptors, two of which are identified), the receptor correlates are less clear for the five female-specific glomeruli. Three receptors are expected to belong to the well-described LFG (King et al., 2000); obvious candidates are the two homologues of the *Bombyx* linalool-receptor BmorOR-19, MsexOR-5 and -6. Reisenmann et al. (2004) described two distinct glomeruli for the enantiomers of linalool (Reisenman et al., 2004). This indicates that the detection of the two enantiomers is mediated by different neuron populations and therefore receptors, probably MsexOR-5 and -6. The expected third LFG-related receptor is probably MsexOR-13, the homolog of the female-specific BmOR-30.

Interestingly, the existence of data from lepidopteran species belonging to three different families (Bombycoidea, Noctuidae, Sphingidae) indicates that there are homologous receptors between the species. Given the evolutionary distance of the three families, and the generally positive selection of OR genes (Tunstall et al., 2007), these receptors might play a central role in lepidopteran olfaction. However, there is no reported function or ligand that readily presents itself as connected to these OR types. This suggests an unknown behavior or an unknown compound with a key role in established paradigms.

The data in this study presents the first near-complete information on the molecular basis of lepidopteran species beside the domesticated *Bombyx mori*. The chosen transcriptomic approach allowed an extensive analysis, which will be fundamental for future studies involving this complex model species as well as extensive cross-species comparison.

Material & Methods

Animals

Manduca (Lepidoptera, Sphingidae) moths were reared as described in Grosse-Wilde et al., 2010 (51). Detailed instructions are in Supplement M.

Extraction of totalRNA

Antennae of adult animals were cut off close to the scapulum, transferred to an Eppendorf cup and total RNA extracted using the Trizol method. For a more detailed description see Supplement M.

Expressed Sequence Tag Generation

RNA extracted from four male and four female animals was unified and further purified using the RNeasy MinElute Clean up Kit (Qiagen, Hilden, Germany) following the manufacturer's protocol. In order to prevent over-representation of the most common transcripts, the reverse transcribed mRNAs converted to double-stranded cDNAs (see below) were normalized using the duplex-specific nuclease method (Zhulidov et al., 2004). Normalized, full-length enriched cDNA libraries were generated using a combination of the SMART cDNA library construction kit (BD Clontech, Mountain View, CA) and the Trimmer Direct cDNA normalization kit (Evrogen, Moscow, Russia) generally following the manufacturer's protocol but with several important modifications and enzyme replacements essentially as described in (Vogel et al., 2010). The resulting normalized ds-cDNAs were used as a template for NextGen sequencing on a Roche 454 FLX using standard chemistry at the MPI for Molecular Genetics, Berlin, Germany. Original data generated in the run has been deposited at <http://www.ebi.ac.uk/ena/data/view/ERP000526>.

For additional description, see Supplement M.

RACE-PCR

To extend fragments of candidate genes to full-length, Marathon and SMART RACE PCR kits (Clontech) were employed using gene specific primers generated with eprimer3 according to recommended specifications and following the manufacturer's instructions.

Bioinformatics

Multiple assemblies using either seqclean or the TGICL package (<http://compbio.dfci.harvard.edu/tgi/>), Seqman NGen (DNAStar, Madison, WI) or CLC Genomics Workbench (CLCbio, Aarhus, Denmark) were performed to facilitate comparison. In each case, reads

and resulting contigs were screened for contaminants, low quality and adaptor/linker sequences using the respective options. GO Annotation was performed both using Blast2GO (Conesa et al., 2005; Gotz et al., 2008) and a Codequest Workstation W8 (Active Motif, Carlsbad, CA). For identification of ORs and IRs, custom databases for Blast and HMM profile searches were used. Candidate sequences for all mentioned gene families were analyzed further using the Lasergene software suite (DNASTar, Madison, WI). Predicted amino acid sequences were aligned using MAFFT (Kato et al., 2005), followed by maximum likelihood analysis with FastTree (Price et al., 2010). Dendrograms were created using MEGA4 (Tamura et al., 2007) and colored in Adobe Illustrator (Adobe Systems, Mountain View, CA). Identified olfactory genes are included in table S1.

Microarrays and data analysis

Sequence assembly of included *Manduca* antennal and gut ESTs (Pauchet et al., 2010) and all publicly available Genbank sequences was used with eArray (Agilent Technologies) for the design of 4 x 44K microarrays based on 60mer oligo probes.

For sex-specific antennal microarray hybridizations, RNA of three individuals of one sex was pooled per preparation, and 5 larvae each were dissected for gut tissue isolation with four biological replicates per sex (antennae) and tissue (gut), respectively. Double purified total RNA was added to Agilent Technologies spike-in RNA and labeled using QuickAmp Amplification kit (Agilent Technologies) and the Kreatech ULS Fluorescent Labeling Kit with cyanine 3-CTP dye following the manufacturer's instructions.

Amplified cRNA samples were used for microarray hybridization, scanned with the Agilent Microarray Scanner and data was extracted from TIFF images with Agilent Feature Extraction software version 9.1. Raw data output files were analyzed using the GeneSpring GX11 and GeneSifter microarray analysis softwares. Data has been deposited at gene expression omnibus (<http://www.ncbi.nlm.nih.gov/geo/>, series entry: GSE27470). More detailed descriptions are available in Supplement M.

Neuroanatomical procedures

Brains were dissected from the head capsule and fixed using ice-cold 4% formaldehyde in phosphate-buffered saline (PBS; pH 7.2). Tissues were permeabilized by dehydration and rehydration using a sequence of ethanol concentrations. Afterwards brains were stained using Lucifer yellow, dehydrated and cleared with methylsalicylate. Image acquisition was performed

using a Zeiss LSM 510 (Carl Zeiss, Jena, Germany). Reconstruction was performed using Amira 4.1.2 (Mercury Computer Systems, Berlin, Germany). For a detailed description see Supplement M.

Image processing

For video visualization, label surfaces were exported from AMIRA and visualized with ImageJ (Fiji). Figure 3 was edited using Adobe Photoshop CS4 (Adobe Systems, Inc.) and compiled with Adobe Illustrator CS4 without any further modification on brightness or contrast.

ACKNOWLEDGEMENTS

This work was funded by the Max Planck Society. The authors would like to thank Sabine Kaltofen and Sylke Dietel for animal rearing, Richard Weniger for valuable support with AL reconstruction, Martin Niebergall and Steffi Gebauer-Jung for IT support and Bernd Timmermann (MPI for Molecular Genetics, Berlin) for sequencing services. The authors want to thank Shannon Olsson for helpful comments on the manuscript.

Supplemental Data

Supplementary Materials & Methods

Animal rearing

Animals were taken from a culture maintained at the Max Planck Institute for Chemical Ecology, Jena, Germany. For breeding, adults were kept in a flight cage containing a *Nicotiana attenuata* plant for oviposition, with artificial flowers providing a sugar solution for nutrition. Three times a week eggs were collected transferred to small boxes with artificial diet (46 g agar, 144 g wheat germ, 140 g corn meal, 76 g soz flour, 75 g casein, 24 g salt, 36 g sugar, 5 g cholesterol, 12 g ascorbic acid, 6 g sorbic acid, 3 g methyl paraben, 9 ml linseed oil, 60 ml 37% formalin, 30 mg nicotinic acid, 15 mg riboflavin, 7 mg thiamine, 7 mg pyridoxine, 7 mg folic acid and 0.6 mg biotin per 1.8 ml water). Eggs and emerging larvae were kept inside a climate controlled chamber at 27°C and 70% humidity. Hatched larvae were transferred into new boxes with artificial diet on metal lattices. On onset of wandering (fifth instar) larvae were allowed to pupate separately in small plastic boxes filled with paper. Pupae were kept in climate chambers until 1 week before likely emergence. Animals used for morphological or microarray experiments were separated as pupae and allowed to emerge individually in paper bags in an environmental chamber at 25°C with 50% relative humidity on a 16-hour/8-hour photoperiod. For 3D reconstructions only naïve adult moths 3-5 days post-eclosion were used (male n = 3, female n = 3).

Extraction of total RNA

Tissues were cooled over liquid nitrogen. The frozen tissue was transferred to a liquid nitrogen cooled mortar and ground. The homogenate was covered with 1 ml Trizol reagent (Sigma-Aldrich, St. Louis, MIS). Further steps were performed according to the manufacturers instruction, replacing chloroform with 1-bromo-3-chloro-propane. Also, an additional DNase (Turbo DNase, Ambion, Austin, TX) treatment was included to eliminate any contaminating DNA. TotalRNA was dissolved in RNA Storage Solution (Ambion) and RNA content and quality was measured photometrically.

Expressed Sequence Tag Generation

RNA extracted from four male and four female animals was unified and further purified using the RNeasy MinElute Clean up Kit (Qiagen, Hilden, Germany) following the manufacturer's protocol. RNA integrity and quantity was verified on an Agilent 2100 Bioanalyzer using the RNA Nano chips (Agilent Technologies, Santa Clara, CA). RNA quantity was determined on a Nanodrop ND-1000 spectrophotometer. In order to prevent over-representation of the most common transcripts, the reverse transcribed mRNAs converted to double-stranded cDNAs (see below) were normalized using

the Kamchatka crab duplex-specific nuclease method (77). Normalized, full-length enriched cDNA libraries were generated using a combination of the SMART cDNA library construction kit (BD Clontech, Mountain View, CA) and the Trimmer Direct cDNA normalization kit (Evrogen, Moscow, Russia) generally following the manufacturer's protocol but with several important modifications and enzyme replacements essentially as described in (78). In brief, 2 µg of total RNA was used and reverse transcription was performed with a mixture of several reverse transcription enzymes for 1h at 42 °C and 90 minutes at 50 °C. cDNA size fractionation was performed with SizeSep 400 spun columns (GE Healthcare) that resulted in a cutoff at ~200 bp. Each step of the normalization procedure was carefully monitored to avoid the generation of artifacts and overcycling. The resulting normalized ds-cDNAs were used as a template for NextGen sequencing on a Roche 454 FLX using standard chemistry at the MPI for Molecular Genetics, Berlin, Germany.

Microarrays and data analysis

The sequences used for microarray probe design included *Manduca* antennal and gut ESTs (63) and all publicly available Genbank sequences for this species, and were jointly assembled using Seqman NGen. A resulting list of 25975 contigs in fasta format was uploaded onto eArray (Agilent Technologies), and two 60mer oligo probes were designed for each predicted OR and a single 60mer oligo probe was designed for the remaining contigs using eArray tools with standard settings. The microarray was designed with a 4 X 44K format with a final number of 37018 non-control probe sets, 1000 replicate controls and 1417 Agilent Technologies built in controls (structural and spike in).

For sex-specific antennal and head capsule microarray hybridizations, RNA of three individuals of one sex was pooled per preparation, and 5 larvae each were dissected for gut tissue isolation with four biological replicates per sex (antennae) and tissue (gut and head), respectively. Total RNA was double purified, quality tested and quantified as mentioned above. Agilent Technologies spike-in RNA was added to 500 ng of total RNA and labeled using a combination of the QuickAmp Amplification kit (Agilent Technologies) and the Kreatech ULS Fluorescent Labeling Kit with cyanine 3-CTP dye following the manufacturer's instructions. Labeled amplified cRNA samples were purified using Qiagen RNeasy MinElute columns and analyzed on a Nanodrop ND-1000 spectrophotometer using the microarray function. Amplified cRNA samples were used for microarray hybridisation only if the yield was >825 ng and the specific activity >8.0 pmol Cy3 per ug cRNA. 1,600 ng of cyanine 3 labeled cRNA was used for each array and hybridization was carried out at 65°C for 17 hours. Slides were washed in GE Wash Buffers according to the manufacturer's instructions (Agilent Technologies). Slides were treated in Stabilization and Drying Solution, scanned with the Agilent Microarray Scanner and data was extracted from TIFF images with Agilent Feature Extraction

software version 9.1. Raw data output files were analyzed using the GeneSpring GX11 and GeneSifter microarray analysis softwares. The data points were normalized between arrays to the median intensity and log base 2-transformation of the normalized data was performed. Genes were classified as differentially expressed in GeneSifter if the P-values (t-test) were < 0.05 after correcting for multiple testing using the Benjamini & Hochberg FDR. Global gene expression patterns were examined using hierarchical clustering in GeneSpring GX11 (Agilent Technologies). Clustering was performed on both probes and condition (tissues and treatments) using Pearson Centered distance metric and Centroid linkage rule. Gene expression (presence/absence) in tissues and sexes was determined using the presence call and threshold criteria implemented in GeneSpring GX11.

Neuroanatomical procedures

Brains were dissected from the head capsule, transferred to ice-cold 4% formaldehyde in phosphate-buffered saline (PBS; pH 7.2) and incubated for at least 2 hours on a shaker. After fixation, brains were dehydrated in an ascending series of ethanol (50%, 70%, 80%, 90%, 95%, and 3x100%, 10 minutes each) and subsequently rehydrated in a descending series to permeabilize tissue and facilitate homogenous dye penetration. Afterwards brains were incubated in 4% Triton X-100 in PBS containing 3% Lucifer yellow (Sigma-Aldrich) for 3 days on a shaker.

Stained brains were dehydrated, cleared with methylsalicylate (M-2047; Sigma-Aldrich, Steinheim, Germany) overnight, and finally positioned and sealed in custom aluminium slides. Brains were examined by confocal laser-scanning microscopy using a Zeiss LSM 510 (Carl Zeiss, Jena, Germany) equipped with a HeNe/Ar lasermodul and a 10x, 0.45-NA objective lens (C-Apochromat, Zeiss, Germany). Optical sections (1024 x 1024 pixel) were taken at intervals of 1-1,5 mm for detailed scans of the AL.

Image segmentation and 3D reconstruction

3D reconstructions were carried out using AMIRA 4.1.2 (Mercury Computer Systems, Berlin, Germany). Individual glomeruli were reconstructed by segmentation of each spherical structure around its center in three focal planes (xy, xz, yz). Subsequent use of the wrapping tool allowed us to interpolate 3D shapes. Brain outlines of adjacent neuropil areas serving as orientation guidelines were reconstructed by segmentation, followed by regular interpolation. Total number of all glomeruli was assessed by complete AL reconstructions of 3 males and 3 females.

Supplementary Figures

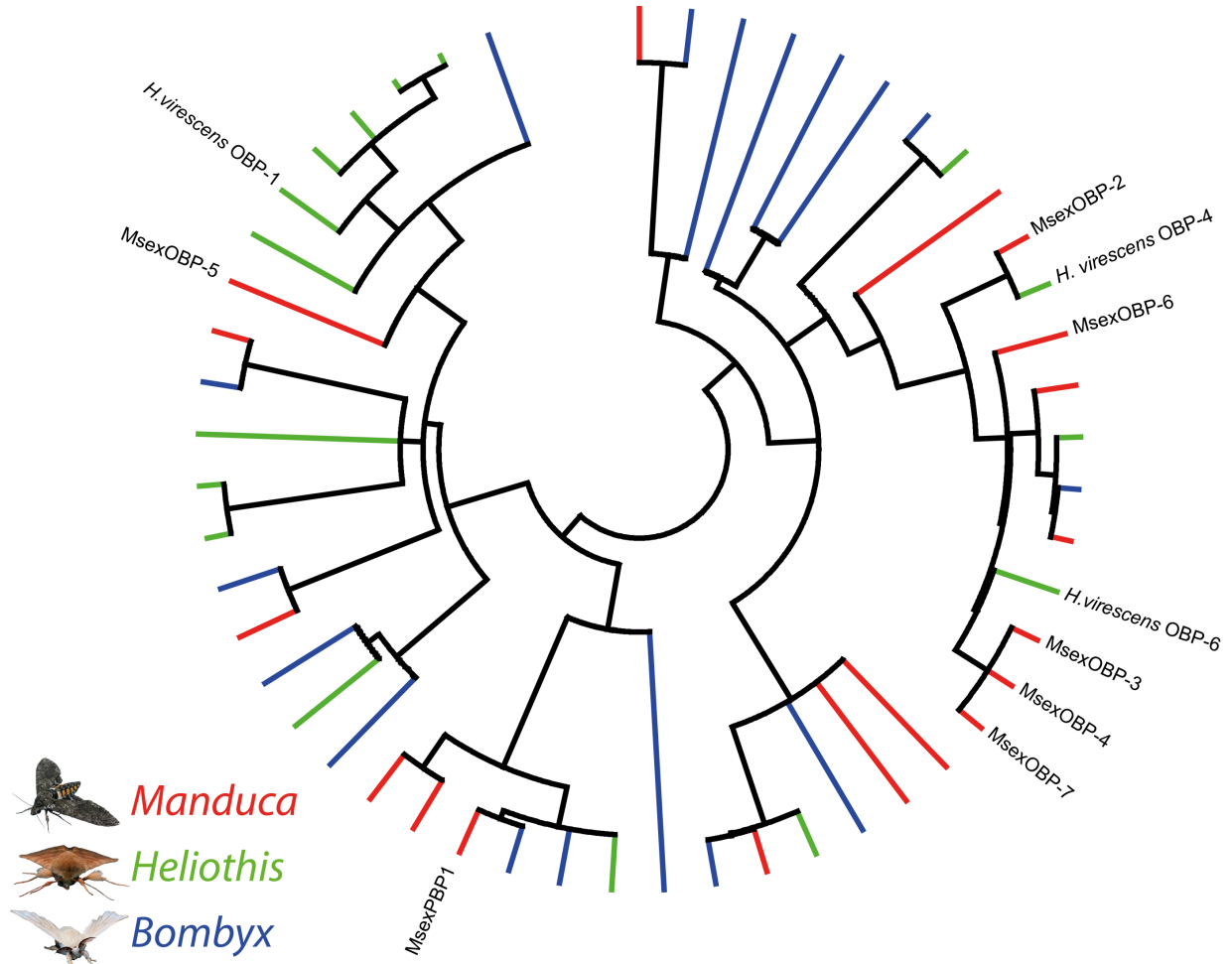


Figure S1: Lepidopteran OBPs (*Heliothis* green, *Bombyx* blue, *Manduca* previously identified yellow, this study red, others black). Linearized dendrogram based on a maximum likelihood analysis of a MAFFT alignment of predicted protein sequences. Newly identified OBPs have been indicated by name, as have been single representatives in other species and MsexPBP1 for orientation. The predicted proteins of *Manduca* show high similarity to other lepidopteran OBPs.

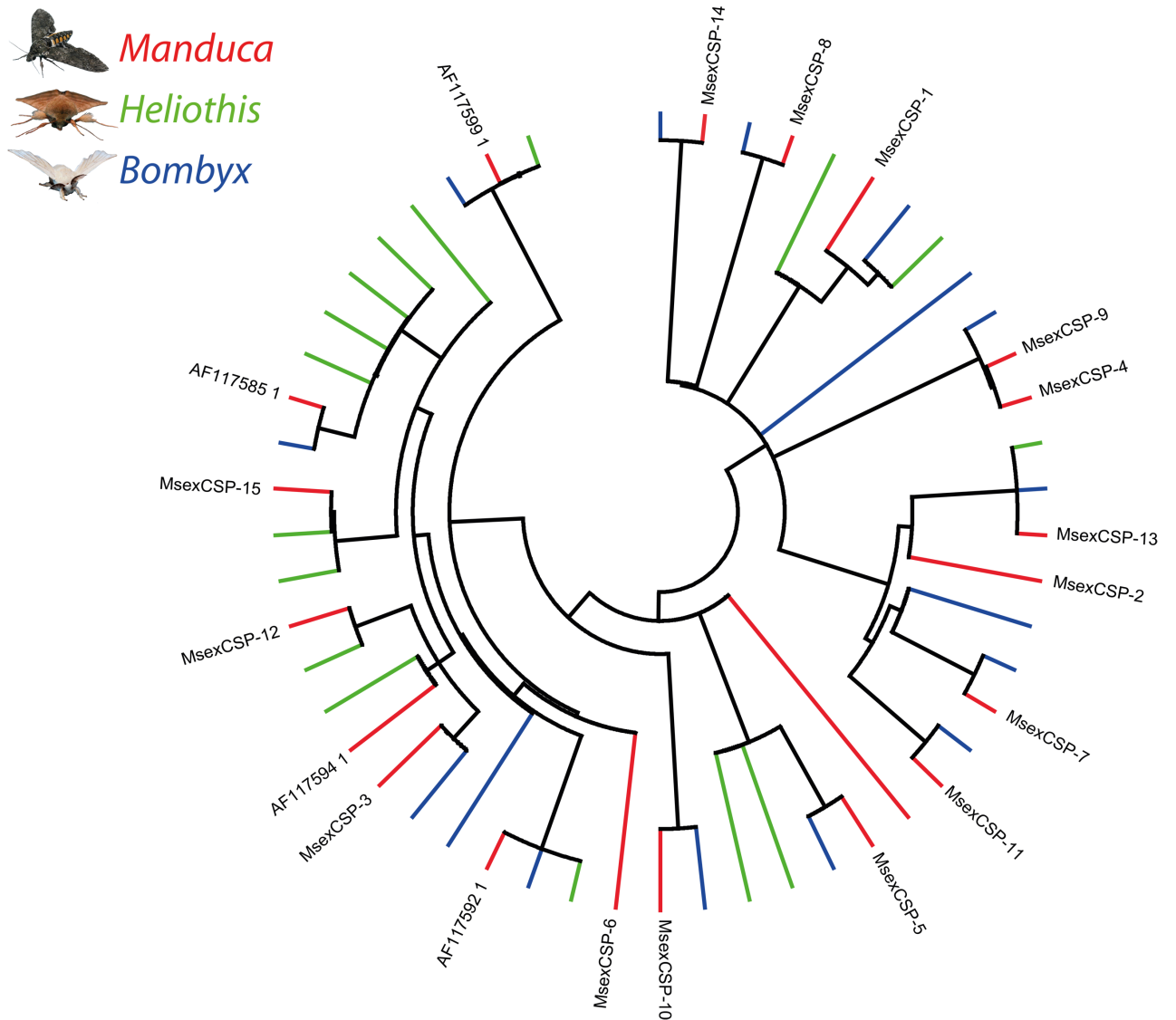


Figure S2: Lepidopteran CSPs and new *Manduca* CSP candidate transcripts, dendrogram calculated and colored as described in Figure 1. The number of predicted CSPs *Manduca* (red) is comparable to *Bombyx* (blue) and *Heliothis* (green). *Manduca* CSPs have been indicated by name or accession number.

Manduca
Drosophila
Bombyx

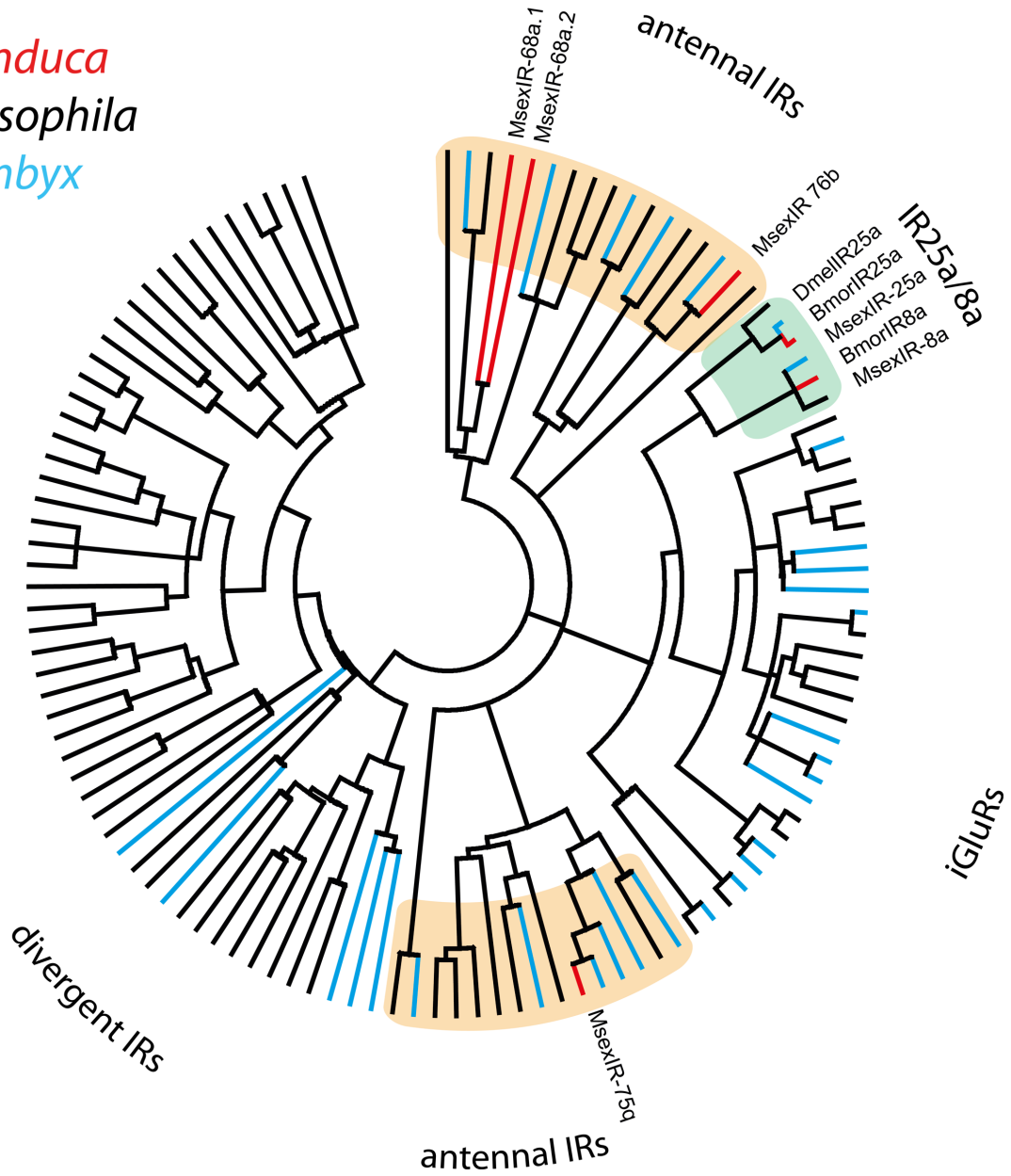


Figure S3: Similarity of *Manduca* IR candidates (red) to IRs/iGluRs of *Drosophila* (black) and *Bombyx* (blue). Depicted is a maximum likelihood dendrogram, calculated based on the alignment of predicted amino acid sequences. Colored boxes indicate the antennal IR (orange) and IR25a/8a subgroups (green).

The antennal transcriptome of *Manduca sexta*

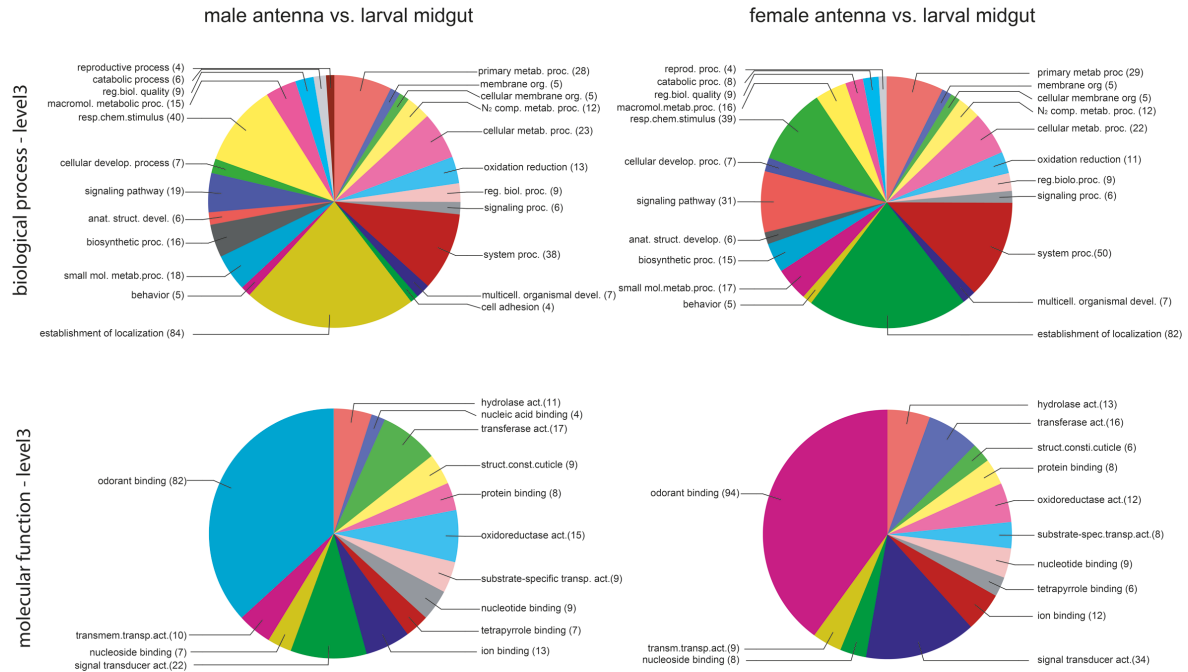


Figure S4: Comparison of male and female gene representation with the larval midgut, using microarray data and GO categorization for biological processes (top) and molecular function (below; both level 3). Depicted are transcripts with presence calls in each respective antennal tissue (male left, female right), but no presence calls in the larval midgut. Total number of gene objects presented in brackets.

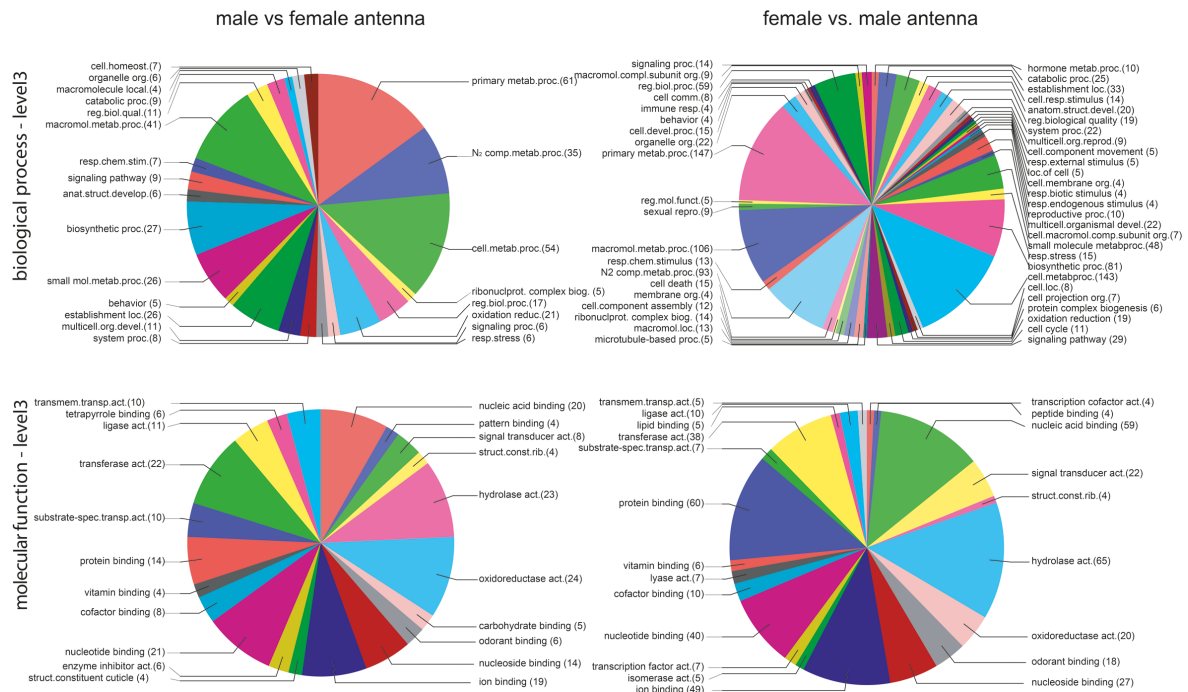


Figure S5: Comparison of male and female gene expression using GO categorization for biological processes (top) and molecular function (below) (both level 3) based on microarray presence calls. Total number of gene objects presented in brackets. The total number of categories for biological processes is higher in the female antenna, as is the total number of gene objects.

The following supplemental Data is supplied at <http://www.pnas.org/>

Figure S6: Reconstruction of the male antennal lobe. The data is presented as 3D data. Glomeruli are presented as schematics, with colors indicating groupings used as basis for nomenclature.

Figure S7: Reconstruction of the female antennal lobe. The data is presented as 3D data. Glomeruli are presented as schematics, with colors indicating groupings used as basis for nomenclature.

Movie S1: Reconstruction of the male antennal lobe. The data is presented as movie file, following the Z-axis. Glomeruli are presented as schematics, with colors indicating groupings used as basis for nomenclature.

Movie S2: Reconstruction of the female antennal lobe. The data is presented as movie file, following the Z-axis. Glomeruli are presented as schematics, with colors indicating groupings used as basis for nomenclature.

Table S1 Olfactory genes identified in this study, FASTA formatted file. Sequences have been named according to existing nomenclature or closest homologue where possible.

Dataset S1-4 Files in fasta format containing the sequences used for the generation of Figures 2 (Dataset 1), S1-S3 (Dataset 2-4).

CHAPTER II

A novel multicomponent stimulus device for use in olfactory experiments

Shannon B. Olsson^{*}, Linda S. Kuebler^{*}, Daniel Veit, Kathrin Steck, Alexandra Schmidt, Markus Knaden
& Bill S. Hansson

^{*}These authors contributed equally to this work

Abstract

Olfactory studies have expanded beyond the study of single compound odor perception to explore the processing of complex mixtures and blends. The spatiotemporal presentation of blend stimuli is a challenging task requiring volatiles with diverse chemical and physical properties to be presented as a unified stimulus. This not only necessitates accurate control of the timing and homogeneity of the odor stream, but requires attention to the concentration of each blend component presented. We have developed a novel, multicomponent stimulus system for use in olfactory experiments that is capable of presenting up to 8 different odors simultaneously or in sequence at defined concentrations and time scales. Each odor is separated to minimize physical or chemical interactions, and stimulations are performed from a saturated headspace of the odor solution. Stimulus concentrations can be measured empirically or estimated using common gas laws. Photoionization detector measurements show that stimuli could be presented as cohesive blends or single components at frequencies of at least 10 Hz without leakage or contamination. Solid phase microextraction measurements also show that the concentration of each component could be equilibrated through regulation of each component line's flow rate based on the different partial vapor pressures of the odorants. This device provides a unique method for introducing complex volatile mixtures for olfactory studies in a variety of animal taxa and allows for accurate control of odor intensities in both time and space.

Keywords: olfaction; stimulation; physiology; behavior; blend; mixture

Abbreviations: PID: photoionization detector, SPME: solid-phase microextraction, PEEK: polyether ether ketone

Introduction

The world is a cacophony of scent. At any moment, our olfactory system is bombarded with hundreds of volatile compounds emanating from every flower, tree, or cup of coffee. What we perceive as a single scent is often several compounds acting in concert to form an odor blend. Despite this fact, most olfactory studies have focused on the perception of single compounds, both for the simplicity of the stimulus and to establish a basic understanding of olfactory processing. Thus, relatively little is known about how odor mixtures are processed to generate a cohesive signal (Lei and Vickers, 2008).

One of the major obstacles encountered in olfactory studies is accurate stimulus presentation. Several olfactometers have been designed to optimize various aspects of odor presentation including increased variety of odors, controlled concentrations, or precise stimulus timing (Vetter et al., 2006). In particular, blend components must be presented concurrently on both temporal and spatial scales. This presents significant challenges. First, natural odorants can possess considerably different chemical and physical properties (see Dunkel et al., 2009 for a database of flavors and scents, “Superscent”). At best, a mixture of ecologically relevant odors will contain chemicals with different vapor pressures and solvent interactions (see Table 1 for an example of the vapor pressure diversity for odors used in this study). In many olfactory experiments, it is common to use an odor cartridge containing an aliquot of liquid odorant placed on an adsorbant surface, such as filter paper. Although the dose of odorant applied is controlled, release rates depend on several factors such as vapor pressure, chemical affinity to the substrate used, solvent, temperature, airflow, and time (Girling and Cardé, 2007). Consequently, odor concentrations must be empirically calculated for each new stimulus using techniques such as stimulus headspace collection and gas chromatography (e.g.; Brockerhoff and Grant, 1999; Koch et al., 2002). It then becomes a rather arduous task to calibrate concentrations for each blend component.

In the worst case, blend components can chemically or physically interact with each other. In the quest to determine the physiological activity of DEET, (Syed and Leal, 2008) discovered that DEET “masks” or inhibits the volatility of odors when they are placed together with DEET in conventional odor cartridges. Syed and Leal instead presented DEET in separate cartridges to the insects. This example emphasizes that improper blend presentation can make it difficult or even impossible to predict the presence, concentration or distribution of components in the headspace of a mixture.

Table 1: Calculated flow rates used for electrophysiological analyses

Blend Component	CAS	Vapor Pressure (mm Hg at 20 or 25°C)	Mole Fraction in air (using equations 1-3)	Flow rate (L/min)
Phenyl acetaldehyde	122-78-1	0.392 ^a	2.78×10^{-8}	0.37 ^c
(+) and (-) Linalool	78-70-6	0.16 ^a	2.16×10^{-8}	0.56
Nonanal	124-19-6	0.37 ^a	2.65×10^{-8}	0.46
(E)-2- and (Z)-3- hexenyl acetate	2497-18-9/ 3681-71-8	1.14 ^a	3.72×10^{-8}	0.32
Hexanol	25917-35-5	0.809 ^a	5.14×10^{-8}	0.24
Benzaldehyde	100-52-7	1.27 ^a	6.02×10^{-8}	0.20 ^d
Mineral Oil	8012-95-1	<.005 ^b	not measured	0.60 ^e
TOTAL FLOW				2.07 ^c

a. SRC PhysProp Database (<http://www.syrres.com/esc/physdemo.htm>)

b. 0.005 mm Hg used as a high estimate for dilutions. Material Safety Data Sheets for Mineral Oil (1. Ameri-Pac, Inc., 751 S. 4th Street, St. Joseph, MO 2. Petroleum Specialties Group, Petrolia, PA 3. Veltek Associates, Inc. 15 Lee Blvd. Malvern, PA)

c. value was set at 0.43 L/min during physiological experiments, raising total flow slightly

d. the most volatile component, set to the lowest adjustable flow rate value

e. set above the highest flow rate to control for any mechanical responses to flow.

We present a multicomponent olfactory stimulator capable of presenting up to 8 different odors simultaneously or in sequence at defined concentrations and time scales. Blend components are stored separately to minimize physical or chemical interactions. Additionally, the use of odor vials closed with check valves allows for stimulation from a saturated headspace of the odor solution, without the use of an adsorbant surface. Photoionization detector (PID) and solid-phase microextraction (SPME) measurements show that this not only reduces leakage and contamination, but allows for fairly accurate control of stimulus concentration. Stimulus concentrations can be measured empirically, or estimated using common gas laws. Finally, odor components can be presented concurrently as a single blend stimulus by passing through a blend chamber that combines the separate headspace aliquots into a single, unified odor stream.

Materials & Methods

2.1 System Overview

This multicomponent olfactory stimulation system was intended for general physiological and behavioral assays that require small, distinct quantities of odor stimuli. It can accommodate up to 8 odors, but additional components could be added to increase the number of odorants and potential combinations. Odorants can be presented in any combination, either simultaneously or in sequence. Each odor component has a dedicated line that is isolated from other system elements before a final central line that presents the blended stimuli to the behaving animal or physiological preparation.

The system consists of three major parts, illustrated schematically in Figure 1: an airflow regulator (Figure 1, A), an odorant delivery system (B), and a final blending and output chamber (C). Compressed air is first separated through a sensor board consisting of a series of 8 flowmeters (one for each odor component). Each line is regulated individually and passed through an odorant delivery system containing a three-way valve and two chambers with check valves for each line. Under normal flow conditions, airflow passes through a distilled water chamber to establish a constant, humidified airstream necessary for many behavioral and physiological preparations. Upon stimulation, the valves transfer the regulated airstream through the odor chamber. The airstream from each chamber (either humidified or odorized) finally passes through a blending and output chamber that combines the 8 lines into a single, unified laminar flow that proceeds to the animal or preparation. Check valves on each side of the chambers prevent leakage or contamination in the absence of airflow. In this manner, combinations of the eight lines can be presented in unison or sequence at any time point. Additionally, because the three-way valves switch between humidified or odorized airstreams that are equivalent in all other respects, total airflow always remains the same, regardless of the nature or length of stimulation.

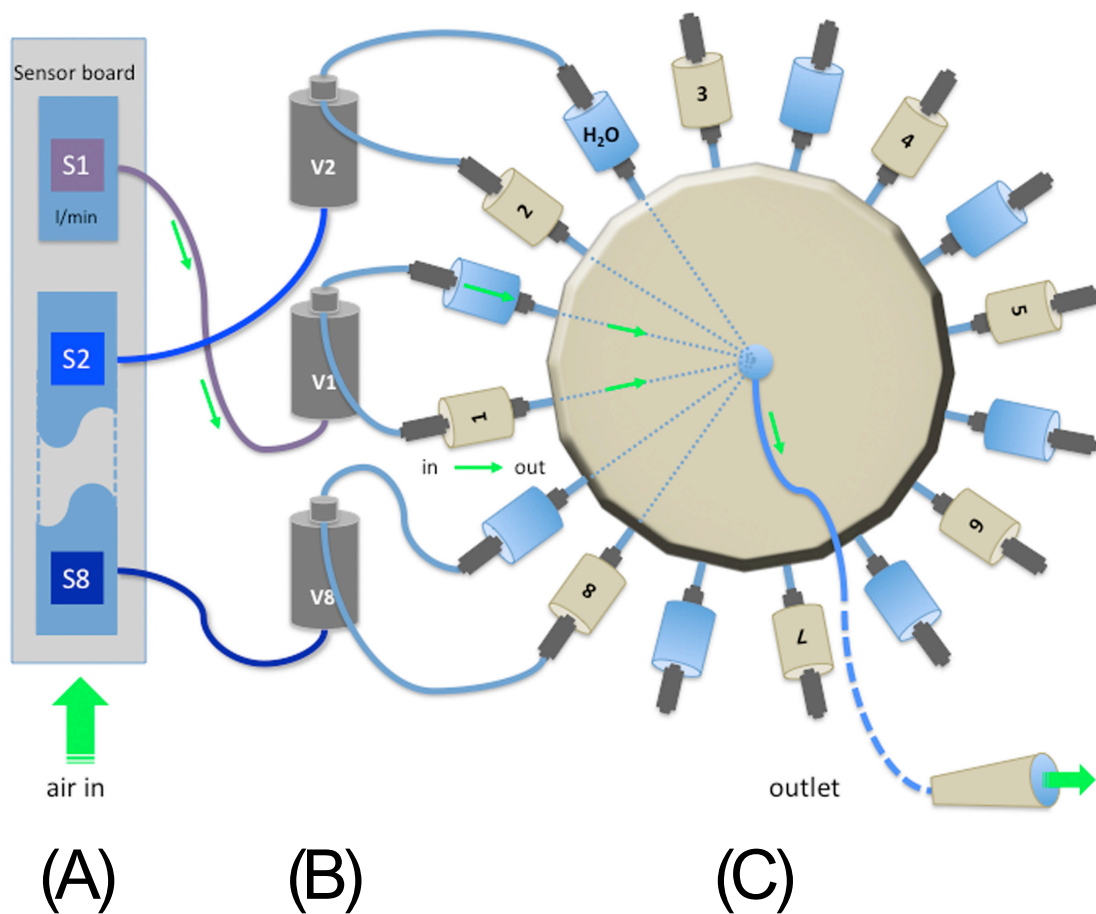


Figure 1: Overview of the multicomponent stimulus system. 8 separate regulated airstreams (A) adjusted for component vapor pressures pass through solenoid valves and odor/humidifying chambers (B) before presentation as a single, unified airstream by the blending chamber (C).

All components were constructed from Teflon (tubing), steel (stainless or nickel-plated; valves, flowmeters and connectors) or polyether ether ketone (PEEK; blending and odorant chambers). These materials were chosen to inhibit contamination of the system or airstream by component parts or chemical residue. In particular, PEEK was chosen for its overall strength and chemical resistance to both organic and aqueous solvents (Parker et al., 2002). It also exhibits thermal resistance to temperatures reaching 300°C, which allows for heated cleaning of the system to remove odorant or solvent residuals. Finally, routine placement of the odorant delivery system within a Faraday cage did not lead to significant noise during electrophysiological recordings.

2.2 Carrier Gas and Airflow Regulation

A constant, charcoal-filtered air stream (filter: AMF150C-F02SMC, SMC Pneumatik, Reutlingen, Germany) was supplied from compressed house air (8 bar) and regulated to a pressure of 2 bar. The pressurized air stream was split via teflon tubing (4 mm O.D. 1 mm I.D.; Ammerflon, Diessen a. Ammersee, Germany) and stainless steel connectors (Jenpneumatik, Jena, Germany) into 8 lines connected to a sensor board (Figure 1 A). The sensor board contained 8 digital flowmeters (PFM7, SMC Pneumatik) used to measure airflow for each line. Separate choke valves (M3M5ES24V, Jenpneumatik) regulated the airstream according to the vapor pressure of the odorant connected downstream of that line (see 2.4 for details). Input airflow temperature was at ambient conditions. Teflon tubing connected each flow meter to the solenoid valves and odor chambers (Figure 1 B).

2.3 Odorant Delivery

The constant airstream from each of the 8 separate lines passed through a three-way solenoid valve (3/2 way, M3M5ES24V, Jenpneumatik) before proceeding to the odor or humidifying chambers (Figure 1 B). Each solenoid valve had two positions. In the normal closed position, air passed through a PEEK vial (Supplementary Figure 1; custom made by MPI's scientific workshop, PEEK: Arthur Krüger, Barsbüttel, Germany) containing distilled water, whereas in the open position, air flowed through an equivalent PEEK vial containing an equal amount of odor, either pure or dissolved in a solvent such as mineral oil (see 2.6.2 for experimental parameters). In this fashion, total airflow from the system always remained the same.

Water or odorants were placed in equal amounts at the bottom of each vial. Each chamber was equipped with a stainless steel plug sealed with a rubber O ring to allow for cleaning and refilling (3/8" external thread, key size 19, VS38AES Jenpneumatik). The inlet and outlet were placed at the top of each vial (Supplementary Figure 1). Thus, any airflow passing through the vials removed only the headspace of the chamber, and did not contact the liquid itself. Each chamber was also equipped with corresponding ball-stop check valves at both inlets and outlets (4 mm , HAIQS M54 and HBIQSM54, Jenpneumatik; or 1.3 mm, mp-cv, Bartels Microtechnik, Dortmund, Germany). The smaller check valves were used for higher frequency experiments. The valves served two purposes. First, they prevented either forward or back pressure from inducing flow through the chambers in the absence of stimulation, and precluded leakage or contamination of odorant into the system. Second, under no-flow conditions they essentially established a closed system within each chamber. This allowed the chamber environment to reach equilibrium and establish the saturated vapor pressure conditions necessary for calibration of odorant concentrations (see 2.4).

Solenoid valves were activated by a TTL pulse (I/O interface, PMD 1208LS, Meilhaus, Puchheim, Germany) transformed via an optocoupler (ILQ55, Conrad, Electronic, Hirschau, Germany) to 24V DC. The TTL Pulse could also be recorded by analogous inputs to a computer, such as via PCI card (see 2.6.1) in order to track stimulus identity and onset. Stimulation was controlled with custom written software using Labview 8. 5 (National Instruments, Austin, TX).

Once the regulated airflow passed through either odor or humidifying chambers, it proceeded through a concentric PEEK blending chamber, which combined all 8 lines into a single unified airstream (Supplementary Figure 2). Each of the 16 odor or humidifying bottles were connected to the blend chamber via stainless steel push-in system connectors and nickel-plated steel screw connectors (2.5 mm diameter I. D., IQSGM54I push-in, M5 screw, Jenpneumatik). A 1 cm steel insert (2.5 mm I. D.) was placed at the inlet of each line to prevent stripping of the PEEK during repeated removal of the screw connectors for cleaning. Inside the blending chamber, the sixteen channels (2.5 mm diameter) fed to a central line (4.2 mm diameter) that then exited the blending chamber via a nickel-plated steel connector (2.5 mm M5, Jenpneumatik). Teflon tubing (4 mm O. D., 1mm I. D., Ammerflon) was then used to connect the airflow to the animal or preparation (see 2.6.2).

2.4 Vapor Pressure Calibration

As noted in 2.3, odor stimulation was accomplished by passing the airflow through the odor chamber headspace for a predetermined length of time. By establishing an essentially closed system within the odor chambers using check valves, the undisturbed headspace odor would reach equilibrium with the liquid odor at the chamber floor. Consequently, odor concentration could be roughly determined for each stimulation by calculating partial pressures of the odor vapor in the headspace.

Two general methods allow determination of partial pressures. In the first, and most straightforward method, one can utilize Raoult's Law (1):

$$P_A = P_A^* \times x_{A,liquid} \quad (1)$$

where P_A is the individual vapor pressure of odor component A (i. e. solute), P_A^* is the vapor pressure of pure A, and $x_{A,liquid}$ is the mole fraction of A in solution. A similar calculation can be performed to determine the vapor pressure of the solvent B (P_B).

Dalton's Law of partial pressures (2) then states that:

$$P_{tot} = P_A + P_B \quad (2)$$

where P_{tot} is the total pressure of the binary odor solution at equilibrium.

To determine the mole fraction of odor A in the headspace, $x_{A,air}$, one must calculate the mole fraction of the total solution in air using P_{tot} divided by the air pressure, P_{air} :

$$x_{A,air} = (P_{tot}/P_{air}) \times x_{A,liquid} \quad (3)$$

By using equations 1, 2 and 3, the mole fractions of all blend components in the headspace can be determined. In order to equilibrate the total moles (i.e. concentration) of each component in the blend stimulation, the flow rates from that odor line can be adjusted on the sensor board (Figure 1 A) according to each odor's mole fraction so the concentration of all components is the same. To reduce the total flow rate of the system, the individual line flows should be set according to the *most* volatile component. See 2.6.2 for a sample of such calculations. A workbook performing the calculations used for the odorants in Table 1 is also included as supplementary data ("Odorant Vapor Pressure Calculations.xls").

Equation (1) assumes that odor A in solvent B is an ideal solution, without any interaction between odor and solvent molecules (which is rarely true). For real dilute solutions used in many olfactory experiments, Henry's Law is applicable (Cometto-Muniz et al., 2003):

$$P_A = H_A \times x_{A,liquid} \quad (4)$$

where H_A is Henry's Law constant in pressure/concentration units. This equation can then be used with (2) and (3) to determine component mole fractions. Although Dalton's Law (2) applies to gases under ideal conditions as well, it is generally considered suitable for real gases in most cases. This second method is more appropriate for real solutions used as stimuli, but see also (Cometto-Muniz et al., 2003) for other experimentally derived calculations of odor pressures.

2.5 Stimulus Measurements

Stimulus timing and blending were assessed using odor chambers filled with 250 μ l or 750 μ l pure ethanol as a tracer odor and photoionization detection (miniPID Fast Response Miniature Photoionization Detector, Model 200A, Aurora Scientific Inc.). During measurements, the PID sensor was placed at the outlet of the stimulator. For blend and frequency comparisons, PID outputs were presented and compared using raw values.

For calibration analyses, 50 μ l of isoamyl acetate and 2-heptanone were placed in microcentrifuge tubes within two separate odor chambers and allowed to equilibrate for at least 2 minutes between stimulations. A holder containing a solid-phase microextraction fiber [100 μ m PDMS, Supelco (Sigma-Aldrich, Munich, Germany)] was placed 2 cm in front of the device outlet. Approximately 2

seconds before stimulation, the fiber was extruded from the holder. A 500 ms pulse containing a blend of the two components either calibrated for vapor pressure (see 2.4; Supplementary Table 2) or uncalibrated at the same flow rate was then presented to the fiber. Approximately 1-2 seconds after stimulation, the holder was removed and the fiber inserted into the inlet of an Agilent Technologies 7890N/5975C GC-MS system in splitless mode (1 min sampling time). A 0.75-mm i.d. glass inlet liner [Supelco (Sigma-Aldrich)] was used for SPME analysis and the system equipped with an HP5ms ui column (30 m × 250 μm × 0.25 μm) with helium (0.5 ml/min constant flow) as carrier gas. Samples were heated to 40°C for 3 min. The temperature was then increased at a rate of 5°/min to 120°C and 50°/min to 250° for 10 min. The TIC (MS EI 70 eV in scan mode) revealed two peaks that were confirmed as the two blend components using the NIST 2005 library and comparison with authentic reference compounds. A separate calibration of the SPME fiber using known quantities of headspace (data not shown) was performed to ensure reasonably equivalent SPME adsorption of the two blend components.

2.6 Operational Examples

2.6.1 Intracellular Preparation and Recording

Female *Manduca sexta* moths were confined in modified Falcon tubes (15ml) and a small window was cut between the antennae to expose the primary olfactory processing centers of the brain (the antennal lobes). A sharp glass recording electrode was inserted into the antennal lobe using a motorized micromanipulator (Luigs & Neumann, Ratingen, Germany). Once intracellular contact with a single antennal lobe neuron was established, the ipsilateral antenna was stimulated and physiological activity recorded. The analog signal of the impaled neuron was amplified, filtered (Bramp 0,1, bridge amplifier NPI Electronic GmbH Tamm, Germany), optimized via an interface (INT-20MX Breakout Box Module, NPI Electronic) and monitored on an oscilloscope (TDS 2000B, Tektronics Inc., Beaverton, OR, USA). The resultant analog signal (mV) was then digitized via a PCI card (6250E, National Instruments, Austin, TX, USA), sampled (50 kHz), and recorded (3 kHz) using customized Labview software (National Instruments, Austin, TX). Action potentials were extracted as digital spikes using Igor Pro software (Wavemetrics, Portland, OR).

2.6.2 Electrophysiological Stimulus Preparation and Odor Stimulation

The following odors were used for electrophysiology (Sigma Aldrich, highest purity available): (+) linalool, (-) linalool, phenyl acetataldehyde, benzaldehyde, hexanol, nonanal or trans-2-hexenyl acetate (used instead of nonanal in some experiments), and cis-3-hexenyl acetate. Each odor was

dissolved at 10^{-4} in mineral oil and 250 μl placed in the bottom of odor chambers. A corresponding amount of distilled water was placed into the alternate humidifying chambers (see 2.3).

Flow rates were calculated from literature-based vapor pressures according to Boyle's Law and a 10^{-3} dilution as a relative estimate of component concentrations for stimulation (Table 1, "Odorant Vapor Pressure Calculations.xls"). Flow rates were set according to benzaldehyde, the component with the highest vapor pressure. This ensured that the overall flow rate was as low as possible. The resultant humidified airflow passed through the central line and ended in a Peek nozzle (diameter 7 mm) positioned 1 cm in front of the insect's antenna. The TTL signal activating each solenoid valve was recorded (sample size 30 kHz) by analogous inputs from the PCI card in order to track stimulus identity and onset. Stimulation was controlled with custom written software using Labview (see 2.3), which also triggered the spike-recording program via a direct network connection (crossover TCP/IP). Thus, stimulus onset and physiological response could be recorded concurrently.

2.6.3 Behavioral Assays

The multicomponent stimulus system was also integrated into a novel behavioral assay (to be detailed elsewhere) in which odor-evoked behavior could be studied in detail using a high-throughput experiment that automatically tracks 16 individual insects. Individual *Drosophila melanogaster* fruit flies were placed in glass tubes (diameter, 1cm; length, 15 cm; Supplementary Figure 3) and exposed to continuous airflow of 35cm/s. Undiluted chemicals were placed in 5 μl aliquots in the bottom of each odor chamber. Stimuli were presented in 500 ms increments to simulate the odor filaments of a turbulent plume. The up-and downwind movement of each individual fly was recorded using a visual tracking system. The tracking system was electrically connected to the multicomponent olfactory stimulation system to dictate recording times. This combination enabled the calculation of stimulus exposure times for each individual fly. The result for each fly was presented as a pre- and a post-odor period.

Results

3.1 Spatial and Temporal Stimulus Delivery

The performance of the multicomponent stimulus device was tested using pure, undiluted ethanol placed at the bottom of 7 odor chambers. A final empty odor chamber was opened along with other stimulus chambers and its TTL pulse recorded in conjunction with PID output to dictate stimulus timing. Figure 2 shows the results of 2-7 ethanol-filled lines opened simultaneously to deliver various stimulus "blends". The figure illustrates that a uniform mixture was delivered regardless of the number of odor chambers used. Pulses increased in height ($R_{\text{sq}}=0.93$), but not width ($R_{\text{sq}}=0.18$), as

more stimuli were presented. The slight biphasic PID peaks shown in the figure were likely because flow rates of the 7 valves differed (Table 1) although only one chemical (ethanol) was presented. This shows that multicomponent stimuli could be presented in the same time frame as single odors, retaining spatiotemporal integrity of both blends and single components equally.

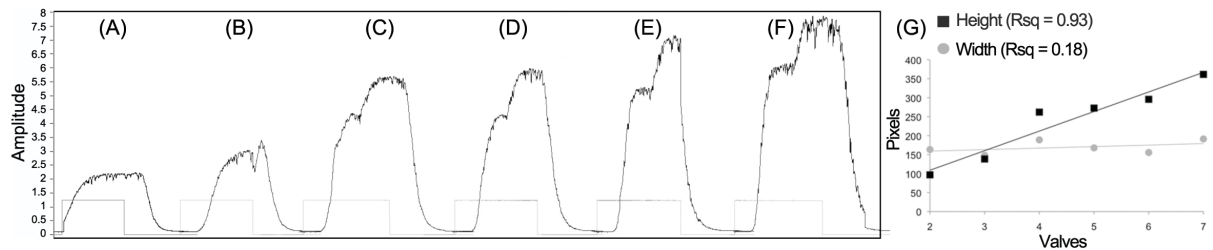


Figure 2: PID measurement of odor mixtures as presented by the multicomponent device. Ethanol was placed into each of 7 odor chambers with line flow rates as listed in Table 1 and the headspace after a 500 ms stimulation measured. Each peak shows a different number of components or valves employed: (A) 2, (B) 3, (C) 4, (D) 5, (E) 6, and (F) 7 valves opened. (G) Peak heights and widths in pixels including the Rsq for each dimension.

Temporal stimulus integrity could also be retained with high frequency stimulation. Figure 3 shows the result of single odor stimulations at 5 to 15 Hz. Each odor pulse was clearly separated from the next, even with 50 ms pulses (Figure 3 D). At 15 Hz, (Figure 3 E) some peak overlap occurred. Furthermore, individual pulses presented by the multicomponent stimulator showed a clear square pulse of odor with little bleed or contamination as compared to a commercial stimulation device (Syntech CS 55, Kirschzarten, Germany; Figure 3 F inset). The figure also shows that initial high frequency peaks (B-E) may be reduced due to mechanical delays in valve operation.

The consistency and delineation of repeated stimulations was also tested on a *Manduca sexta* antennal lobe neuron (Figure 3 G). Intermittent 1 Hz stimulations showed highly consistent and clearly separated responses ($n = 7$, 10.3 ± 0.6 Hz, s.e.m.) suggesting that repeated stimulations retained spatiotemporal integrity.

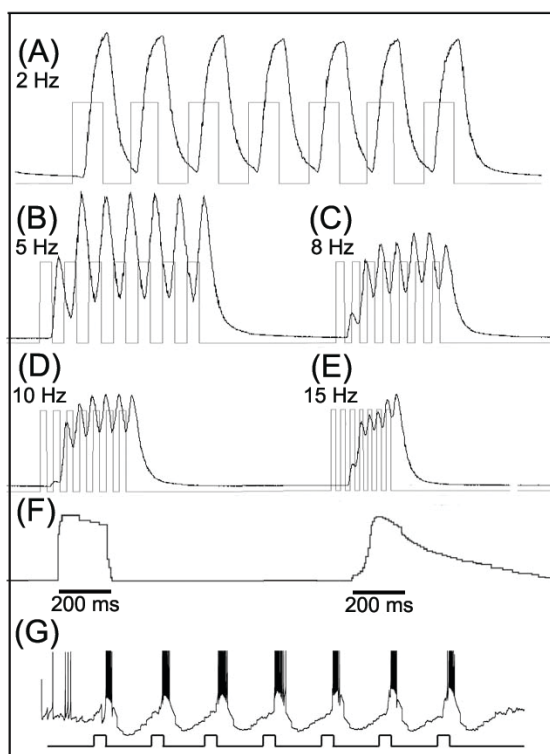


Figure 3: PID measurement of odor pulses at various frequencies (A) 2 Hz; (B) 5 Hz; (C) 8 Hz; (D) 10 Hz; and (E) 15 Hz. (F) compares a 200ms pulse of odor between the multicomponent device and another commercially available stimulator (CS-55 Stimulus Controller, Syntech, Kirchzarten, Germany). Finally, the consistency of the system was tested on a *Manduca* antennal lobe neuron at 1 Hz (G; n=7; 10.3 +/- 0.6 Hz, s.e.m.).

3.2 Stimulus Concentration Control

The concentration of stimuli delivered by the stimulus device could be controlled in three ways. First, odors could be diluted in varying amounts of solvent and the total concentration present in the odor chamber headspace calculated by Raoult's or Henry's Law (see 2.4). Stimuli could also be delivered over longer periods of time, thus releasing more total odorant. Finally,

concentrations could be equilibrated across the 8 odor chambers by controlling for the different vapor pressures of each odor (see 2.4). Flow rates of each line were set according to the vapor pressure of each odorant in that line (Table 1). In this way, stimulus pulses from each odor chamber would release an equivalent concentration of odorant as calculated using 2.4 Equations 1-3.

Altering the flow rate of an individual odorant (ethanol; Figure 4) linearly increased the concentration of odor in a stimulus pulse as measured by PID (Rs_q based on peak areas or height = 0.92).

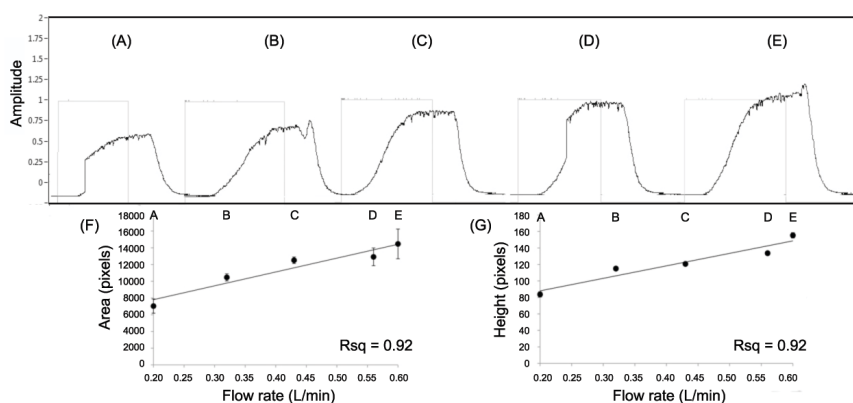


Figure 4: PID measurement of odor pulses from different odor chambers and flow rates (A) 0.20; (B) 0.32; (C) 0.43; (D) 0.56; and (E) 0.60 L/min. (F) and (G) graph mean PID peak areas and heights in pixels with error bars for three replications at each flow rate. A trendline notes the relative linearity of the points as shown by the Rs_q in the corner of each graph.

Thus, flow rate could accurately be used to equilibrate concentrations of various odors using each odor's partial vapor pressure. To illustrate this, two pure odorants, isoamyl acetate and 2-heptanone (saturated vapor pressures of 5.6 and 3.86 mm Hg respectively; SRC PhysProp Database) were placed in separate odor chambers. Equations 1-3 were used to calculate the flow rates needed to release similar concentrations of each pure, undiluted odorant from its saturated headspace at four different values (calculated flow rates listed in Supplementary Table 2). Figure 5 (A) and (B) show that calibration greatly improved equilibration of the two concentrations. When presented at similar flow rates (1), 2-heptanone was released at an average of 50.9% less than isoamyl acetate, the more volatile component. Yet, when equilibrated according to their vapor pressures using the gas law equations (Supplementary Table 2), the two compounds were released at roughly equivalent concentrations (2; 1.2% average difference). Nevertheless, higher flow rates [Figure 5 (C)] increasingly reduced the similarity of the two concentrations, with at 53.2% average difference between the two components at the highest flow rate (0.5 L/min).

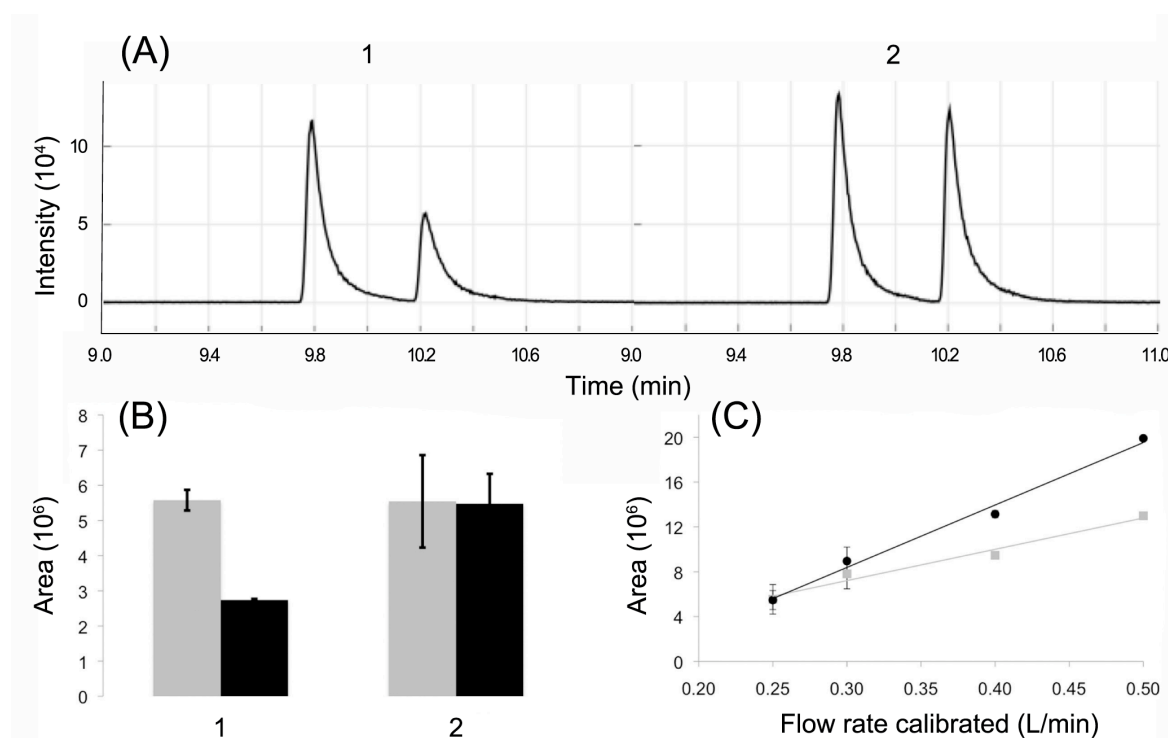


Figure 5: SPME measurement of a single pulse containing a blend of 2 pure components [isoamyl acetate (gray) and 2-heptanone (black)]. (A) sample chromatograms and (B) mean chromatogram peak areas for 1. uncalibrated (n=3) and 2. calibrated (n=4) components at 0.25 L/min (relative to isoamyl acetate) (C) mean chromatogram peak areas for calibrated components presented at four flow rates (n=3-4 for each rate relative to isoamyl acetate; Supplementary Table 1)

3.3 Operational Examples

3.3.1 Intracellular Electrophysiology

The multicomponent stimulus device was used to present single and multicomponent stimuli while recording from single neurons in the *Manduca sexta* antennal lobe. An example of three such recordings are shown in Figure 6.

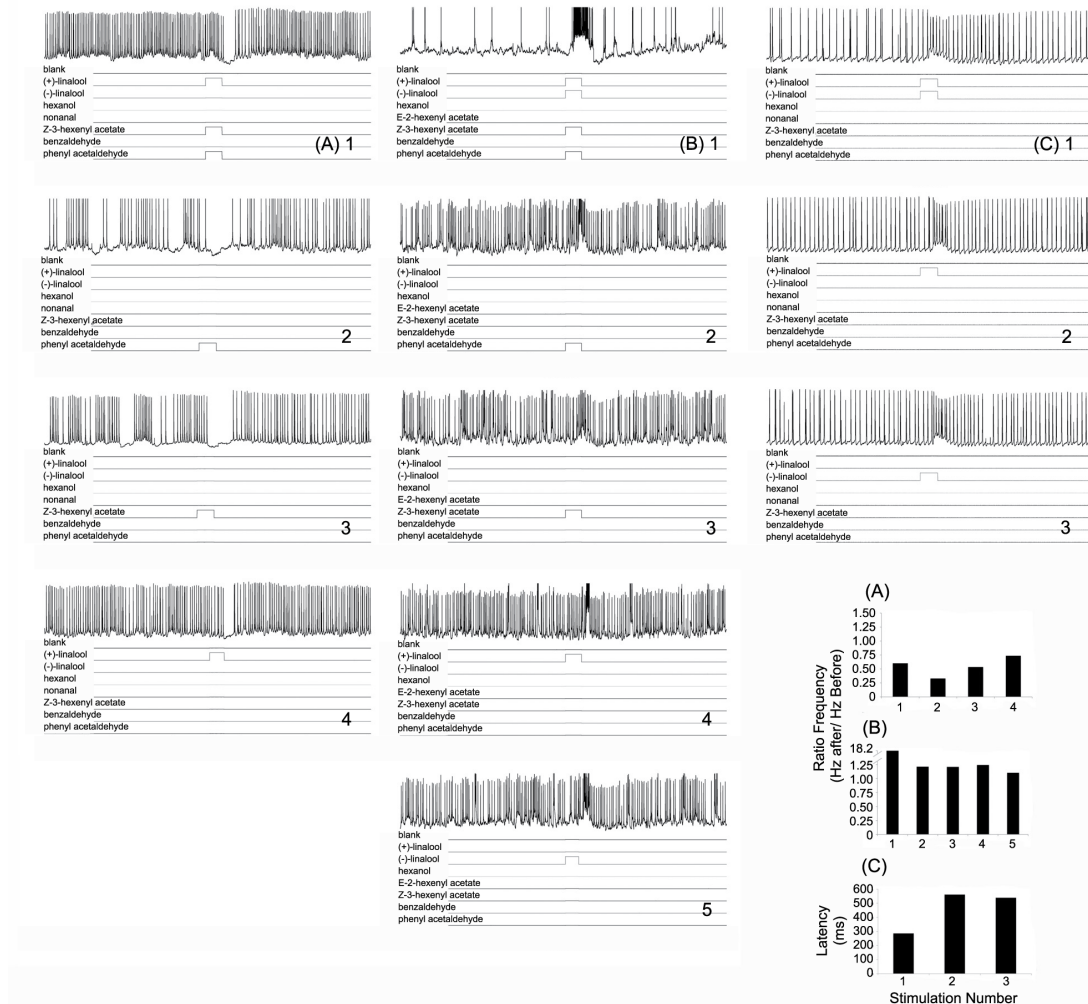


Figure 6: *Manduca sexta* antennal lobe neurons stimulated with the multicomponent stimulus device. Cell (A) exhibits an inhibitory response to calibrated stimuli, while Cells (B) and (C) exhibit an excitatory response. Traces 1-5 for each cell represent different stimuli: For Cell (A) 1. Blend of equal concentrations of (+)-Linalool, (Z)-3-hexenyl acetate and phenyl acetaldehyde, 2. phenyl acetaldehyde alone, 3. (Z)-3-hexenyl acetate, 4. (+)-Linalool. For Cell (B) 1. Blend of equal concentrations of (+) and (-)-Linalool, (Z)-3-hexenyl acetate and phenyl acetaldehyde, 2. phenyl acetaldehyde alone, 3. (Z)-3-hexenyl acetate, 4. (+)-Linalool and 5. (-)-Linalool. For Cell (C) 1. Blend of (+)- and (-)-Linalool, 2. (+)-Linalool alone, and 3. (-)-Linalool alone. The graphs at the bottom right depict frequency ratios (Hz after stimulation/ Hz before stimulation) for 1.5 seconds following stimulation in traces shown in (A) and (B), or latency to response maximum [ms; (C)].

Cell A exhibited an inhibitory response (a drop in spike frequency) to a 3-component blend and each of its components, while Cell B displayed an excitatory response to a 4-component blend. In each cell, the response to the blend (trace 1 in all cases) produced a non-linear response from that expected by the blend components. In cell A, the blend elicited a suppressive response (decreased inhibition) when compared to blend components, particularly compared to components 2 and 3. Cell

B exhibited a highly synergistic response to the blend (increased excitation) when compared to the single components. Additionally, Cell C displayed an excitatory response to a blend of two components that occurred nearly twice as fast (i.e. latency from stimulus onset to maximum response) than the response to the components themselves. The ability to detect various blend interactions among the separate cells further illustrates the accurate blending capability of the multicomponent device. Note that the blend responses exhibit a single, uniform signal, but display clear differences in magnitude (frequency or latency) as compared to the single components. These non-linear responses would only be apparent if the components were blended accurately into a cohesive stimulus.

3.3.2 Behavioral Assays

We have established a behavioral assay that automatically tracks individual flies exposed to a current laminar airflow carrying olfactory stimuli produced by the multicomponent stimulus device (Figure 7). The accurate on- and offset of the valves did not generate any change in airflow, and allowed a solely chemical stimulation of the animals without producing a mechanical stimulus. However, when a 500 ms pulse of balsamic vinegar (a blend known to be highly attractive to the flies) was added to the constant flow, the majority of flies moved upwind toward the odor source, while the flies did not respond to an empty control (i.e. the switching of valves in the absence of any odors).

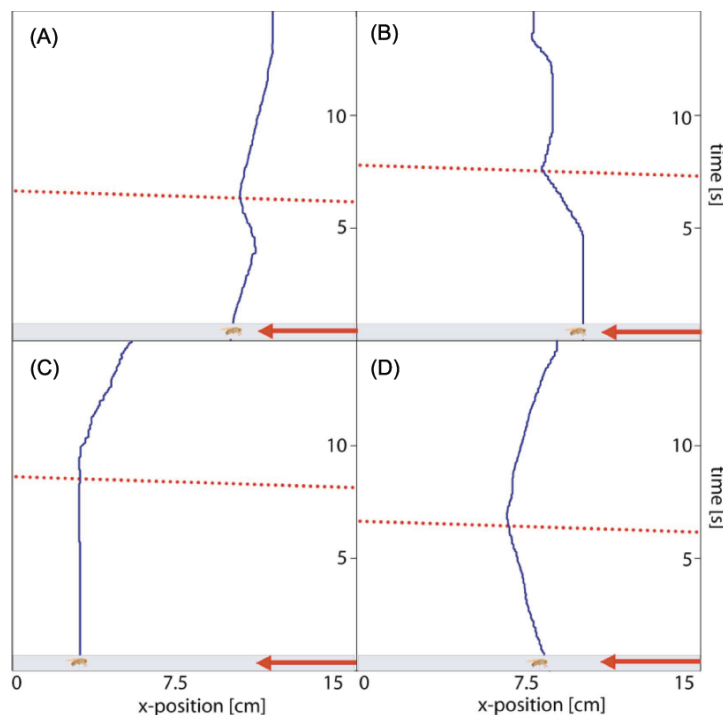


Figure 7: Behavioral paradigm. Individual flies in glass tubes (grey bar; diameter, 1cm; length, 15 cm) were exposed to continuous airflow of 35cm/s (red arrow depicts wind direction) and were tracked for 15 s. A defined olfactory stimulus (headspace of balsamic vinegar; stimulus duration, 500 ms) entered the tube after 6 or 8 seconds at x-position 15cm and travelled within 0.43 s moving at a constant speed of 35 cm/s towards x-position 0cm. Blue line, x-coordinate of the fly within the tube over time; red dotted line, x-coordinate of stimulus within the tube over time. In panels A, B, C and D the odor pulse evoked a change in the flies' movement. In panel A, B and D the flies changed direction of their movement from down- to upwind, whereas in panel C the fly was first sitting still and then started to move upwind in response to the stimulus pulse.

The examples in Figure 7 depict four sample trials where the flies were moving downwind directly before they had contact with the stimulus (Figure 7 A, B and D, blue traces) or were sitting still (Figure 7 C, blue trace). When presented with the vinegar stimulus (the red dotted line) the flies moved upwind towards the odor source, exhibiting attraction to the stimulus. However, the change of speed in the presence of an attractive stimulus was tiny and could have been easily overlooked. Thus, the olfactory stimulus generated by the multicomponent stimulus device was able to elicit a clear, repeatable change in behavior, and the communication between this device and the automatic tracking system allowed us to quantify this odor-evoked behavior reliably. Most of the previously established *Drosophila* behavioral assays use large numbers of flies and/or stimuli less defined in concentration and duration (e.g. (Ruebenbauer et al., 2008; Semmelhack and Wang, 2009)). Therefore the coupling of the multicomponent stimulus device with the multichannel bioassay allows a more accurate assessment of flies' olfactory sensitivity and behavioral latency to single odors or blends. We are now quantifying the flies' responses to a large set of stimuli (different odors with different concentrations) that will be published in a separate manuscript.

Discussion

Here we present a novel multicomponent stimulus device that can present up to 8 simultaneous odor components at various time scales. Odor components were accurately blended into a unified odor pulse (Figure 2), and pulses could be separated at frequencies of at least 10 Hz with little bleed or contamination (Figure 3). Odor pulses were also consistent and repeatable (Figures 4 and 5).

As with any olfactory device, contamination and leakage of the stimulus is a significant concern. This device has been designed to address this issue in a number of ways. First, all components are composed of chemically inert materials including steel, PEEK, and Teflon, which resist adsorption of chemicals on to their surfaces. Second, each line is dedicated to a single component and is equipped with check valves as an alternative to reverse flow (Cardé et al., 1984), to prevent flow or leakage in the absence of stimulation. Third, as the same outlet is used for both stimulation and constant flow, the system is constantly flushed with clean air to restrict any adsorption of the stimuli on the system surfaces. Fourth, the system contains 8 lines, so one of the lines can be used as a blank or control line to test for any evidence of contamination (as in the electrophysiology examples, 3.3.1). Long term testing of the system over several months with electrophysiology provided no evidence for leakage or contamination. Finally, repeated stimulations showed no evidence of leakage (Figure 3), and PID measurements indicated that a clean, square pulse of odor was released (Figure 3 F). Nevertheless, the use of particularly heavy volatiles (such as some pheromones), or those with

certain functional groups may indeed introduce long-term buildup in system components. It is for this reason that all components, particularly tubing, are easily cleaned and replaced if needed. As this system was designed primarily for testing non-pheromonal food and host blends, the use of the apparatus for less volatile, high molecular weight stimuli has not been tested.

The concentrations of two compounds (isoamyl acetate and 2-heptanone) were equilibrated through regulation of each component line's flow rate based on the different partial vapor pressures of the odorants (Figure 5). Vapor pressure calibration showed a vast improvement in equilibrating concentrations over uncalibrated, equal flow conditions. Although this method produced fairly consistent concentrations at low flow rates (<0.4 L/min), the difference between the two concentrations increased at higher flow rates. This suggests an apparent limitation of the device in equilibrating concentrations of compounds at high flow rates, potentially due to increased pressure in the system at higher airflows. Additionally, as angle and distance of the animal in relation to the stimulus outlet can drastically alter airborne concentrations and subsequent response magnitudes (Moore, 1984), care should be taken to always present stimuli at the same position relative to the olfactory system in question. A flexible outlet has been created (Figure 1) to allow for optimal placement of the outlet in relation to the animal or preparation.

The spatiotemporal delivery and simple TTL control of this device make it suitable for a variety of olfactory tasks requiring accurate stimulus delivery and recording in diverse taxa such as insects, rodents, and humans. Two such examples, invertebrate electrophysiology and behavioral assays have been shown here. This device is also currently being used in other olfactory experiments including calcium and two-photon optophysiological experiments (S. Sachse, personal communication). Several odors can be tested by adding larger or multiple blending chambers. The odor and blending chambers are also relatively inexpensive and portable, allowing each experiment to have its own dedicated setup to reduce cross-contamination. Heated and/or automated cleaning with purified air can also reduce contamination within each setup.

When using such a device, care should be taken to ensure that stimuli can be consistently presented during the experimental trials. Sufficiently large odor chambers should be chosen for high frequency experiments to ensure that the saturated headspace is not depleted between stimulations. The use of a larger chamber will also require a greater resting period between trials to allow vapor equilibrium to be reached. High frequency stimulations may also show uneven initial pulses (Figure

3) due to delays in valve opening on the odor chambers. Additionally, theoretical calculations to regulate stimulus concentrations based on common gas laws should be checked empirically (such as through PID or gas chromatographic measurement) to ensure that real concentrations match those predicted. Finally, multiple stimuli may be limited to those with relatively similar vapor pressures to avoid the high flow rates needed to compensate much less volatile stimuli.

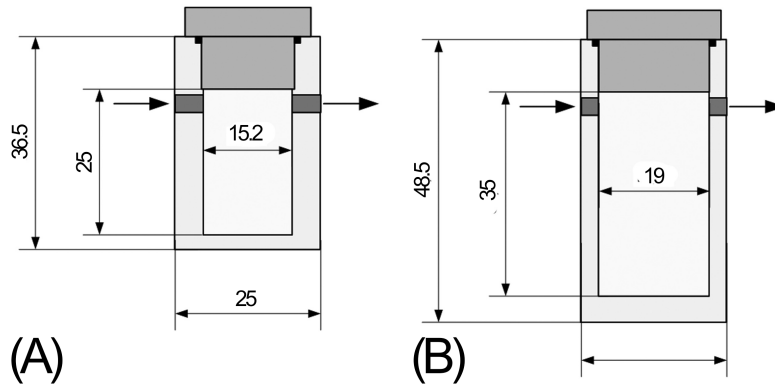
In summary, this multicomponent device provides a much-needed method to deliver accurate blends of volatile stimuli for current studies on olfactory processing of complex mixtures in many animals. As we progress further in our understanding of the role of blends in olfaction, we hope that this device will serve as a starting point for further improvements on accurate stimulus delivery in both spatial and temporal scales.

ACKNOWLEDGEMENTS

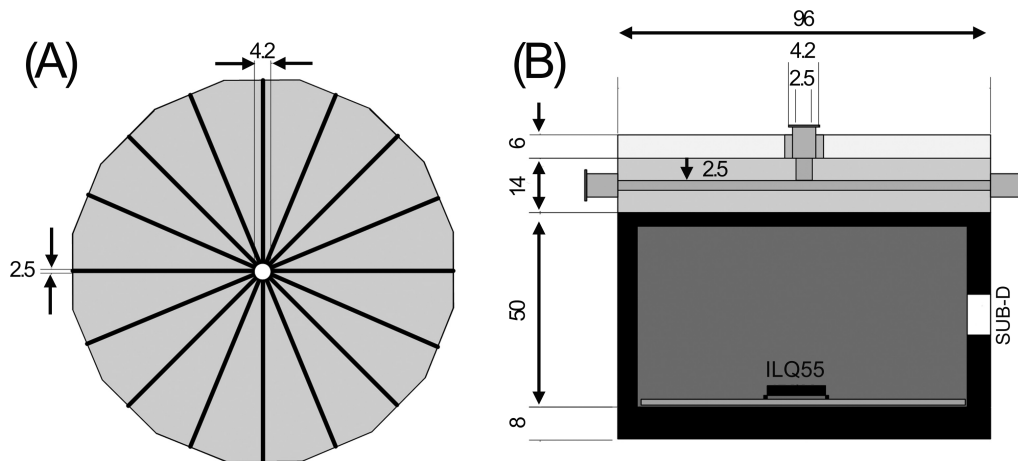
This research was funded by the Max Planck Society and the EU 6th Framework Programme. The authors wish to thank Julian Gardner and Andreas Reinecke for advice on vapor pressure calculations and concentration calibration. SO and LK funded by iChem (EU 6th Framework Programme), KS, AS, MK and BH funded by the Max Planck Society.

Supplemental Data

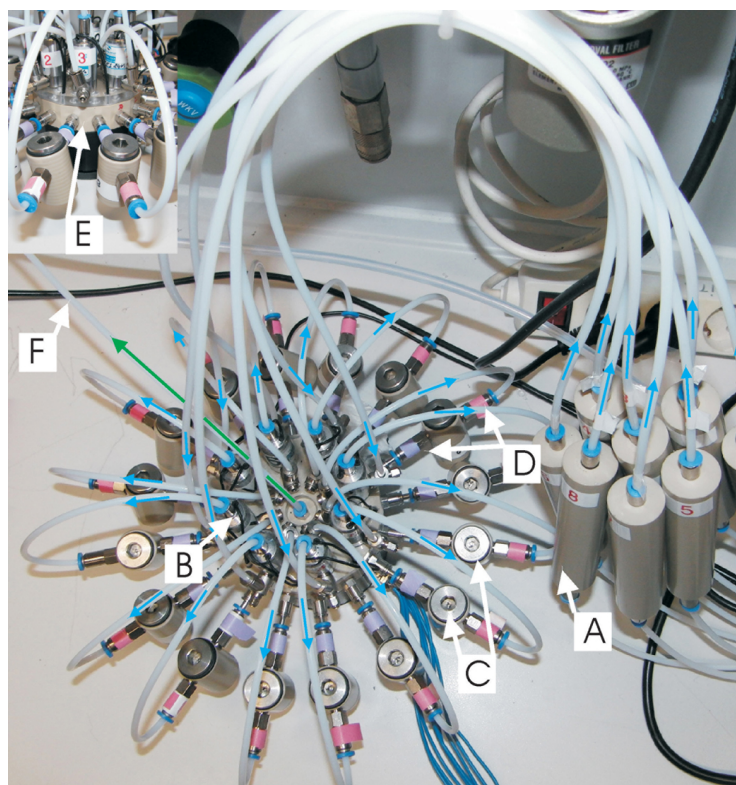
Supplementary Figures



Supplementary Figure 1: Schematic overview of odor/humidifying chambers for (A), behavioral and (B), electrophysiological assays. All dimensions are shown in mm.



Supplementary Figure 2: (A; top) and (B; side) view of blending chamber. (B) shows the chamber affixed above the optocoupler (ILQ55) and SUB-D connection for valve activation. Odors enter and exit via inlets and central outlet shown at the top of (B). All dimensions in mm.



Supplementary Figure 3:
Multicomponent stimulus system as used for behavioral paradigms.
 (A) humidifier filled with 3ml distilled water; (B) solenoid valves connected to stimulus chambers, (C), which contain 5 μ l of pure odor or the empty control. When the valve switches to one vial, the pressure opens the check valves (D) so that the vial's headspace can reach the blend chamber (E; inset). (F): stimulus release tube.

Supplementary Tables

Supplementary Table 1. Calculated flow rates used for calibration analyses

Blend Component	CAS	Vapor Pressure (mm Hg at 25°C) ^a	Mole Fraction in air (using equations 1-3)	Flow rate (L/min) ^b				
				uncalibrated	calibrated			
Isoamyl Acetate	123-92-2	5.6	0.007	0.25	0.25	0.30	0.40	0.50
2-heptanone	64-17-5	3.86	0.005	0.25	0.36	0.44	0.58	0.73
TOTAL FLOW				2.8 ^c				

a. SRC PhysProp Database (<http://www.syrres.com/esc/physdemo.htm>)

b. Values were set according to isoamyl acetate, the most volatile component

c. Total flow was equilibrated with unused valves

CHAPTER III

Neuronal processing of complex mixtures establishes a unique odor representation in the moth antennal lobe

Linda S. Kuebler, Shannon B. Olsson, Richard Weniger & Bill S. Hansson

Abstract

Animals typically perceive natural odor cues in their olfactory environment as a complex mixture of chemically diverse components. In insects, the initial representation of an odor blend occurs in the first olfactory center of the brain, the antennal lobe (AL). The contribution of single neurons to the processing of complex blends in insects, and in particular moths, is still largely unknown. Using a novel multicomponent stimulus system, we performed intracellular recordings of projection and interneurons in an attempt to thoroughly characterize blend representation and integration properties by single AL neurons in the moth.

We found that the fine spatiotemporal representation of blends within and between single neurons in the AL revealed a highly combinatorial, non-linear process for coding host blends presumably shaped by the antennal lobe network: 82% of blend responding projection neurons (PNs) and local interneurons (LNs) showed non-linear spike frequencies in response to an odor mixture, exhibiting an array of interactions including suppression, hypoadditivity, and synergism. Our results indicate that odor blends are represented by each cell as a unique combinatorial representation and there is no general rule by which neurons compute the mixture in comparison to single components. On the single neuron level, we show that those differences manifest in a variety of parameters, including the spatial location, frequency, latency, and temporal pattern of the response kinetics.

Introduction

Behaviorally relevant host odors are composed of complex mixtures of compounds that create a spatially and temporally dynamic olfactory environment through which insects navigate. An insect's ability to perform odor-mediated behavior (e.g. nectar feeding, host location or mate finding) requires the olfactory system to process and reliably identify complex volatile signals in a constantly

changing background. Nevertheless, the mechanism by which single neurons generate a unique blend percept in the olfactory system remains largely unclear.

The antennal lobe (AL) of the insect brain is a conglomeration of anatomically discrete subunits of neuropil known as glomeruli, which confine synapses among four types of neurons (Stocker, 1994; Mori and Yoshihara, 1995; Shipley and Ennis, 1996; Hansson and Anton, 2000). Olfactory sensory neurons (OSNs) expressing the same receptor proteins at the periphery send their axons to a single glomerulus where they synapse with AL-intrinsic local interneurons (LNs) connecting glomeruli (Christensen et al., 1993) projection neurons (PNs) that transmit information to higher brain areas (Shepherd, 1972; Tolbert et al., 1983; Boeckh and Tolbert, 1993) and modulatory centrifugal input (Kent et al., 1987). Therefore, AL output is shaped by both excitatory and inhibitory activity requiring interglomerular connectivity (Vosshall and Stocker, 2007). The AL thus serves as the primary processing center for generating blend information from the combined activity of OSNs.

Single neurons may process odor mixtures either as the linear sum of the constituent chemicals (elemental processing) and/or non-linear computation creating a unique blend representation (configural processing; Rescorla, 1972). In vertebrates, non-linear mixture interactions have been observed both at the periphery (Duchamp-Viret et al., 2003) and in the central nervous system (Tabor et al., 2004; Lei et al., 2006; Lin et al., 2006; Davison and Katz, 2007; Johnson et al., 2010). In contrast, mixture interactions among insects have been witnessed mainly in the CNS (for review see Lei and Vickers, 2008, but see Akers and Getz, 1993; Ochieng et al., 2002; Hillier and Vickers, 2011). Optophysiological studies observing the response of (predominantly) OSNs in the insect AL showed that responses to odor blends could generally be predicted from the single component responses (Silbering and Galizia, 2007). Yet strong mixture interactions at the PN level were prominent (Silbering and Galizia, 2007) suggesting significant levels of non-linear information processing among single neurons within the AL.

In moths, one of the key insect models of olfaction, odor processing has been extensively studied among single pheromone-receptive neurons (Christensen and Hildebrand, 1987; Christensen et al., 1995; Anton et al., 1997; Barrozo et al., 2010; Lei and Vickers, 2008). In contrast, the nature of complex host blend processing by single AL neurons remains unclear, although, recent studies using optophysiological and multi-unit recording suggest that both linear and non-linear processing may occur (Carlsson et al., 2007; Riffell et al., 2009a; Riffell et al., 2009b). In the present study, we performed intracellular recordings of single LNs and PNs in female *Manduca sexta* while presenting the antenna with various host volatile blends. Neurons were stimulated with up to seven different

host compounds and their mixtures using a novel multicomponent stimulus system. We asked two major questions:

1) What is the degree and spread of non-linear interactions among single neurons in the antennal lobe? 2) How do cellular aspects of AL neuron responses contribute to blend processing? Results addressing both of these issues are discussed in relation to first order processing within the AL.

Material & Methods

Animals

Manduca sexta (Lepidoptera, Sphingidae) larvae were reared on an artificial diet (Bell and Joachim, 1976). Sexes were separated as pupae and animals used for physiological experiments were isolated individually before eclosion in paper bags in an environmental chamber at 25°C with 50% relative humidity on a 16-hour/ 8-hour photoperiod. All experiments were performed with naïve adult females 3-5 days post-eclosion.

Odor stimulation

The stimulation device is detailed in (Olsson and Kuebler et al., 2011). Briefly, compressed air was regulated through a series of 8 flowmeters (one for each odor component and the blank). Each line then passed through a three-way valve attached to two chambers with check valves in each direction. Under normal flow conditions, airflow passed through the headspace of a distilled water chamber to establish a constant, humidified airstream. Upon stimulation, the valves switched the regulated airstream through the headspace of the odor chambers to release the stimulus. The airstream from each chamber was then combined among all 8 lines into a single, unified laminar flow that proceeded to the antenna as a blend or single component.

The following odors were used: (+)-linalool, (-)-linalool, phenyl acetaldehyde (PAA), benzaldehyde, hexanol, nonanal or trans-2hexenyl acetate (E2HA) and cis-3-hexenyl acetate (Z3HA; Table A1 in Appendix). As nonanal did not provide appreciable responses for most neurons, it was substituted with the Z3HA isomer, E2HA. All odors were acquired from Sigma at highest purity available. Odors were selected because of their ecological and physiological relevance as shown in previous studies of *Manduca sexta* (King et al., 2000; Shields and Hildebrand, 2000; Fraser et al., 2003; Hansson et al., 2003; Reisenman et al., 2004; Hoballah and Turlings, 2005). New odor dilutions were prepared approximately once per month and unused vials were kept at 4°C. Odor mixtures were obtained by switching up to 7 valves simultaneously. A set of 50 bottles (7 concentration stages per odor +

control) were available in order to alter concentrations. To achieve the same relative odor concentrations during presentation, the vapor pressure of each component was considered and single component airflows were altered accordingly (Olsson and Kuebler et al., 2011). For intracellular analyses, odors were always presented in a similar repetitive sequence across animals (stimulation protocol, 500 ms odor pulse). Recorded cells were first presented with all 7 components simultaneously (“all”), followed by a fully randomized stimulation sequence, testing each of the 7 single components separately (“single”) with the control stimulus (mineral oil) in between. Stimulation brakes and random testing was crucial to rule out adaptation and cross adaptation effects (Stopfer and Laurent, 1999). Components that induced a response were subsequently presented together as a blend (“blend”). Hence, each cell was tested with an individual blend composed of variable number components [ranging from 2 (binary blend) up to 7 components]. Finally, cells were randomly tested with the single components at appropriate “blend” concentrations (e.g. for a tertiary mixture, single components were again tested using threefold concentration, 3×10^{-4} ; “single+”). This was necessary to compensate for concentration differences between the blend and its single components (Olsson and Kuebler et al., 2011; Silbering and Galizia, 2007). In this fashion, we were able to assess the response of various mixture interactions, including synergism. Due to time constraints related to the complex odor set used, execution of multiple trials per component was unfeasible. However, to justify this approach we pretested cells and showed stable and reliable response patterns for repeated stimulation (compare Olsson and Kuebler et al., 2011)). We are thus confident that analyzed responses in this study were robust and consistent regardless of number of repetitions. Only stable recordings (>40min) of cells that successfully passed the entire stimulation protocol process were analyzed.

Intracellular recordings

For electrophysiological recordings, moths were firmly restrained in plastic tubes (modified Falcon tubes 15ml) with the head exposed and immobilized with dental wax (Surgident, Heraeus Kulzer, Dormagen, Germany). The head capsule was opened with a razor blade and labial palps and cibarial musculature removed to allow access to the brain. Obstructing trachea and parts of the neurolemma covering the ALs were removed with fine forceps to facilitate insertion of the recording electrode. The brain was superfused constantly with physiological saline solution containing (in mM): 150 NaCl, 3 CaCl₂, 3 KCl, 10 TES buffer, and 25 sucrose, pH 6.9 (Heinbockel et al., 2004).

Sharp glass-capillary electrodes were produced from borosilicate tubing (1.0 mm OD, 0.5 mm ID, World Precision Instruments, Sarasota, Fla., USA) using a CO₂ Laser based micropipette Puller (P-

Neuronal processing of complex mixtures establishes a unique odor representation in the moth antennal lobe

2000, Sutter Instrument, Novato, CA, USA). Tips of the micropipettes were loaded with a 3% solution of Lucifer yellow (Sigma-Aldrich) in 0.2 M LiCl, or 2% neurobiotin (Molecular Probes, Carlsbad, CA, USA) in 0.2 M KCl. Shafts were filled with 2M LiCl (Lucifer) or 2M KCl (neurobiotin). Electrode resistances, measured in the tissue, ranged from 110 to 320 Mohm. The recording electrode was inserted randomly into the antennal lobe using a motorized micromanipulator (Luigs & Neumann, Ratingen, Germany). Typically, one neuron was recorded per animal. When intracellular contact was established, the ipsilateral antenna was stimulated and the activity of the neuron was recorded. The analog signal of the impaled neuron was amplified, filtered (Branp 0.1, bridge amplifier npi Electronic GmbH Tamm, Germany), synchronized with the external stimulation device via an interface (INT-20MX Breakout Box Module, npi Electronic) and monitored on an oscilloscope (TDS 2000B, Tektronics Inc., Beaverton, OR, USA). The resultant signal was then digitized via a PCI card (6250E, National Instruments, Austin, TX, USA). Action potentials were recorded with a custom-made Labview 8.5 program (National Instruments) and stored on the PC. Spike analyses were performed using IgorPro software (Wavemetrics, Portland, OR). After physiological characterization, neurons were injected iontophoretically with either Lucifer yellow by passing hyperpolarizing current (0.5–4 nA) for 3–40 min or neurobiotin (depolarizing current). Potentially stained brains were further processed as noted below.

Neuroanatomical techniques & confocal microscopy

Brains were dissected from the head capsule and immediately transferred to ice-cold 4% formaldehyde in phosphate-buffered saline (PBS; pH 7.2) for at least 2 hours on a shaker. To visualize neurobiotin-injected neurons, brains were additionally incubated with Alexa-conjugated streptavidin (Molecular Probes; Invitrogen, Eugene, OR, USA) for 3 days at 4°. All brains were then dehydrated in an ascending series of ethanol (50%, 70%, 80%, 90%, 95%, and 3x100%, 10 minutes each), cleared in methyl salicylate (M-2047; Sigma-Aldrich, Steinheim, Germany) overnight, and finally positioned in custom aluminium slides, each sealed with a coverslip. Neurons were examined by laser-scanning confocal microscopy using a Zeiss LSM 510 (Zeiss, Jena, Germany) equipped with a HeNe/Ar laser module and a 10, 0.45-NA objective lens (C-Apochromat, Zeiss,). Optical sections (1024 x 1024 pixel) were taken at intervals of 0.8µm for detailed scans of the AL. In addition, serial 2µm optical sections through the entire brain were performed for stained projection neurons in order to visualize the fine arborizations in higher brain areas, such as mushroom bodies.

3-D reconstruction & image processing

3D reconstructions were carried out in AMIRA 4.1.2 (mercury Computer Systems, Berlin, Germany). Individual glomeruli were reconstructed by segmentation of each spherical structure around its center in three focal planes (xy, xz, yz). Subsequent use of the wrapping tool in Amira 4.1.2 allowed us to interpolate 3D shapes from just a few segmented slices. Single neurons were reconstructed using the skeleton-tool. Composite visualization of the neural architecture of different preparations was achieved by using landmark and label field registration techniques (compare (Rybak et al., 2010)) All figures presented here were edited by using Adobe Photoshop CS4 (Adobe Systems, Inc.) and compiled with Adobe Illustrator CS4 without any further modification on brightness or contrast.

Spike analysis

Analog intracellular data (mV) was sampled (50 kHz) and recorded (3 kHz) using customized Labview software (National Instruments, Austin, TX). Action potentials were extracted as digital spikes using Igor Pro software (Wavemetrics, Portland, OR). The number of spikes was counted 1.5 s before (prestimulus) and 1.5 s after stimulus onset (poststimulus) to determine response frequency (Figure 1D). To compensate for mechanical stimulus delay, spikes were counted 100 ms after stimulus onset (Figure 1D2 and E2, *blue dotted line*) as dictated by PID (photoionization detector) measurement of stimulus presentation (“Olsson et al., unpublished observations”). For analysis, response frequencies for each trial were normalized to spontaneous activity as a ratio (Hz 1.5 s after stimulus onset / Hz 1.5 s before onset; Figure 1D2 and E2)

Interspike intervals (ISIs) were calculated between successive spikes (Figure 1D2, red bar). For cells exhibiting an inhibitory response (a drop in spike frequency), response latency was determined as the time between stimulus onset (including the 100 ms mechanical delay) to the beginning of the longest ISI (i.e. the beginning of the inhibitory response; Figure 1E2, orange bar indicates loISI). For cells exhibiting an excitatory or biphasic response (an increase in spike frequency), latency was calculated as the time between stimulus onset (including the 100 ms mechanical delay) to the beginning of the shortest ISI (i.e. the point of highest frequency response; Figure 1D2, sISI, magenta bar). To assess temporal patterns, raw spike frequencies were calculated in 50 ms bins and compared from 100 ms – 1500 ms following stimulus onset.

Blend interactions

Definition of blend interactions was based on Duchamp-Viret (Duchamp-Viret et al., 2003) and Silbering and Galizia (Silbering and Galizia, 2007) as illustrated in Figure 6 in the Appendix. Consider a neuronal response to two compounds, a and b: if there are no interactions between the components, the blend of a and b will be perceived as the sum of the response to a and b alone. This is known as linear summation (A). Alternatively, if there is synergism between the two compounds (B), the blend of a and b will produce a response greater than the maximum response of the single components at the same total concentration as the blend (in this case, a + a). Suppression (C) causes a blend response that is less than at least one of the single components. Finally, hypoaddivitivity (D) occurs when at least one of the components of the blend is ignored and the blend response resembles that of a single component.

In order for a blend interaction to be considered non-linear, the blend response of an antennal lobe neuron must have exceeded the cell's response to the single components of that blend by at least one standard deviation of all single compound responses. For synergism to occur, the blend response must be at least one standard deviation above the maximum response to the single components when tested at the same concentration as the total blend (Tabor et al., 2004). In other words, if a blend contained four components, the blend response was compared to the single components tested at 4x their base concentration. Suppression constituted a blend response at least one standard deviation less than the maximum response to the single components. Hypoaddivitivity was defined as a blend response between those two extremes, which would make the blend response similar to at least one of the single components. Anything else was considered a linear response. Standard deviations were used to account for the diversity of single compound responses. Although increasing the criteria to 2 S.D. did not change overall ratios of linear/non-linear responses, it inflated the number of hypoaddivitive responses. Thus, 1 S.D. was chosen as a more conservative measure for linearity. This method also ensured that only blend responses with highly divergent kinetics would be considered non-linear. The equations for determining blend interactions were thus as follows:

Inhibitory Responses

Synergism: Blend Hz < Minimum single component Hz tested at the same concentration as the blend - standard deviation of single component Hz.

Suppression: Blend Hz > Minimum single component Hz + standard deviation of single components

Neuronal processing of complex mixtures establishes a unique odor representation in the moth antennal lobe

Hypoadditivity: Minimum single component Hz - standard deviation of the single components < Blend Hz < Maximum single component Hz + standard deviation

Excitatory/Biphasic Responses

Synergism Blend Hz > Maximum single component Hz tested at the same concentration as the blend + standard deviation of single component Hz.

Suppression: Blend Hz < Maximum single component Hz - standard deviation of single components

Hypoadditivity: Maximum single component Hz - standard deviation of single component Hz < Blend Hz < Maximum single component Hz + standard deviation

Non-linear latencies were determined in a similar fashion with blend responses compared to maximum or minimum latencies of the single component responses. However, blend latencies exhibiting synergism were at least one standard deviation less than the minimum latency to the single components when tested blend concentrations. Suppressed blend latencies constituted a blend response at least one standard deviation greater than the maximum latency to the single components. Thus, latency synergism was defined as a short latency blend response, and the reverse for suppression.

Statistical analysis

Fisher's exact test was used to compare percentages of projection and interneurons exhibiting various response characteristics. Temporal patterns were assessed using areas under the curve measured from each response PSTH (peri-stimulus time histogram; 50 ms bins; 100-1500 ms following stimulus onset). Areas were measured for each response profile using the trapezoid rule for each data bin. These areas were then divided by the time to establish a frequency average for each response. These averages were compared using independent Student's t-tests separately for each type of response (excitatory, inhibitory, and biphasic). Differences in response latencies have been revealed using Wilcoxon Matched Pairs and T-test. All analyses were performed using PASW (SPSS) v 18 software.

Results

Odor-evoked electrophysiological responses were recorded from a total of 50 single projection and local interneurons innervating ordinary glomeruli [and the female-specific glomeruli (LFGs)]. Among these, 16 were discounted due to incomplete protocols (see material & methods). The remaining 34 neurons were used in subsequent analyses.

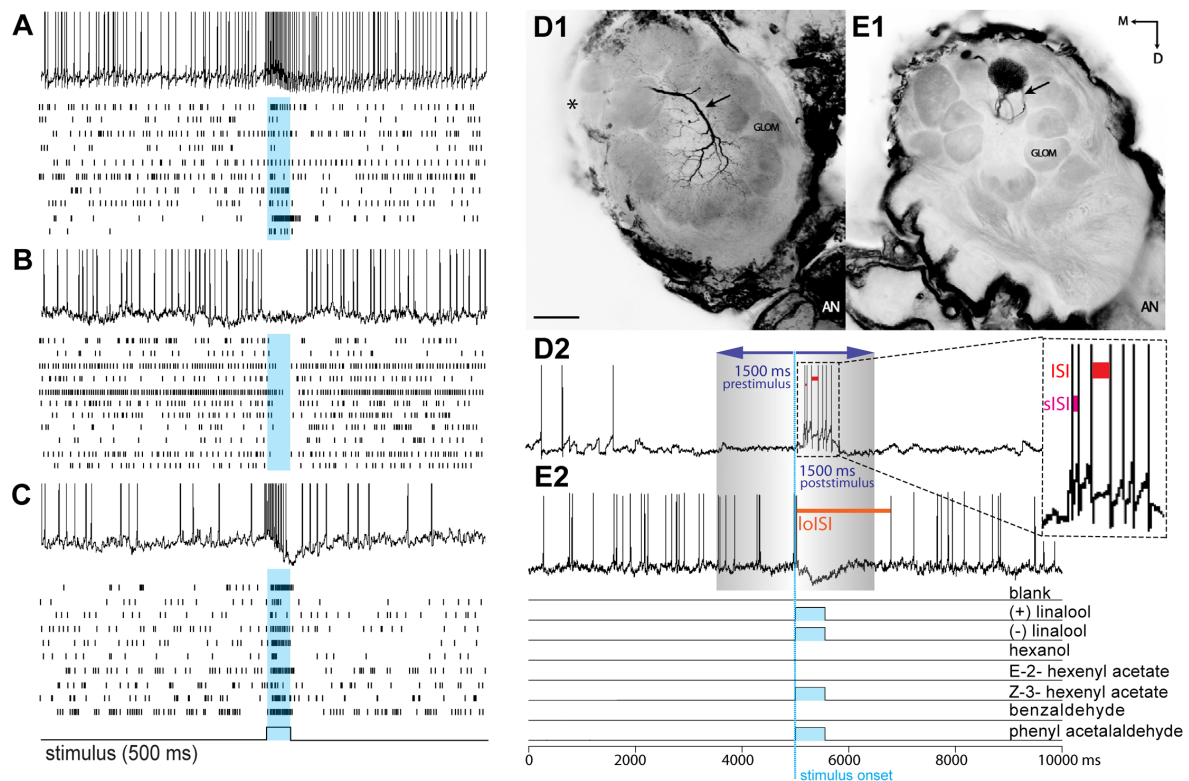


Figure 1: Response profiles of single AL neurons to a complex odor blend. Left panel (A-C): The three basic *Manduca* response types: (A) Excitatory. (B) Inhibitory. (C) Biphasic. Each block shows one example of an intracellular recording trace and complete raster plots of action potentials for all analyzed cells of the dataset in response to plant odor mixtures. Blue squares and vertical bars indicate the 500 ms odor stimulus period. **Right panel:** Example of two common morphological types of AL neurons in the female *Manduca sexta* brain responding to an identical blend of four components. Both neurons innervate the right antennal lobe. (D1) Typical local interneuron (LN) with a broad symmetrical arborization profile, branching in the vast majority of glomeruli with soma situated in the lateral cell cluster (not visual in the confocal plane but indicated by asterisk); LN neurites are restricted to the antennal lobe; excitatory response profile (D2). (E1) Uniglomerular projection neuron exhibiting dense dendritic arborization occupying one single ordinary glomerulus; soma antero-ventral, axon innervating the mushroom bodies via the inner antennocerebral tract (IACT, compare FIGURE 4E and F); inhibitory response profile (E2). Pictures were obtained by confocal microscopy of two separate whole mount brain preparations; anterior inverted projection view of picture stack ((D) = average of 50 pictures; (E)= 11); M, medial; D, dorsal; AN, antennal nerve; GLOM, glomerulus; Scale bar, 100 microns. (D2, E2) To determine response frequencies the number of spikes was counted 1.5 s before (prestimulus period) and 1.5 s after stimulus onset (poststimulus period; stimulus onset: blue, vertical dotted line). To determine latency, interspike intervals (ISIs) were calculated between successive spikes (red bar; shortest ISI, sISI, magenta bar; longest ISI, loISI, orange bar).

Response to antennal stimulation exhibited three basic response types, characterized by either an abrupt depolarization with increased spiking (excitatory response), hyperpolarization leading to a suppression of spiking (inhibitory response), or a biphasic response with an early excitatory phase followed by a period of hyperpolarization (Figure 1A-C). Another very rare fourth profile was defined

Neuronal processing of complex mixtures establishes a unique odor representation in the moth antennal lobe

as a bimodal response, where a single cell showed divergent response types for different stimuli. Although there was variation in the response pattern across single cells (compare Figure 1) the main characteristics of the basic response types (e.g. no inhibitory phase in excitatory response profiles) were apparent and therefore led to robust categorization of each cell.

Blend interactions

In general, the number of neurons responding to an odor mixture remained relatively sparse. Roughly 20 cells were contacted before obtaining a response to any of the 7 tested compounds. Interestingly, 100% of all blend-responsive cells responded to (+)-linalool (both PNs & LNs), 86% responded to the levo-rotatory enantiomer (-)-linalool and 90% responded to phenyl acetaldehyde (see Table A1 “Table of compounds” in Appendix). Apart from one exceptional case, no specific “blend” neurons were found: if a neuron responded to a blend it also responded to the single components and vice versa.

TABLE 1: Degree and spread of blend interactions across the four major response types

A FREQUENCY	Linear	Synergism	Suppression	Hypoadditivity	TOTAL
Excitatory	20/2	10/1	40/4	30/3	10
Inhibitory	18/2	0	9/1	73/8	11
Biphasic	20/2	0	40/4	40/4	10
Bimodal	0	33/1	33/1	33/1	3
TOTAL	18/6	6/2	29/10	47/16	34
	18%	82%			100%
B LATENCY	Linear	Synergism	Suppression	Hypoadditivity	TOTAL
Excitatory	20/2	0	20/2	60/6	10
Inhibitory	64/7	0	9/2	27/4	11
Biphasic	0	10/1	50/5	40/4	10
Bimodal	0	33/1	33/1	0	3
TOTAL	27/9	6/2	26/10	41/14	34
	27%	73%			100%

A high percentage (>80%) of neurons show non-linear integration properties in response to the blend, based on the analysis of spike frequency and latency (%/n; n = Number of antennal lobe neurons exhibiting each characteristic).

Table 1 displays the array of blend interactions observed among the 34 antennal lobe neurons. Stimulus responses fell in each of the four response type categories described above. Blend Interactions were calculated separately for response frequency (A) and latency (B). Although some linear responses to the blend were observed, 82% of the cells showed non-linear spike frequencies in response to the blend and 73% displayed non-linear response latencies. Among these non-linear interactions, the majority of cells exhibited hypoadditivity (45% for spike frequency and 41% for latency), where the response to the blend was similar to at least one of the single components within that blend. Suppression (a diminished response compared to the single components) was also observed in approximately 25-30% of cell blend responses, whereas synergism (an enhanced response compared to the single components) was witnessed in only 2 cells for each response characteristic.

While the three major response types were equally distributed across recorded cells (excitatory 29%, inhibitory 32%, biphasic 29%), bimodal responses were only witnessed in three out of 34 cells. Interestingly 50% of hypoadditive frequency interactions were composed of inhibitory cells. Suppression, the second most common blend interaction, was predominantly displayed by excitatory and biphasic cells (80% of all suppressive cells for frequency, 70% for latency). Synergism, although very rare ($n=2$), was exhibited by one excitatory and one bimodal cell.

The number of compounds tested in the blend (2-7; Table A1 in Appendix) did not alter the percentage of non-linear blend responses. However, it is possible that “silent” compounds (i.e. compounds that did not elicit a significant response) could have imposed some non-linearities on the total blend response. We thus compared the response of single components to the initial trial that tested all 7 compounds simultaneously (Table A3 in Appendix). Although the overall proportion of non-linear responses to the complete mixture did not change appreciably, the percentage of non-linearities increased by roughly 10% for both frequency and latency. This indicates that a small proportion of “silent” compounds may indeed have an effect on the blend response.

Morphology

25 antennal lobe neurons were intracellularly stained and 18 identified either as local interneurons (LN, $n=8$, e.g. Figure 2G-I) or projection neurons (uniglomerular PN, $n=7$, e.g. Figure 2C-F multiglomerular PN, $n=2$, e.g. Figure 2B). Among these, 9 PNs and 5 LNs were included in the blend interaction analysis. Seven other stained neurons could not be clearly characterized due to incomplete or multiple staining and were therefore excluded from the study.

Neuronal processing of complex mixtures establishes a unique odor representation in the moth antennal lobe

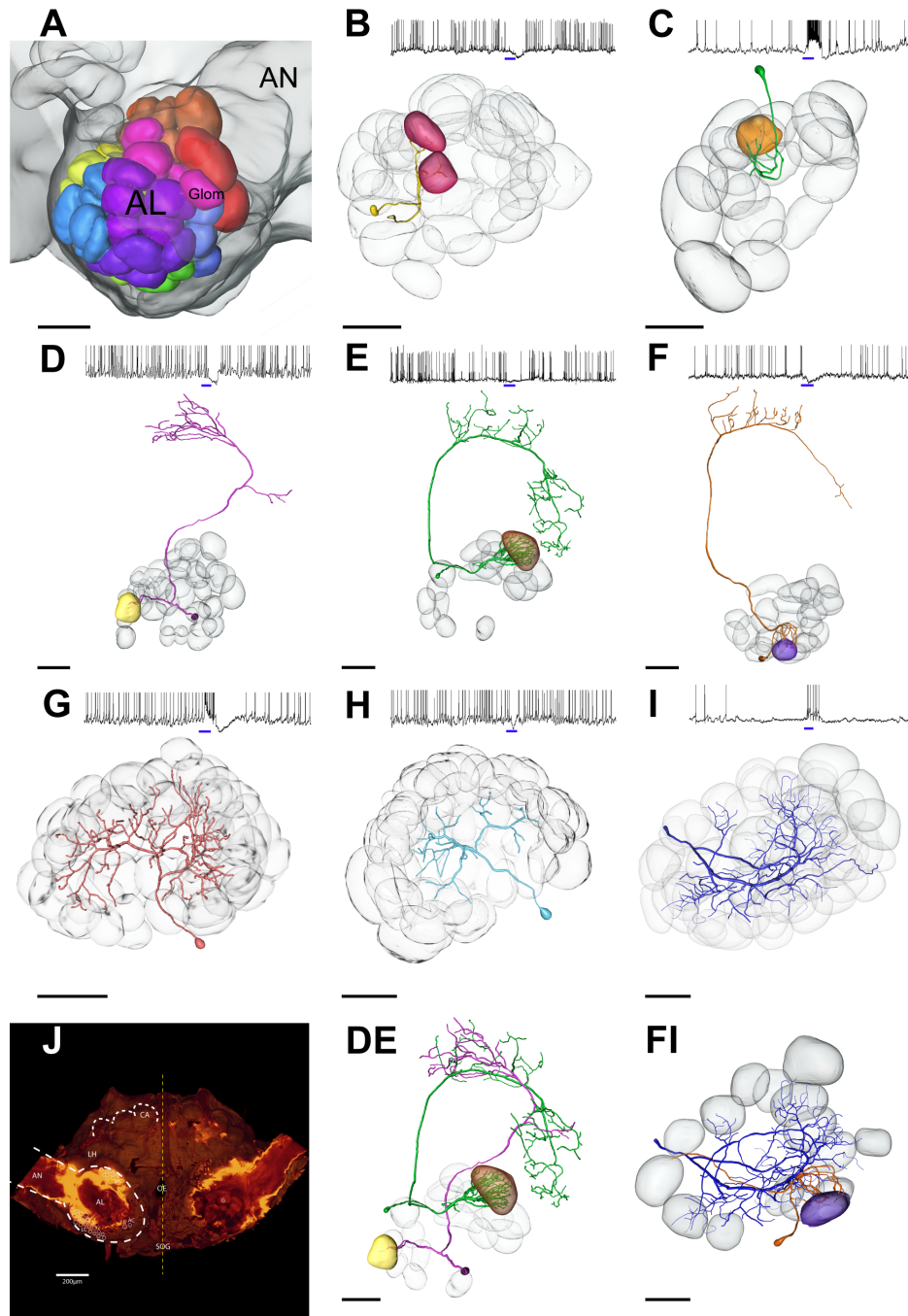


Figure 2: Three dimensional morphological reconstruction of blend responsive neurons in the Manduca brain. (A) Color coded map of antennal lobe (AL) glomeruli, female specific glomeruli depicted in red. **(B–i)** Subset of stained AL neurons (PNs and LNs) responding to the same blend of four components: (+)-linalool, (-)-linalool, phenyl acet-aldehyde, and cis-3-hexenyl acetate. Multi- **(B)** and uniglomerular **(C–F)** PNs show remarkably different innervation patterns as well as varying response profiles; blue bars indicate blend stimulus, 500 ms. **(De)** Composite picture of two PNs running directly opposed tracts. **(Fi)** Transformation of one LN and one uniglomerular PN responding to the same quadruple mixture; note that the purple glomerulus innervated by the Pn **(F)** is not innervated by the LN **(i)**, although responding to the same stimulus. Transparent, gray glomeruli serve as landmarks for PNs in **(B–F)**, and depict all innervated glomeruli in LNs **(g–i)**. **(J)** Overview of the Manduca brain. AL, antennal lobe; AN, antennal nerve; CA, mushroom body calyces; AC, MC, LC, cell clusters; Oe, esophagus; LH, lateral horn; black scale bars, 100 μ m.

Neuronal processing of complex mixtures establishes a unique odor representation in the moth antennal lobe

Most local interneurons (n=7) were "symmetrical", exhibiting a broad, symmetrical arborization pattern throughout the antennal lobe, as originally described (Matsumoto and Hildebrand, 1981). PNs arborizing in both uni- and multiglomerular patterns travelled to higher processing centres via all three antennocerebral tracts (Homberg et al., 1988, for example see also Figure 2D and E).

Figure 2 depicts a subset of stained neurons (Pn n=5, LN p=3) responding specifically to the same blend of four components [(+)-linalool, (-)-linalool, phenyl acetaldehyde, and cis-3-hexenyl acetate]. By careful comparison with landmark neighbors, the spatial position of innervated glomeruli within the antennal lobe (AL) was designated and assigned to the glomeruli indicated on the AL map (Figure 2A). Although responding to the same blend, reconstructed PNs revealed remarkably different innervation patterns. None of the 5 PNs targeted the same glomerulus. Transformation of one LN and one PN together on the map (Figure 2 FJ) also showed that although responding to the same components, LN arborizations did not innervate the glomerulus strongly arborized by the dendrites of the uniglomerular PN.

PNs could be physiologically distinguished from LNs on the basis of the spike width measured during spontaneous activity at the base of spikes above threshold membrane oscillations. Mean spike width for morphologically identified LNs ($LN_{(morph)} 9.7 \pm 3.9$ ms, n=6) was significantly different from that measured in PNs ($PN_{(morph)} 4.9 \pm 1.7$ ms, n=9; t-test $p=0.028$, Figure 3). Spontaneous spike width did not differ notably during the recording (± 0.27 ms in $PNs_{(morph)}$, ± 0.54 ms in $LNs_{(morph)}$; measured for 5 consecutive spikes) and therefore was selected as a consistent character across cells. Several other inspected properties, including IPSP (inhibitory post-synaptic potential) and spontaneous activity (Mann-Whitney U Test $p=0.96$) did not differ between these two morphological types. Also the spontaneous firing rate was very similar between stained PNs and LNs with a mean of 7.3 spikes/s for LNs and 8.3 spikes/s for PNs (same median ISI=31ms for LNs and PNs).

Neuronal processing of complex mixtures establishes a unique odor representation in the moth antennal lobe

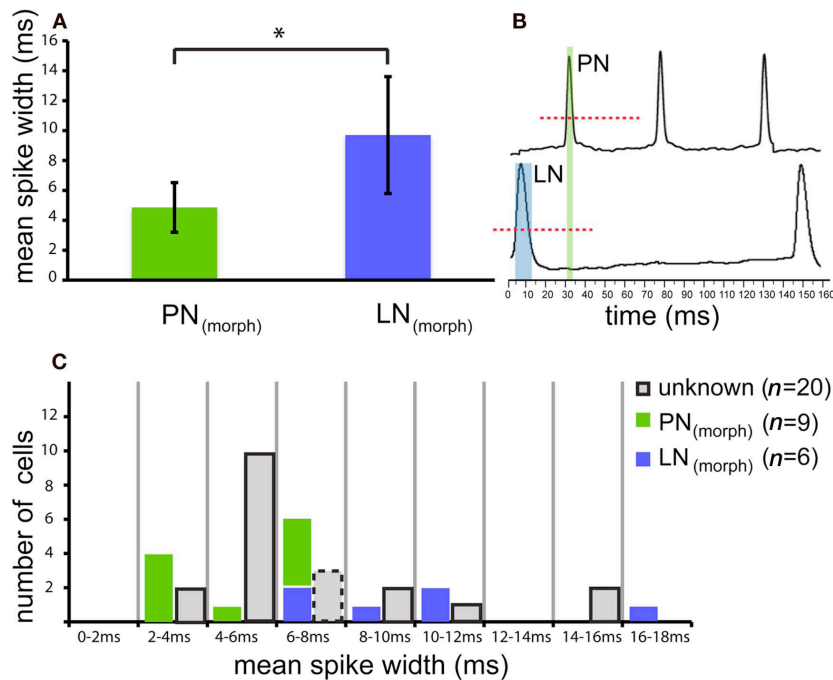


Figure 3: Projection neurons and LNs reveal different action potential characteristics. (A) Comparison of spike kinetics for morphologically confirmed local neurons [LN(morph), blue] were significantly different from those measured in projection neurons [PN(morph), green; t-test $p = 0.028$]. Average spike duration (mean spike width) measured during spontaneous activity of nine randomly selected PNs was roughly half the value (4.9 ± 1.7 ms; mean \pm SD) found in LNs (9.7 ± 3.9 SD, $n = 6$). **(B)** Spontaneous action potential width was measured at the base of spikes above threshold membrane oscillations (dashed red line). **(C)** Based on this robust character, 17 other unknown neurons (gray) could be categorized as physiologically designated neurons [PN(phys) $n = 12$, LN(phys) $n = 5$]. Three unknown neurons possessed intermediate spontaneous spike widths (between 6 and 8 ms, gray, dashed outline) and therefore could not be determined.

Based on the robust spike width character, 12 other unidentified neurons could be categorized as PN_(phys) (physiologically designated PNs) according to their spontaneous action potential width, and 5 categorized as physiologically designated LNs (LN_(phys)). Three unknown neurons possessed intermediate spontaneous spike widths and therefore could not be typed (see dashed outline cells, Figure 3C). The categorization of cells on the basis of spike width is not exhaustive and was not intended to replace the accurate but tedious staining method of morphological identification. This method rather offers an alternative approach to compare the two cell populations based on a solely physiological characteristic. Using this physiological method, Figure 7 in the Appendix shows the relative proportions of PNs and LNs ($n=31$, including stained neurons) across the four response types and four blend interaction categories. Fisher's exact test found no difference in response type or blend interaction for either response frequency or latency between PNs and LNs (both morphologically and physiologically confirmed cells, $p > 0.05$ for all comparisons).

Latency

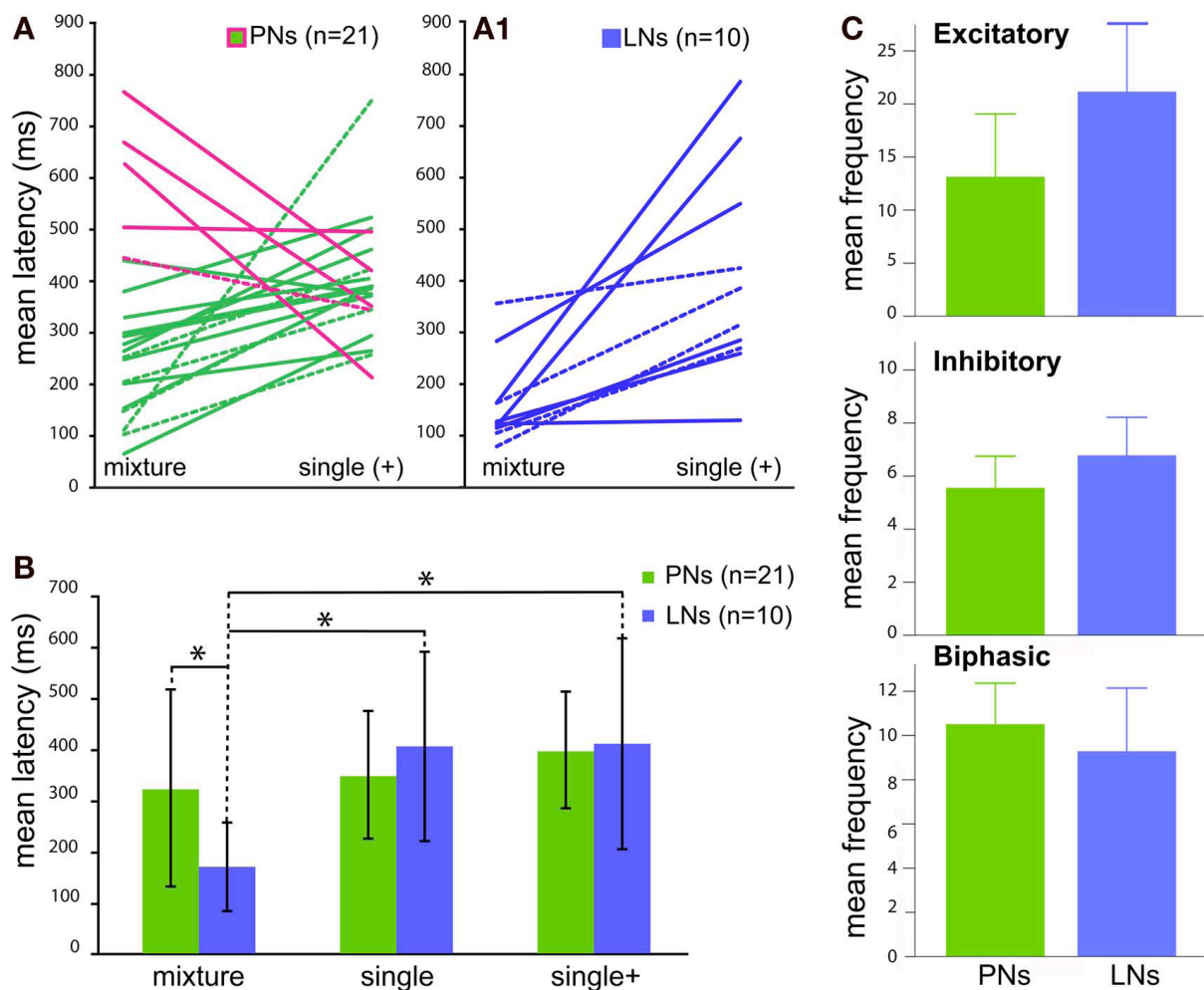


Figure 4: (A1) All local interneurons (LNs, blue) show significantly shorter latencies to the blend, whereas five [(A), magenta line] out of 16 projection neurons (PNs, green) depict shorter latencies to single components (LNs $p = 0.0020$, PNs $p = 0.103$). Single components were tested at the higher blend concentration (single+). (B) Average response latencies show differences between blend vs. single component latencies at the two different concentrations for LNs (blue) but not PNs (green). (C) Comparison of mean temporal patterns to blend stimuli between projection neuron (PN) and interneuron (LN) responses (both morphologically confirmed and physiologically designated neurons). Traces represent PNs (green) and LNs (blue) respectively. Graphs are arranged as Excitatory, Inhibitory and Biphasic responses. Bar graphs depict total mean frequencies calculated from areas under the PSTH curves (not shown, compare Figure 5).

Figure 4 depicts mean latencies of response onset to the blend and its single components tested at the higher blend concentration (single+) within each type of neuron. Mean paired latencies were calculated for both morphologically and physiologically confirmed cells (Figure 4A1, PNs $n=21$; Figure 4A2, LNs $n=10$). Absolute latencies to the blend were highly variable and ranged between 65ms (min) and 766ms (max) for PNs and 86-358ms for LNs. Single component latencies varied from 257 to 749ms in PNs and from 129-788ms in LNs. Mean response latencies of PNs to single components were not different from those of LNs [Figure 4B; t-test, $p=0.85$ for single+ in PNs (396 ± 114 ms) and LNs (408 ± 205 ms) and $p=0,28$ for single]. However, responses to the blend were significantly shorter

in LNs [t-test, $P = 0.0046$ for LNs ($168 \pm 86\text{ms}$) vs. PNs ($322 \pm 192\text{ms}$)]. Latencies of LNs to the blend were also significantly shorter than to the single component (single+) within individual neurons (blend vs. single+, Wilcoxon matched pairs LNs $p=0,0020$), but not PNs ($p=0,133$). Moreover, average response latencies to the blend were shorter for LNs only (blend vs. single T-Test, LNs $p=0,003$, PNs $p=0,28$; blend vs. single+ LNs, $p=0,005$, PNs $p=0,85$). Thus local neurons always responded significantly faster to the blend than to single components. The observed differences in latency were not caused by an ambiguously shorter latency to one of the single components (Anova; morphologically designated LNs_(morph) $p=0,758$ and PNs_(morph) $p=0,631$, Figure 8 in Appendix).

Temporal coding

The response frequency of each of the 34 cells was separated into 50 ms bins encompassing 100 ms to 1500 ms following stimulus onset to generate peri-stimulus time histograms (PSTHs) for each trial (excluding mechanical stimulus delay). Figure 5 displays mean PSTHs for responses to blends, single compounds (single), and compounds tested at the higher blend concentration (single+). In this figure, PSTH's are presented as lines rather than histogram bars. Separate graphs are presented for excitatory (Figure 5A), inhibitory (Figure 5B), and biphasic (Figure 5C) response profiles. Bar graphs to the right present mean frequencies based upon areas under the curve created by the PSTHs. Although no significant difference was detected among inhibitory cells, both excitatory and biphasic cells showed differences in response pattern to the three types of stimuli ($p < 0.05$ for both response types). Notably, excitatory responses showed a difference in the single compound response as compared to higher concentrations. Alternatively, biphasic responses showed a difference in the blend response as compared to the single compound responses (at both concentration steps).

PNs and LNs typed either by morphological staining or spontaneous spike width measurement (see above) were also compared by their temporal pattern (see Figure 9 in Appendix). In response to blend stimuli, PN and LN response patterns did not differ for any type of response. Thus, temporal response patterns to blends did not differ based upon morphological neuron type.

Neuronal processing of complex mixtures establishes a unique odor representation in the moth antennal lobe

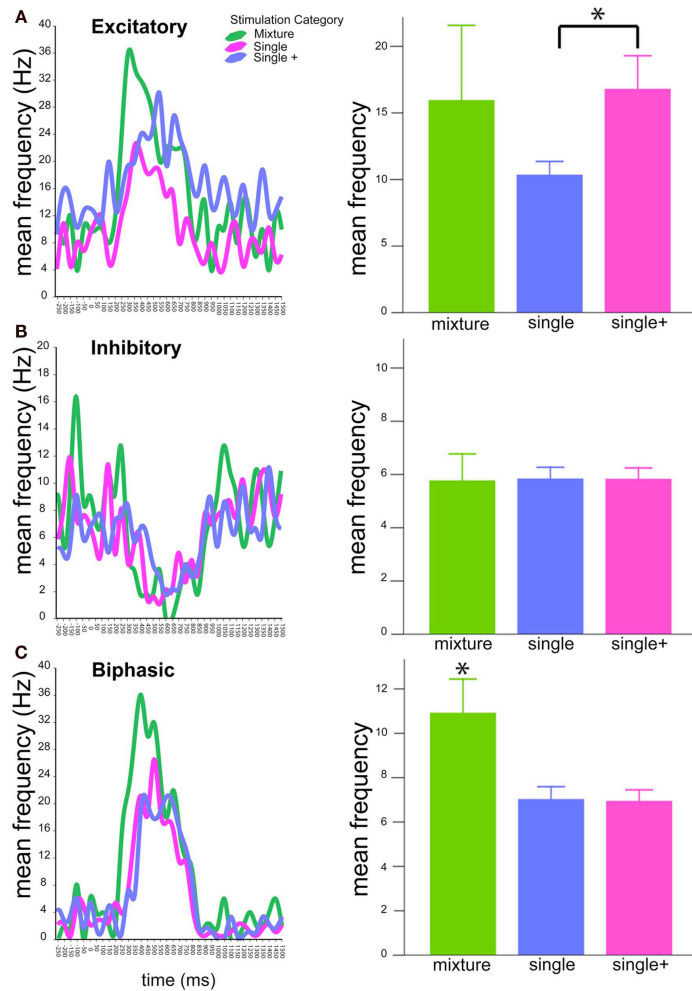


Figure 5: Temporal patterns of antennal lobe neuron responses. Graphs at left depict PSTHs of mean response frequencies (Hz) to blends (green), single compounds (magenta), and single compounds tested at the mixture concentration (blue). PSTHs are presented as lines rather than bars to allow simultaneous comparison of stimulus responses. Graphs are arranged as (A) Excitatory, (B) Inhibitory, (C) Biphasic responses. Bar graphs (right) depict total mean frequencies calculated from areas under the PSTH curves after stimulus onset (0 ms). Asterisks indicate significant differences according to Student's t-tests. Bars \pm SE.

Discussion

We found significant non-linear blend processing among 34 projection and interneurons examined in the *Manduca sexta* antennal lobe. The high degree of across-fiber patterning shown in this study suggests the generation of a novel “blend representation” within individual neurons throughout the antennal lobe.

Our findings reveal important aspects of AL neuronal processing of complex odor blends. In examining the cellular and spatiotemporal aspects of single AL neuron responses, at least 3 different cellular parameters appear to be involved in establishing the blend response: (1.) the morphology and location of neurons within the AL, (2.) the firing rate of individual neurons (frequency and temporal pattern), and (3.) the neuronal response latency. Conversely, stimulus concentration is encoded by the slow temporal patterning of single vs. higher concentration responses. We discuss

each of these aspects of blend processing below in relation to the overall network processing of blends within the antennal lobe.

Degree and spread of non-linear interactions

The degree of multi-component response neurons in the antennal lobe (AL) was relatively sparse: Only 1 out of roughly 20 cells per animal responded to the 7 compounds tested. This translates to approximately 60 blend responsive cells for these compounds in the entire animal [1200 total PNs and LNs, Homberg et al., 1988]. Blend coding in *Manduca* thus represents a highly selective system, where less than 100 AL cells integrate information received from hundreds of OSNs. Admittedly, in order to avoid non-selective OSN responses the odor concentration used in our study (10^{-4}) was in the lower part of the dynamic range of the dose–response curve (King et al., 2000; Reisenman et al., 2008) and may partially explain such high selectivity. Nevertheless, the blend-responsive cells exhibited clear and robust signals (Figure 1, Figure 2).

Most blend coding studies have utilized binary mixtures (De Jong and Visser, 1988; Galizia and Menzel, 2001; Deisig et al., 2003; Ditzen et al., 2003; Broome et al., 2006; Carlsson et al., 2007; Rospars et al., 2008; Fernandez et al., 2009; Niessing and Friedrich, 2010) but only 15% of all cells in our study responded to two compounds. Indeed, most cells responded to tertiary (26%) or quaternary mixtures (41%), whereas responses to quinary (12%) or six or seven components remained comparably sparse (3%; Table A1 in Appendix). This suggests that investigations of blend interactions involving several compounds may reflect the natural processing of host odors more accurately, even though our selected compounds were still extremely limited compared to the plethora of odors *Manduca* encounters in nature.

Morphological aspects of blend processing

Non-linear interactions were observed among both projection and interneurons (Figure 7 in Appendix). In their review, Lei and Vickers suggest that multiglomerular innervation would aid blend coding because single neurons integrate information directly from multiple OSN input channels (Lei and Vickers, 2008). The presence of synergism and suppression in uniglomerular projection neurons in our study indicates a significant role for the across-fiber network in generating the unique blend presentation. This assumption is also supported by our 3D morphological reconstructions. Tracing of four uni- and one multi glomerular projection neuron responding to the exact same blend of four components [(+)-linalool, (-)-linalool, phenyl acetaldehyde, and cis-3-hexenyl acetate] showed

radically different innervation patterns (Figure 2). This suggests that the blend percept of even a relatively simple four-component blend is represented globally across the AL network.

Additionally, we showed that PNs and LNs exhibited similar levels of non-linear blend interactions for both response frequency and latency (Figure 7 in Appendix), suggesting that neuron identity does not impact blend response linearity.

Temporal aspects of blend processing

Response Rate

We showed that 82% of the cells in this study exhibited non-linear spike frequencies in response to the blend and 73% displayed non-linear response latencies (Table 1). Among these non-linear interactions, the majority of cells exhibited hypoadditivity or suppression. Our findings on the single cell level correspond well to previous network-level studies of mixture interactions using calcium imaging (Carlsson et al., 2005; Deisig et al., 2006; Silbering and Galizia, 2007) or multi-unit recordings (Riffell et al., 2009a). Nevertheless, concentration effects and different dose response properties among blend components can also establish non-linearity in the odor response of single cells (Sachse and Galizia, 2003; Wright et al., 2005; Stopfer et al., 2003). We therefore equilibrated the concentration for each single component stimulus to the appropriate corresponding blend concentration (Silbering & Galizia, 2007; Olsson and Kuebler et al., 2011). Testing odors (10^{-4}) in the lower part of the dynamic range of the dose–response curve (King et al., 2000; Reisenman et al., 2008) can prevent artificial non-linearity caused by eventual saturation. Moreover, fully randomized testing prevented adaptation and cross adaptation effects as the repeated exposure to odors, even without a reward, can lead to plasticity in the AL (Stopfer and Laurent, 1999).

Although rare, synergism has been observed between essential behaviorally relevant components in oriental fruit moths (Pintero et al., 2008). In our data set, all four cells exhibiting synergism responded specifically to the same four volatiles [(+) / (-)-linalool, phenyl acetaldehyde, and (Z)-3-hexenyl acetate]. These compounds are all found in the odor bouquet of the flowers and plants on which *Manduca* feeds and oviposits. It is possible that synergism is restricted to very select cells responding in a context-dependent manner to important behavioral cues, although other cells responding to these same four compounds did not exhibit synergism. Interestingly, nearly all blend responsive cells responded to (+)-linalool, a compound suggested as particularly important for oviposition behavior in *Manduca* (Reisenman et al., 2010). Future behavioral trials with female *Manduca* may clarify the correlation between compound identity and behavioral relevance, as has been shown recently for male feeding behavior (Riffell et al., 2009).

Response Latency

Sensory information incorporating both rate (i.e. average rate of spike firing) and spike timing allows for processing of complex mixtures by a limited number of cells, with blends coded not only by where and how cells fire, but when. The concept of a “latency code” is not novel (Krofczik et al., 2008). Indeed, response onset is the first information transmitted from the network (Krofczik et al., 2008). Applying different latencies for single components and mixtures can provide fast and definitive information about stimulus identity. Our results showed that blend latencies not only revealed non-linear interactions when compared to single component responses (Table 1) but revealed significant differences between the two AL neuron classes: We report that blend response latencies were significantly shorter than single compound latencies in local interneurons, but not in projection neurons (Figure 4). In order for projection neurons to respond to a blend, they must either be directly innervated by all OSNs responding to the blend components, or be connected to the local interneuron network. 80% of the blend-responsive projection neurons were uniglomerular, and therefore unable to directly connect to all OSN populations specific to the blend components. Consequently, the response latencies of interneurons would reasonably be shorter as they must first transmit the relevant blend information to the output projection neurons. Nevertheless, Krofczik et al. hypothesize that a “latency code” cannot accurately reflect both concentration and identity simultaneously (Krofczik et al., 2008). For this reason, the authors indicated that the temporal firing pattern of AL neurons could act in concert with latency to represent different stimuli.

Response Profiles

Interestingly, the relevance of the temporal response patterns seemed to differ depending on the response profile of the neuron recorded. Inhibitory responses did not show an overall difference in response pattern regardless of the type of stimulus presented. These cells also showed the highest level of hypoadditivity (73%, Table 1), indicating that the blend response generally resembled at least one of the single components. Thus, inhibitory responses do not appear to provide any information about either identity or concentration, but may instead provide more binary information on the presence or absence of odor. On the other hand, excitatory responses showed a difference between low and high concentrations, regardless of whether the high concentration was a blend or not (statistical significance only compared to single+ values). This indicates that excitatory responses may encode the concentration of the stimulus. Finally, blend responses in biphasic cells were significantly different from both concentrations of single compound stimuli, suggesting that biphasic cells may carry the brunt of identity coding in the AL. Nevertheless, further investigations

using dose response curves for single odorants and blends would be necessary to test this hypothesis.

Conclusions

Our results suggest a global, highly combinatorial and non-linear scheme for processing complex host blends that is shaped by the AL network. On the single neuron level, blend responses exhibit an array of interactions including suppression, hypoaddivitivity, and synergism that establish a new neuronal representation of the blend that differs from single component responses. By assessing single neuron kinetics of blend processing, our results suggest that each neuron utilizes a variety of parameters to produce the novel, unique signal representing the entire blend. This suggests that analysis of blend input from OSNs cannot unambiguously predict AL output on any spatial or temporal scale. Furthermore, simultaneous analysis of the entire antennal lobe network (rather than just the surface or a neuronal subset) is necessary to properly demonstrate the “blend representation”, already occurring in AL.

Across single antennal lobe neurons, inhibitory responses may signify the general presence of an odor, while excitatory and biphasic responses indicate odor concentration and identity, respectively. All neurons exhibited high levels of non-linearity for both response frequency and latency, indicating that both response rate and latency are important for coding the unique blend identity. Finally, although both types of AL neurons analyzed were similar in terms of response patterns and types, LNs exhibited significantly shorter latencies. Along with the finding that uniglomerular PNs with similar response profiles revealed remarkably different innervation patterns, this supports the role of LNs in the first level of blend processing in the AL and strengthens the assumption that blends are represented globally across the AL network.

Due to the obvious complexity of the system, and the inability to record all neurons involved, our findings cannot be interpreted in terms of a single model. Moreover, when studying early olfactory processing, we must consider that downstream events (e.g. Mushroom bodies and/or lateral horn) may significantly alter blend representations by combining information pooled across different channels (Laurent, 1999; Perez-Orive et al., 2002). However, our results on the single neuron kinetics of blend processing provide a novel foundation for future studies on complex blend processing.

ACKNOWLEDGEMENTS

We thank Daniel Veit for engineering the stimulus delivery system and solving technical problems. We are grateful to Christoph Kleineidam and Kirk Hillier for support and helpful advice on electrophysiology. We also thank Jürgen Rybak for invaluable advice on 3D- reconstructions and Sonja Bisch-Knaden for statistical help. We would like to express our gratitude to the Ichem consortium for fruitful discussion.

This work was supported by Ichem (6th programme of the EU) and funding from the Max Planck Society to BSH.

ABBREVATIONS

AL, antennal lobe; LN, local interneuron; OSN, olfactory sensory neuron; PN, projection neuron.

Supplemental Data

Supplementary Figures

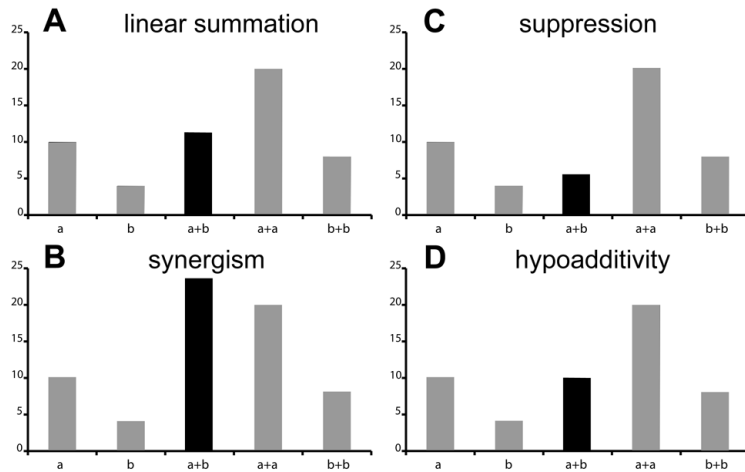


Figure 6: Definition of blend interactions. Schematic graphs depicting various types of non-linear interactions: (A) Linear Summation (B) Synergism (C) Suppression (D) Hypoadditivity

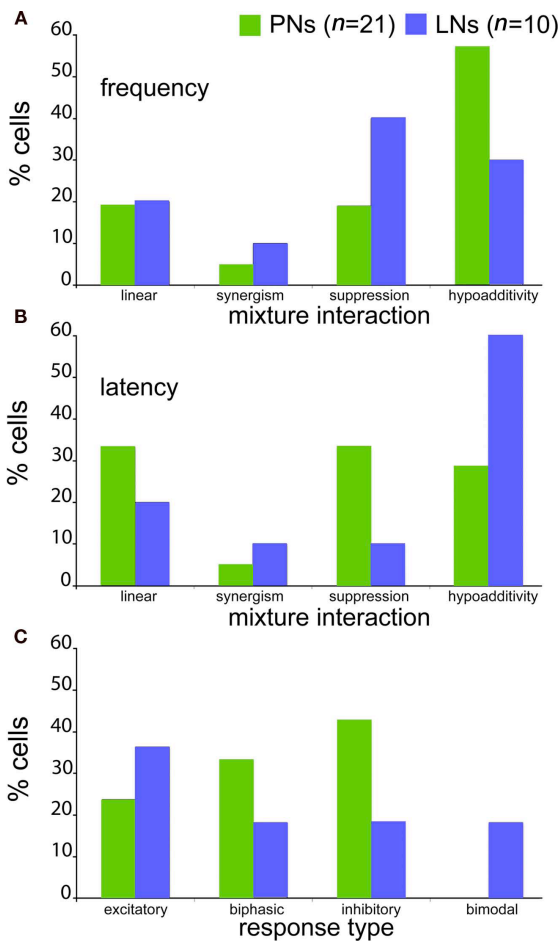


Figure 7: Projection and local interneurons exhibit various blend interactions and response profiles but show no differences in response frequency or latency (both morphologically and physiologically confirmed cells). (A) Percentage of neurons exhibiting response frequency interactions to the blend. (B) Percentage of neurons exhibiting response latency interactions. (C) Percentage of neurons demonstrating various response profiles.

Neuronal processing of complex mixtures establishes a unique odor representation in the moth antennal lobe

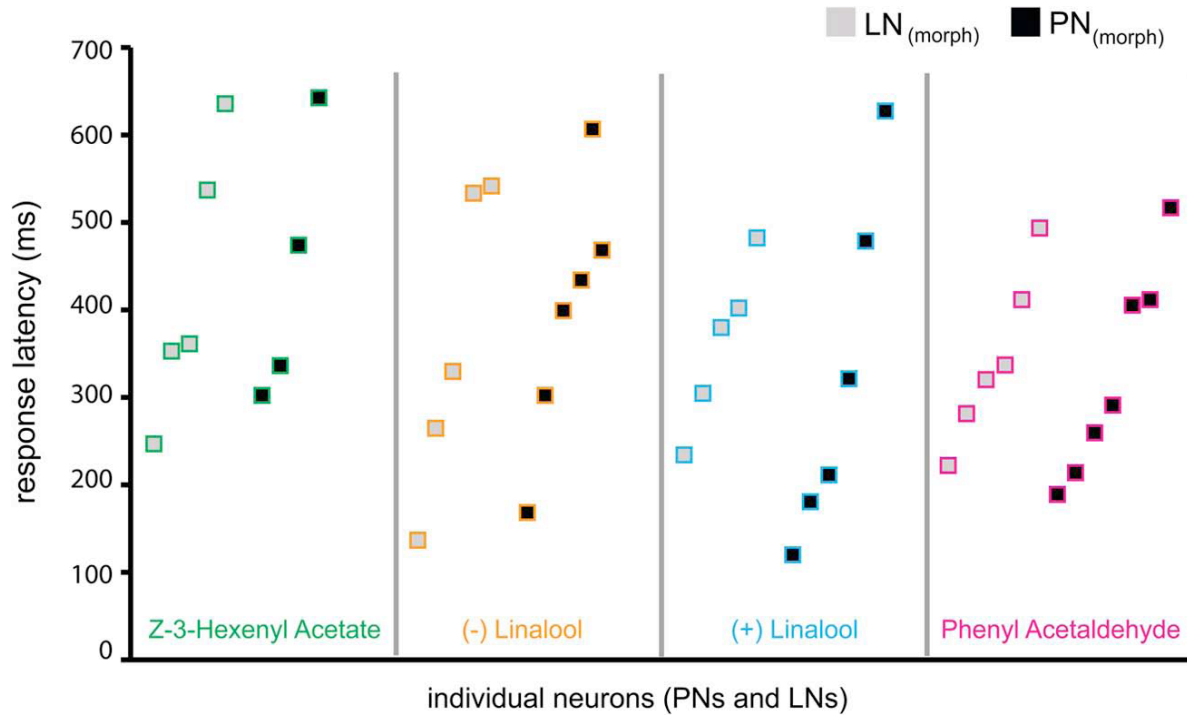


Figure 8: Comparison of response latencies across cell populations. Example of absolute response latencies (time delay between stimulus onset and start of the response) of single stained neurons to the four most abundant blend components. We found no significant difference in latency to the four odors, for both local interneurons [LN(morph), $p = 0.75$; gray squares] and projection neurons [PN(morph), $p = 0.631$; black squares]. This indicates that compound identity does not influence latency for mixtures incorporating those components.

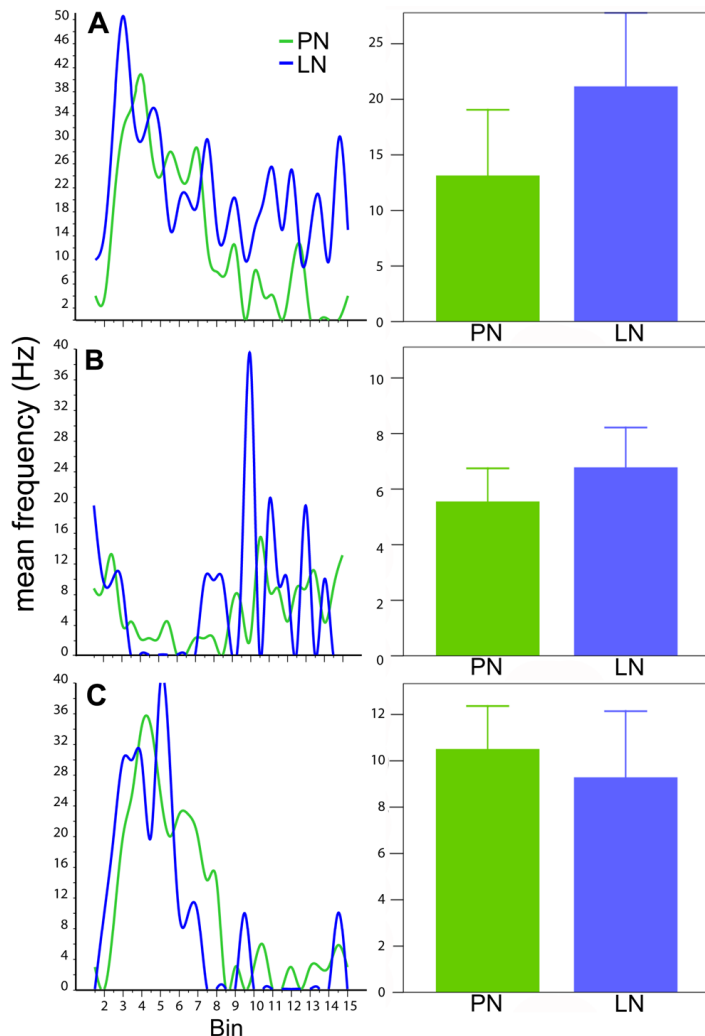


Figure 9: Comparison of mean temporal patterns to blend stimuli between projection (PN) and interneuron (LN) responses (both morphologically confirmed and physiologically designated neurons). Traces represent PNs (green) and LNs (blue) respectively. Responses are arranged and analyzed as in Figure 5.

Neuronal processing of complex mixtures establishes a unique odor representation in the moth antennal lobe

Supplementary Tables

TABLE A1| Table of compounds: Summary of interactions across the four major response types listed for each tested compound
 Nearly 90% of cells (n=34) respond to linalool and phenyl acetaldehyde

		Total Cells	PAA	(+) Linalool	(-) Linalool	Z3HA	E2HA	Nonanal	Hexanol	Benzaldehyde
RESPONSE TYPE	Inhibitory	11	11	11	10	7	1	0	2	2
	Excititory	10	9	10	8	5	0	1	2	0
	Biphasic	10	8	10	10	6	2	0	1	0
	Multiple Response Types	3	2	3	2	3	0	0	0	0
	Total	34	30	34	30	21	3	1	5	2
		Total Cells	PAA	(+) Linalool	(-) Linalool	Z3HA	E2HA	Nonanal	Hexanol	Benzaldehyde
CELL TYPE	ProbablePN	21	19	21	20	11	3	1	3	2
	ProbableLN	10	9	10	8	8	0	0	1	0
	Total	31	28	31	28	19	3	1	4	2
		Total Cells	PAA	(+) Linalool	(-) Linalool	Z3HA	E2HA	Nonanal	Hexanol	Benzaldehyde
INTERACTION	Linear	6	4	6	5	3	2	0	2	1
	Synergism	2	2	2	2	2	0	0	0	0
	Suppression	10	9	10	8	6	1	0	1	0
	Hypoadditivity	16	15	16	15	10	0	1	2	1
	Total	34	30	34	30	21	3	1	5	2
		Total Cells	PAA	(+) Linalool	(-) Linalool	Z3HA	E2HA	Nonanal	Hexanol	Benzaldehyde
Frequency	Linear	9	8	9	9	4	1	0	2	2
	Synergism	2	2	2	2	2	0	0	0	0
	Suppression	9	6	9	7	5	1	0	0	0
	Hypoadditivity	14	14	14	12	10	1	1	3	0
	Total	34	30	34	30	21	3	1	5	2
		Total Cells	PAA	(+) Linalool	(-) Linalool	Z3HA	E2HA	Nonanal	Hexanol	Benzaldehyde
Latency	Linear	9	8	9	9	4	1	0	2	2
	Synergism	2	2	2	2	2	0	0	0	0
	Suppression	9	6	9	7	5	1	0	0	0
	Hypoadditivity	14	14	14	12	10	1	1	3	0
	Total	34	30	34	30	21	3	1	5	2
NUMBER OF BLEND COMPOUNDS										
		Total Cells	2	3	4	5	6	7		
RESPONSE TYPE	Inhibitory	11	0	4	5	1	0	1		
	Excititory	10	2	3	4	0	1	0		
	Biphasic	10	2	2	3	3	0	0		
	Multiple Response Types	3	1	0	2	0	0	0		
	Total	34	5	9	14	4	1	0		

Numbers indicate quantity of cells responding to each compound

TABLE A2| Degree and spread of blend interactions depending on the number of blend components

A FREQUENCY

no. of components	Linear	Synergism	Suppression	Hypoadditivity	TOTAL
2	40/2	0	40/2	20/1	5
3	11/1	0	33/3	56/5	9
4	7/1	14/2	22/3	57/8	14
5	25/1	0	50/2	25/1	4
6	0	0	0	100/1	1
7	100/1	0	0	0	1
TOTAL	6	2	10	16	34

B LATENCY

	Linear	Synergism	Suppression	Hypoadditivity	TOTAL
2	20/1	0	60/3	20/1	5
3	33/3	0	33/3	33/3	9
4	22/3	14/2	14/2	50/7	14
5	25/1		25/1	50/2	4
6				100/1	1
7	100/1				1
TOTAL	9	2	9	14	34

%/n; n= Number of antennal lobe neurons exhibiting each characteristic

Neuronal processing of complex mixtures establishes a unique odor representation in the moth antennal lobe

TABLE A3| Degree and spread of blend interactions across the four major response types as compared to a mixture of all 7 possible components

A FREQUENCY	Linear	Synergism	Suppression	Hypoadditivity	TOTAL
Excitatory	29/2	29/2	29/2	13/1	7
Inhibitory	17/1	0	0	83/5	6
Biphasic	22/2	0	56/5	22/2	9
Bimodal	0	0	100/2	0	2
TOTAL	21/5	8/2	38/9	33/8	24
	8%		92%		100%
B LATENCY	Linear	Synergism	Suppression	Hypoadditivity	TOTAL
Excitatory	14/1	0	29/2	57/4	7
Inhibitory	33/2	17/1	33/2	17/1	6
Biphasic	0	12/1	44/4	44/4	9
Bimodal	50/1	0	50/1	0	2
TOTAL	16/4	8/2	38/9	38/9	24
	16%		84%		100%

%/n; n = Number of antennal lobe neurons exhibiting each characteristic

CHAPTER IV

Novel blend patterns: simultaneous optophysiological studies at multiple levels of the moth AL

Linda S. Kuebler, Marco Schubert, Shannon B. Olsson. & Bill S. Hansson

Abstract

Insects typically perceive their olfactory environment as a complex mixture of natural odor cues. The initial percept of an odor blend detected by olfactory sensory neurons (OSNs) is conveyed to the first olfactory center of the insect brain, the antennal lobe (AL). Afferent input determined by the response profile of OSNs is modified via mostly inhibitory local connections (LNs) and the resultant information of this computation is transferred by projection neurons (PNs) to higher order brain centers. The resultant neuronal representation of an odor mixture may either retain the monomolecular information of single blend components, or reveal non-linear interactions different from the sum due to signal processing in the AL network. The goal of this study was to expand our understanding of olfactory processing beyond the receptor level and reveal patterns of blend responses at different levels in the AL of the hawk moth, *Manduca sexta*. To assess blend processing, we performed optophysiological studies to record odor evoked calcium changes in the AL to five host volatiles and their mixture. We simultaneously measured OSN network input in concert with PN output across the glomerular array. By comparing activity patterns and intensities of input and output neurons, we could directly determine the degree of AL network processing within a single animal. Our data reflects combinatorial and non-linear processes involved in the coding of complex odor blends in *Manduca sexta*. This non-linear signal modulation results in a novel blend pattern even at the earliest stage of olfactory processing in the insect brain, the AL.

Introduction

Nearly all animals are capable of detecting and orienting to chemical stimuli. For many insects, olfactory cues play a major role in most aspects of life (e.g foraging, communication and host localization). The sense of smell is the most prominent sensory modality in the insect's sensory world (Hölldobler and Wilson, 1990; Wilson and Mainen, 2006). In fact, most natural odors are

complex mixtures of diverse chemical compounds providing the animal a valuable source of information about the environment.

In insects, odorant molecules are detected by olfactory sensory neurons (OSNs) and transduced into electrical potentials that transfer information about the odorant molecule to the brain. The response spectra of host plant responsive OSNs are known to be either specific or broadly tuned (Rostelien et al., 2000a; Rostelien et al., 2000b; Shields and Hildebrand, 2000; Hansson, 2002; Hillier et al., 2006; Hillier and Vickers, 2011). OSNs expressing the same olfactory receptor protein converge onto the same glomerulus in the antennal lobe (AL), the initial olfactory processing center and insect analog of the mammalian olfactory bulb (Ressler et al., 1994; Mombaerts, 1996; Vosshall, 2000). Glomeruli are spherical neuropil of high synaptic density constituting the functional units of the AL. In the moth AL, the massive afferent input of roughly 250000 OSNs converges onto two categories of AL neurons: roughly 900 projection neurons (PNs) and 360 local interneurons (LNs; Homberg et al., 1989). PNs subsequently relay AL output to higher brain centers including the mushroom bodies (MB) and the lateral horn (LH). LNs exclusively branch within the AL, interconnecting glomeruli and relaying information between them (for reviews see Homberg et al., 1989; Hildebrand and Shepherd, 1997; Hansson and Anton, 2000; de Bruyne and Baker, 2008).

Separation of blend information into different OSN channels requires subsequent integration of at least a subset of these channels to establish the unique blend feature. Nevertheless, little is known about the mechanisms by which these channels are combined. Therefore, it remains unclear how the insect's olfactory system processes and reliably identifies complex volatile signals in a constantly changing background.

As a consequence of OSN targeting, odors are represented as stable, spatial patterns of neuronal activity in the AL, as shown by optophysiological studies in both vertebrates (Friedrich and Korsching, 1998; Rubin and Katz, 1999; Uchida et al., 2000; Meister and Bonhoeffer, 2001; Fried et al., 2002) and in insects (Joerges et al., 1997; Galizia et al., 1999a; Sachse and Galizia, 2002; Wang et al., 2003; Skiri et al., 2004; Carlsson et al., 2005; Silbering and Galizia, 2007). Recent recordings in the insect AL show that responses to an odor mixture generally could be predicted from the single component responses at input- but not output levels (Silbering and Galizia, 2007). These prominent "mixture interactions" in the *Drosophila* AL are consistent with our previous electrophysiological study in moths that revealed more than 80% non-linear spatiotemporal responses among projection (PNs) and local interneurons (LNs) in response to the blend versus its individual compounds (Chapter III).

The relative simplicity of the *Manduca* olfactory system, as well as its prominent size and durability offers an ideal model to analyze complex odor processing. Additionally, the gross structure and connectivity of first order processing is regarded as consistent across the Lepidoptera, and general odorant processing may be comparable across several insect orders (Eisthen, 2002; Wilson and Mainen, 2006).

In the current study, we measured odor-evoked calcium responses of AL input and output neurons simultaneously using optophysiological techniques. By applying two different calcium sensitive dyes, we quantified the odor information fed into the network (OSN input) as well as the resultant output of network processing (PN output). With this tool, we were able to push our understanding of olfactory processing beyond the receptor level and directly measure how the cellular network of the AL shapes the spatial representation of odor blends relayed by the receptor neurons. Our combined physiological approach indicates that LNs modulate PN output response patterns in the moth AL, resulting in a unique blend feature that cannot be deduced from the peripheral input.

Material & Methods

Animals & preparation

M. sexta (Lepidoptera, Sphingidae) larvae were reared in the laboratory on an artificial diet (Bell and Joachim, 1976). Female pupae were isolated individually in paper bags in an environmental chamber at 25°C with 70% relative humidity on a 16-hour/ 8-hour light/dark photoperiod. Physiological experiments were performed with naïve adult females 3-5 days post-eclosion. For optophysiological measurements, moths were firmly restrained in 15 ml plastic tubes with the head exposed and immobilized with dental wax (Surgident, Heraeus Kulzer, Dormagen, Germany). The head capsule was opened and labial palps and cibarial musculature removed to allow access to the brain and superfused with physiological saline solution containing (in mM): 150 NaCl, 3 CaCl₂, 3 KCl, 10 TES buffer, and 25 sucrose, pH 6.9 (Heinbockel et al., 2004).

Odor stimulation

Each animal's antennae were exposed to a constant, charcoal-filtered air stream (compressed house air, 8 bar) regulated to a pressure of 2 bar and split into 6 independent channels, each controlled by a digital flowmeter with choke valve (SMC Pneumatik, Reutlingen, Germany). Channels fed into a concentric arrangement of solenoid valves (3/2 way M5, Jenpneumatik, Jena, Germany) surrounding a central line, establishing the novel self-developed and custom-made stimulus delivery system (for

detailed description of the multicomponent stimulus device (see Olsson et al., 2011; ChapterII). The resultant airflow passed through the central line and ended in a Peek nozzle (diameter 7 mm) positioned 1cm in front of the insect's antenna. Stimulus pulses were presented for 2s and controlled with custom written software using Labview 8.5 (National Instruments, Austin, TX). The quintuple odor mixture was obtained by switching on 5 valves simultaneously. A set of 11 bottles (2 concentration stages per odor and mineral oil as control) were used to alter concentrations. To achieve the same relative odor concentrations during presentation, the vapor pressure of each component was considered and single component airflows were altered accordingly (Olsson, Kuebler et al., 2011).

The following odors were used: (+)-linalool, (-)-linalool, phenyl acetaldehyde (PAA), trans-2hexenyl acetate (E2HA) and cis-3-hexenyl acetate (Z3HA). All odors were acquired from Sigma at highest purity available and diluted in mineral oil. Odors were selected because of their ecological and physiological relevance as shown in previous studies of *M. sexta* (King et al., 2000; Shields and Hildebrand, 2000; Fraser et al., 2003; Hansson et al., 2003; Reisenman et al., 2004; Olsson et al., 2011). For optical recordings, stimuli were presented in a similar repetitive sequence across animals: We performed three experimental runs, first presenting each animal with a random stimulation sequence, testing each of the five single components separately with the control stimulus (mineral oil) interspersed in between, followed by the complete quintuple mixture. Animals were finally randomly tested with the single components at the appropriate "blend" concentrations (5x 10⁻⁴). This was necessary to compensate for concentration differences between the blend and its single components.

A total of 140 moths were double stained. Among these, 28 showed successful dye penetration both at input and output levels, thus allowing for simultaneous recording. However, only 8 of these animals showed sufficient calcium responses to olfactory stimuli at both levels allowing us to record complete, repetitive odor stimulation runs.

Dye loading & optophysiology

We combined two approaches simultaneously in one animal, using two different calcium sensitive dyes: 1. Bath application of membrane-permeable calcium green-2 AM (Galizia et al., 1998) monitoring neuronal activity dominated by afferent input to the AL (OSNs); 2. Retrograde selective staining of projection neurons (PNs) with Fura- 2 dextran (Sachse and Galizia, 2002; 2003). For bath application, the membrane permeate form of a fluorescent calcium indicator (30 μ mol, Calcium

Novel blend patterns: simultaneous optophysiological studies at multiple levels of the moth AL

Green-2 AM, Invitrogen) was dissolved in physiological saline solution with 6% Pluronic F-127 (Invitrogen). 40 μ l of the dye solution was applied to the exposed brain and the preparation was incubated for 2h at 4°C. Then the brain was rinsed several times with physiological saline solution to remove excessive dye.

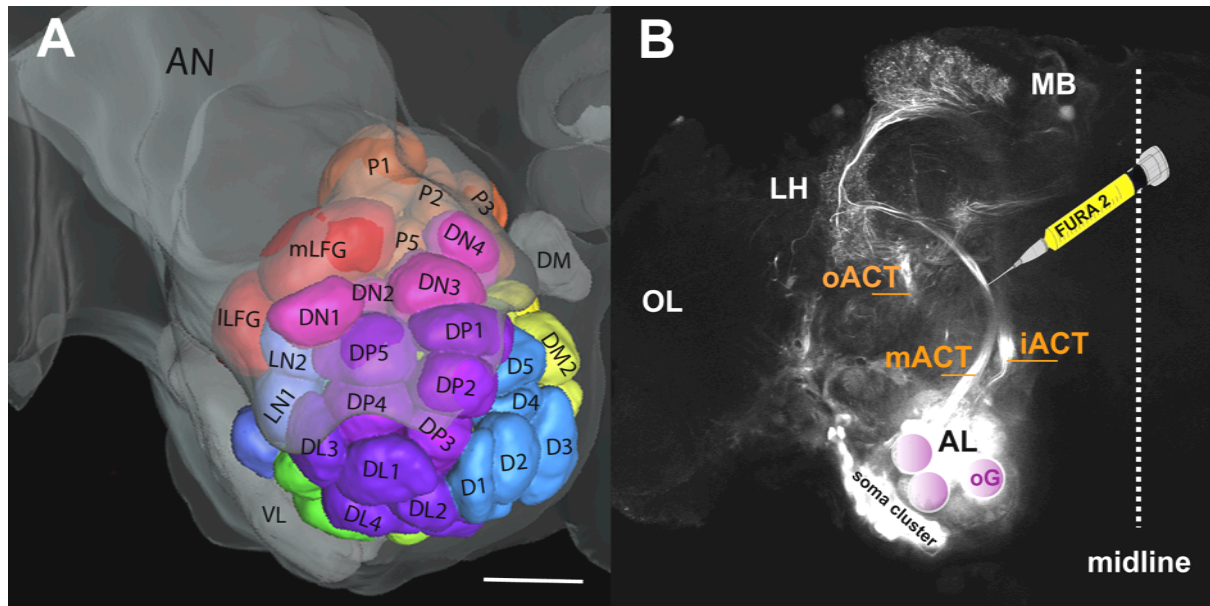


Figure 1: The olfactory pathway of *Manduca sexta*.

A. Color coded map of antennal lobe (AL) glomeruli (Große-Wilde et al 2011). 3D reconstruction of the female antennal lobe depicts a ventral view of reconstructed glomeruli ($n=70\pm 1$). Scale 100 μ m, DM dorsomedial somata cluster, VL ventrolateral somata cluster. (3rd group of AL neuron somata, the anterior group (AC) not shown.)

B. Example of the right hemisphere of the female *Manduca sexta* brain with focus on the AL and its efferent innervation by projection neurons (PNs). Projection view of confocal optical orthogonal slices depicting an anterograde micro-ruby mass fill of the AL output tracts and their projections in the MB and LH. MB mushroombody, LH lateral horn, CB central body, OL optic lobe, glom glomerulus.

Retrograde staining was performed by injection of dye into the PN antennocerebral tracts using a glass electrode coated with crystals of Fura-2 dextran (potassium salt, 3000 MW, MolecularProbes, Eugene, OR) dissolved in 4% bovine serum albumin solution. This dye application method has been shown to be specific and effective in honeybees (Sachse and Galizia, 2002). The glass electrode (diameter 15 μ m) was manually inserted into the deutocerebrum close to the midline of both hemispheres, aiming for both the -inner and outer antenno-cerebral tracts (ACTs, Figure 1). Preliminary studies with tetramethylrhodamine-dextran (micro ruby, Molecular Probes) were conducted to determine the location and projection of the different ACTs in *Manduca* (Figure 1). Micro ruby was inserted into the AL using an identical injection procedure applied for Fura-2 dextran. Dyes were allowed to travel for 2h (micro ruby) and 7h (Fura-2 dextran) at room temperature. Successful PN loading was determined by strong staining of the lateral soma cluster (Figure1).

Imaging was performed using a T.I.L.L. Photonics imaging system (Martinsried, Germany). Appropriate filter settings allowed simultaneous measurement of the two calcium-sensitive dyes. Monochromatic excitation light alternated between 340nm, 380nm (fura) and 475nm (calcium green). As filters, a dichroic beamsplitter (505DRLPXR) together with an alpha longpass emitter (emissionfilter, 515ALP) were used. Light emitted by stained cells peaked at wavelengths of 536nm and 510nm after excitation for Calcium Green-2 AM and Fura-2 dextran, respectively. The imaging set-up consisted of a CCD camera (Olympus U-CMAD3) mounted to an upright microscope (Olympus BX51WI) equipped with a water immersion objective (Olympus, 10x/0.30). Four-fold symmetrical binning resulted in 344 x 260 pixels images with one pixel corresponding to an area of 4 μm x 4 μm . Single experimental trials were recorded with a sampling rate of 4 Hz for 10 s, corresponding to 40 frames for each of the two calcium-sensitive dyes. Light was shut off between frames. Stimulation began 2 seconds after recording onset for a period of 2 seconds (frames 8-16). Several automated processing steps, e.g. background-, bleaching- and movement correction were applied using custom written software (IDL, ITT Visual Information Solutions) to enhance the signal-to-noise ratio. Details of this data processing are described in detail elsewhere (Sachse and Galizia, 2002; 2003).

Raw Data Processing & attribution of activity patterns

In this study, the olfactory response to an odor mixture versus its single components was directly compared at two different processing levels (OSNs and PNs) within a single animal. Olfactory responses leading to increased neural activity were monitored as spatially restricted activity regions of increased fluorescence (F) in the antennal lobe. Fluorescence input signals (Calcium Green-2 AM, 475 nm measurements) were calculated as $(F-F_0)/F_0$ ($\Delta F/F$) with background F_0 as the average of fluorescence in frame 3-7. Output signals (Fura-2 measurements) were first calculated as the ratio of the emitted light (340 nm / 380 nm, multiplied by 1000) and then compared as $\Delta F/F$. Fura ratios are approximately proportional to changes of the intracellular calcium concentration. Absolute values, however, are influenced by several experimental parameters, like staining intensity, background fluorescence, filter properties and light exposure time, and therefore vary greatly between individuals.

Input and output signals were attributed to regions of high activity. In order to compare both levels within individual animals, we had to compensate for different background fluorescence and different maximal activities by setting the strongest response region of each animal to 100% and scaling each response accordingly. In each animal the odor responses were normalized to the

maximal response for each dye separately (max $\Delta F/F$ for Calcium Green, max ΔR (340 nm / 380nm) for Fura-2). Maximal responses measured in each activity region had to exceed 2x SD above noise level for excitatory and 1x SD for inhibitory responses. Noise was determined as the standard deviation of the spontaneous activity between frames 3-7 (before stimulus onset) and averaged across all measurements within one animal. The applied differences in response criteria were necessary because inhibitory signals in general displayed weaker intensities than excitatory signals. Single glomeruli could not be visually identified under fluorescence light, and thus regions of activity were set and analyzed separately for each individual. Coordinates were established to mark the center of activity regions and to superimpose square areas of interest in which the mean activity were calculated over 11x11 pixels covering an area of 30x30 μm . The areas of interest corresponded to 50% of an averaged sized AL glomerulus in *Manduca* (Figure 1). We assigned individual coordinates to 5- 10 activity regions per animal. False-color pictures display the delta in fluorescence between two single frames, frame 4 (background) and 15 (response). A threshold was set to show only active regions and remove noise.

Input/output comparison & measurement of odor similarity in the moth AL

The aim of this study was to measure and compare odor representations at the in- and output levels based on Ca^{2+} signals elicited by stimulation with a blend and its 5 single components. Odor evoked calcium changes in OSNs and PNs of 8 animals were analyzed. For each trace, regions of statistically significant activity were defined as coordinates in an n-dimensional space (n defined by the number of coordinates, ranging from 5-10; Galizia et al., 1999c; Sandoz et al., 2003; Deisig et al., 2006). To measure similarity of odor-evoked activity patterns and compare input and output Ca^{2+} responses in the moth AL, the following analytical approaches were applied:

Vector analysis & Correlation Matrices

A resultant vector was calculated for each trace within an individual using all responding coordinates, and the dot product between vectors used to compare different traces by determining the angle between them [$\arccos(\text{dotproduct})$]. The dot product is a scalar value expressing the angular relationship between two vectors and each vector could be defined as a radius ($|\text{vector length}|$) and Θ (angle) in comparison to another trace. Thus, compared traces with similar spatial responses would generate angles close to 0° , while traces with exclusive patterns would establish an angle of 90° .

In this manner, traces were compared between input/output, high/low concentrations, and blend/single component pairs (supplemental Figure 1). Moreover, using the mean cosine of all

angles across animals, every possible odor pair correlation could be displayed as a correlation matrix for in- and output respectively (Figure 4). More precisely, a 0° angle indicating maximum similarity of odor presentation resulting in a $\cos(\Theta) = 1$ is displayed as a red square in the heat map (max positive correlation), and an angle of 90° , $\cos(\Theta) = 0$, displayed as blue (min positive correlation). The resulting two matrices were tested for significance using the Mantel test, a dedicated random permutation test (Mantel, 1967).

Statistical analysis & scientific artwork

Statistical analysis was performed using PASW 18.0 (SPSS, IBM, Inc.) and R statistical packages. Correlation matrices were generated in PAST, Paleontological Statistics Software Package for Education and Data Analysis. 3D scatter plots were created using Origin (OriginLab Corporation, Northampton, MA, USA). Scientific artwork was polished for publication with Adobe Photoshop & Illustrator CS4 (Adobe Systems, Mountain View, CA).

Results

To reveal the mechanisms of antennal lobe (AL) network processing of complex olfactory information in *M. sexta*, we analyzed AL responses to 5 monomolecular single components and their quintuple mixture. Odor-evoked calcium changes were recorded simultaneously for input (compound signal, dominated by OSN activity) and projection neuron (PN) output. This elaborate, combined physiological approach enabled us to directly measure how the cellular network of the AL shapes the spatial representation of an odor blend compared to its single components.

Response patterns

Odor-evoked calcium changes to monomolecular odorants and their quintuple mixtures lead to specific spatial activity patterns in the AL. In our study, 8 moths (out of 140 potentially stained animals) showed clear, reliable calcium responses at both processing levels and allowed us to record complete stimulus protocols. One animal was not tested to high concentrations of the single odorants and therefore was excluded from some analyzes (e.g. supplemental Figure S1). Two-second odor pulses led to reliable excitatory responses (intracellular calcium increase) resulting in odor specific activity patterns at the input level (OSNs, compound signal, Figure 2 green). Most recorded PN responses were also excitatory, however in roughly 10% of output responses ΔR decreased significantly in response to odor delivery (intracellular calcium decrease in 6 out of 8 animals; Figure 2B&E; Figure 3F). For the compound signal, without any stimulation, no calcium

changes were observed. In contrast, PNs revealed spontaneous activity in the absence of stimuli. These differences in activity support that the measurements from the 2 channels are indeed independent of each other. Successful dye loading in PNs could be easily determined by strong staining of the soma clusters (Homberg et al., 1988, Figure. 2A&B asterisks) and single somata showed strong excitation and /or inhibition to odor stimuli (Figure 2, excited somata.). The blend and its single components induced signals in different combinations and numbers of activity regions, ranging from 5 to 10 between individuals. Each activity region covered an area of 30x30 μ m, corresponding roughly to 50% of an average sized AL glomerulus in *Manduca* (Figure 1). This seemed appropriate as PN responses were in general more sparse as compared to the combined signal (Figure 2). Depending on the odorant tested, activity regions at the output showed complex response patterns: For example, in Figure 2A activity region 7 (blue trace) showed an inhibitory PN response to PAA & Z3HA, whereas for the blend & E2HA excitation was detected. Linalool elicited no response in region 7 for either enantiomer. Inhibitory signals were defined as negative ($\min \Delta F/F$ for Calcium Green, $\min \Delta R$ 340 nm / 380nm for Fura-2) responses detected after stimulus onset that exceeded the threshold $-1 \times SD$ below noise level for inhibitory responses. Conversely, excitatory signals were defined as $+2 \times SD$ above noise. A close examination of the global response for the various stimuli revealed a complex picture: The two Linalool enantiomeres (2C,D) showed differences of activation areas (region 6, light green and 9, pink) in the input, whereas their output patterns matched (but see region 5). In contrast the cis- and trans-isomers varied already in their input pattern and- as stated before- the output showed a strong inhibitory activity in region 7 for Z3HA that turned into an excitation for E2HA. PAA, the only aromatic compound in our odor set elicited the most difference in response pattern between channels. Interestingly, the very strong blend response resulted in a much broader pattern when compared to the single components and a total 10 activity regions were excited by the blend in this animal. In the output pattern of one region (4 turquoise), the activity was also missing.

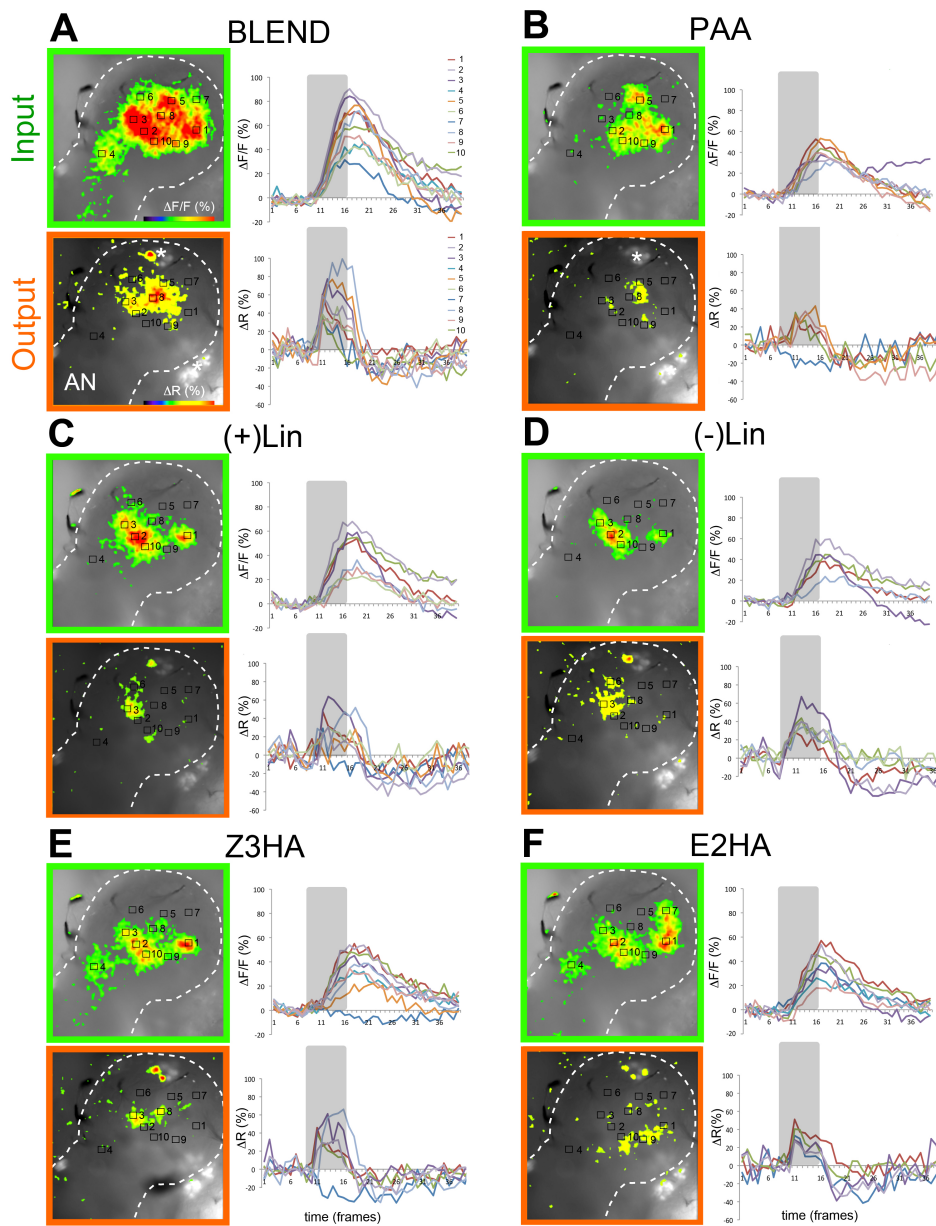


Figure 2. Representative example of simultaneous imaging within a single *Manduca* female AL. Olfactory responses to an odor mixture vs. its single components leading to increased neural activity was monitored as spatially restricted activity regions of fluorescence change (ΔF) in the AL at two different processing levels (Input, compound green frame and output, PN, orange frame). Left panel: False color coded AL patterns evoked by the blend and its single components are overlaid on the intrinsic fluorescent background. Clear spatial differences in odor-evoked activity patterns between input and output indicate AL network modulation. The AL border is marked with a dotted line with the antennal nerve (AN) entering from the lower left corner. Asterisks indicate stained PN soma clusters. Note that glomerular structure is not visible. Right panel: Time course of the raw calcium signals in individual activity regions. Each recording trial lasted 10s (40 frames) with odor stimulation (2s) indicated by grey bars. With both staining methods, odor application lead to a strong change in calcium levels. Odor responses were normalized to the maximal response for each dye separately. PN responses show a characteristic faster rising and decay time than the prolonged compound signals. Note that at the output level odors evoked both excitation and inhibition in PNs (e.g. B, E inhibitory signal in activity region 7).

Response Latency

Interestingly, considerable inconsistencies in the temporal pattern of in- and output timing occurred: Odor evoked PN responses showed faster temporal dynamics when compared to the simultaneously measured compound signals in all animals. On average, output signals to the blend reached a maximum value of $1.6 \pm 1.6s$ SEM after stimulus onset, whereas the significantly slower compound signal took $2.7 \pm 0.7s$ SEM to reach maximum. The observed difference in latencies is possibly due to dye dynamics of the AM or to differences in the calcium influx and buffering mechanisms of PNs and OSNs (Sachse and Galizia, 2003). In general, calcium green responses showed a phasic-tonic shape, with a slow return to baseline after stimulus offset and in some cases a prolonged tonic component with no return to baseline within the 10 sec recording ($>7s$, Figure 2 A, C, E, F). In contrast, Fura recordings were clearly phasic, returning to baseline very shortly (~ 2.5 sec after stimulus onset, Figure 2). Thus PN responses showed a characteristic faster rising and decay time when compared to the prolonged compound signals. Therefore, the temporal aspects comparing input to output were not considered further.

However, when compared within one processing level, response latencies did differ significantly depending on the given stimulus. In the compound signal, the mean latency of the blend was significantly shorter when compared to 4/5 single components (PAA, E2HA and both linalool enantiomers $p < 0.05$, compare Table 1). In contrast in the Fura signals only PAA showed a significantly longer latency of response onset when compared to the blend ($p = 0.015$).

It cannot be determined if the shorter latency observed for the blend is caused by network properties or simply reflects an ambiguously shorter latency to one of the single components (e.g. Z3HA input, (-) Lin output).

Table 1: Mean latencies (in seconds) of response onset to the blend and its single components tested at the higher blend concentration [c] at the two processing levels.**

Stimulus	BLEND	PAA	(+)Lin	E2HA	Z3HA	(-)Lin
Processing level	low[c]	high[c]	high[c]	high[c]	high[c]	high[c]
INPUT (Ca ²⁺ green signal)	2.65 ± 0.0	$3.11 \pm 0.2^*$	$3.17 \pm 0.2^*$	$2.95 \pm 0.1^*$	2.57 ± 0.21	$3.09 \pm 0.1^*$
OUTPUT (Fura signal)	1.55 ± 0.12	1.52 ± 0.3	$2.40 \pm 0.3^*$	2.43 ± 0.45	2.48 ± 0.70	0.94 ± 0.31

(Asterisks indicate significant differences for paired mean latencies blend/single component according to Student's t-tests)

Input vs. Output: Patterns of network interactions

Blend patterns at the two processing levels

To assess the predictability of response patterns, a projected blend for each animal was created (Fig. 3 black bars). The maximum fluorescence change in each activity region across all single component responses was set as the projected blend response for each individual animal (in- and output respectively). A first comparison of the recorded blend patterns (magenta bars) with the projected blend (black bars) at the input level (top trace) showed similar patterns in 6/7 animals (but compare 3D). This indicates that the blend representation of the compound signal can generally be predicted from the response patterns of the individual components (Figure 3.) and suggests that no strong network modulation at the OSN level took place. However, in one single case the blend response activated less activity regions than predicted by the single component patterns (Figure 3D, activity region 2&5).

In comparison, an opposite picture emerges at the output, indicating strong network interactions. To decipher in which ways the PN blend response was modified via the local network, we differentiated between two main network interaction types, synergism and suppression (compare Chapter III, Duchamp-Viret et al., 2003; Silbering and Galizia, 2007). Our criteria was highly restrictive: to be considered as a suppressive interaction at least one of the activity regions in the blend pattern (magenta bars) had to completely disappear in comparison to the projected blend (black bars). In turn, to match the criteria for a synergistic response a new activity area (magenta bar) had to be recruited. Following these simple rules, on the output level 4 out of 7 animals showed strong suppressive effects in the PN response (Figure 3B, D, E, G). Synergistic effects were less common but also found in 3 animals (Figure 3C, D, F). As a result blend response patterns of output neurons could not be predicted from the single component response in 6/7 animals. Areas that were highly activated by the single components disappeared completely in the blend pattern and vice versa (Figure 3 except A).

Comparison between the two processing levels revealed predominantly suppressive effects and synergism was witnessed in only one animal: In this case, in addition to a clear suppressive effect (3F, clear inhibition in region 7) a new activity region was recruited that was not active at the input level (synergism, area 9). The recruitment of additional active glomeruli in the output indicates disinhibition effects among GABAergic LNs. However, as we cannot completely ensure that our manual dye application always stained the entire neuronal population, conclusions drawn between the two levels are tenuous.

Novel blend patterns: simultaneous optophysiological studies at multiple levels of the moth AL

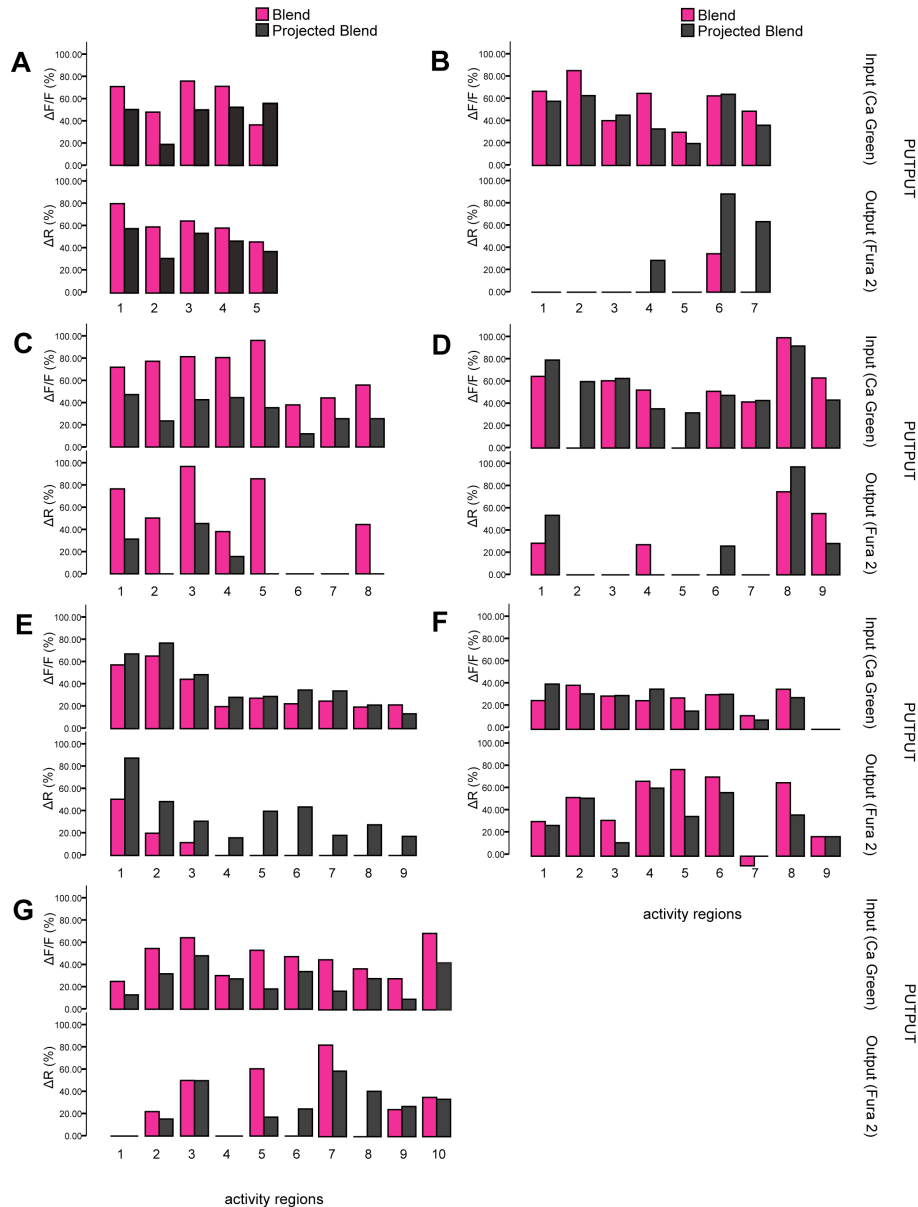


Figure 3: Comparison of blend representations in the AL at both input and output processing levels shows strong interactions in PNs suggesting network modulation. Magenta bars depict the normalized response activity for each activity region (number differs between animals A-G from 5-10). To assess the predictability of response patterns, a projected blend for each animal was created (black bars) using the maximum fluorescence change in each activity region across all single component responses (in- and output respectively). Comparison of the measured blend response (magenta bars) with the created projected blend (black bars) showed that at the input level, the blend representation could generally be predicted from the response patterns of the single components. PN blend responses showed substantial loss and gain of activity regions as compared to single component patterns. Thus, output patterns of single components did not typically reassemble the blend response.

Comparison of the blend pattern vs. its single components

In order to thoroughly assess how the odor representation changes from in- to output, we converted the spatial neural representation of each odor to a vector (supplemental Figure S1 & Figure 4A, see also material & methods). This simple approach does not provide details of specific

Novel blend patterns: simultaneous optophysiological studies at multiple levels of the moth AL

coordinates, but offers a comparison of patterns across tested individuals. Figure 4A compares the blend (red) mean angle vs. its single components across all animals at both processing levels, respectively. The clear spread at the output level, most obvious for PAA (yellow vector), Z3HA (blue) and (+)Lin (magenta), indicates substantial network interactions. Please note that all single components in Figure 4A were calculated and shown in relationship to the blend, therefore no conclusions between single components can be drawn (but see 4B). Moreover the blend response pattern also changed considerably from input to output (supplemental Figure S1, PUTPUT). Comparison of angles across animals (supplemental Figure S1) additionally revealed inter-individual differences: Whereas single components overall diverged more from the blend in the output (blend/low concentration $p=0.005$; Origins's F-test), there is no obvious pattern concerning each single component. Indeed, only PAA (yellow vector) was found to be nearly significantly different when compared to the blend ($p=0.08$; Origins's F-test).

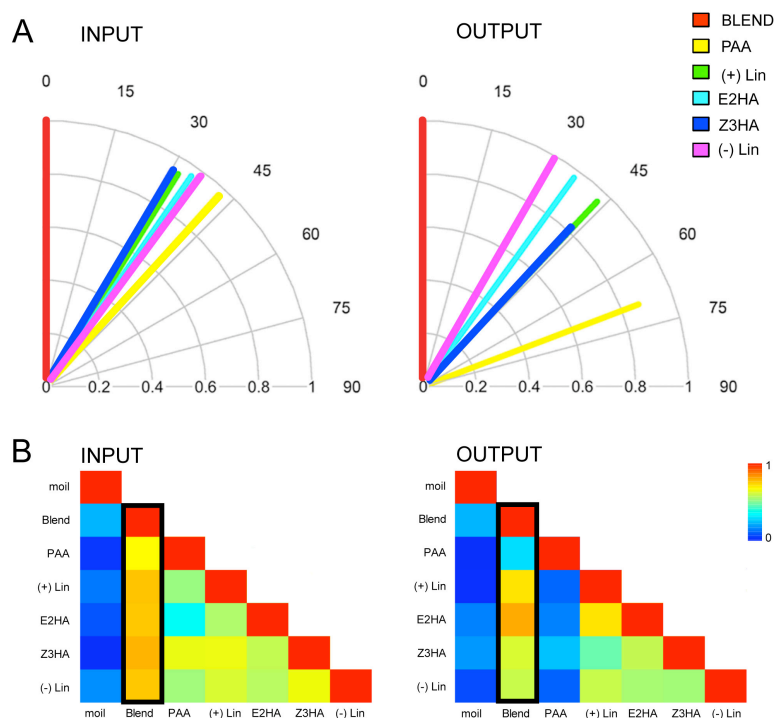


Figure 4. Odor representation changes from in- to output in the *Manduca* AL

A. Odor representation changes from input to output in the AL network. A resultant vector for each response pattern was calculated, and the dot product between vectors used to compare different traces by determining the angle between them [$\arccos(\text{dotproduct})$]. Comparison of the mean blend angle across all individuals vs. the mean of the single components shows a spread at the output level indicating network interactions. This is most obvious for PAA, Z3HA and (+) Lin.

B. Comparison of response patterns for all possible odor pairs at the 2 processing levels. A correlation matrix depicts the mean value of the vector cosines for in- and output respectively. Values are shown as a heat map with cosine values ranging from 0 to 1. A value of 1 (red) indicates an exact match in response patterns. As the values approach 0, the odor representations become more distinct (eg. 0=blue, moil or control). Black limits depict the data that can be directly compared to the corresponding angles in A (blend vs. single components). Both matrices correlate significantly $r=0.64$, $p=0.012$, Mantel test, Spearman's r .

Figure 4B provides a correlation matrix for both in- and output responses, using the mean cosine of the compared angles across all 8 animals. In this matrix, every possible odor pair correlation is shown. The data column with the black border can be directly compared to the corresponding angles in Figure 4A (blend vs. single components). Different colored squares indicate similarity between odor patterns, from maximum similarity (red square, 0°) to minimum pattern similarity (blue, 90°). The matrix shows that individual components in general were more different from the blend at the output. PAA again revealed decreased pattern similarity (blue) at the output level vs. the input, indicating strong network interactions- not only when compared to the blend but also to each single component. Indeed this was also the case for (+) Lin and Z3HA. This shows that the components exhibiting the most obvious spread in relation to the blend also revealed minimum pattern similarity to each other. It is likely that the reported differences in the blend pattern between the two processing levels were to a great extent shaped by these three components, thus increasing the coding capacity by decorrelating glomerular patterns. Conversely, (-)Lin and E2HA may play a minor role in generating the blend representation. Nevertheless, their relatively unchanged input/output patterns could indicate a labeled-line method of processing for these specific components.

Discussion

Applying optical calcium imaging techniques, we directly compared the olfactory responses to an odor mixture and its single components simultaneously at two different processing levels (OSN input and PN output) within a single animal.

Input / output comparison reveals patterns of network interactions

Recording odor-evoked activity to five monomolecular odors and their mixtures showed that the resulting input blend pattern could generally be predicted from the single component responses. This is in agreement with previous studies (Galizia et al., 1999b; Deisig et al., 2006; Carlsson et al., 2007; Silbering and Galizia, 2007). However, on the output level, strong interactions occurred in six out of seven animals: four animals showed strong suppressive effects in the PN response (Figure 3B, D, E, G), whereas synergism also occurred in two animals (Figure 3C recruitment in area 2&8, 3F strong inhibition in region 7). Interestingly, in one single case, both interactions were witnessed equally (Figure 3D, synergism/recruitment in area 4, suppression region 6). These results are consistent with our previous electrophysiological study, investigating blend processing and mixture

interactions at the single neuron level (Chapter III). The current results may even underestimate the numbers of interactions due to our conservative approach. In this study, any non-linearities were the result of a complete loss or gain of regions of activity in the blend as compared to single components (compare results, Figure 3). Our conservative analysis may therefore overlook weak suppressive (e.g. hypoaddivity) or synergistic effects, but also avoids the generation of false positives. However, the finding of clear and strong interactions in six out of seven animals supports our conclusions concerning the important role of the modulatory network and thus underpins the idea of a novel feature percept generated by the AL. Moreover, the agreement with our previous electrophysiological study in *Manduca* shows that the mechanisms of blend processing revealed on the single neuron level were maintained across the glomerular array.

Concentration effects of odor processing

Concentration effects and different dose response properties among blend components may establish non-linearity in the odor response resulting in eventual saturation (Sachse and Galizia, 2003; Stopfer et al., 2003; Wright et al., 2005). In order to prevent artificial non-linearity and compensate for concentration differences between the blend and its single components, monomolecular odors were presented in the lower part of the dynamic range of the dose–response curve (10^{-4}) (King et al., 2000; Reisenman et al., 2008) and also at “blend” concentrations (high [c]**, see supplemental Figure 1 and material & methods). Optophysiological recordings in moths show that response patterns vary with concentration and become increasingly coherent as the concentration increases (Carlsson and Hansson, 2003). These previous studies, conducted at the input level, investigated concentration effects over a range of several log units, whereas the high concentration used in the present study is still within one log step [10^{-4}]. Regarding our results, the recruitment of additional olfactory receptor neurons by high concentrations (Vareschi, 1971; Firestein et al., 1993; Duchamp-Viret et al., 2003) is unlikely.

Relevance of single components in blend processing

Comparing patterns of odor representation at the two processing levels revealed increased network interactions for specific components. We showed that the similarity of odor patterns diverged remarkably from input- to output for PAA, Z3HA & (+) Lin. These three compounds not only revealed minimum pattern similarity at the output level compared to the blend (Figure 4A) but also to the other single components (Figure 4B). Interestingly despite their chemical similarity, the two isomers and enantiomers depicted less change from input to output indicating weaker interactions across

the glomerular array: When compared across all animals in general (+)/(-)Lin and E2HA/Z3HA did not differ in their similarities to each other between the two processing levels (Figure 4B, correlation matrix, (+)/(-)Lin and E2HA/Z3HA both lemon green in input and output). However a closer look at individual cases may change the picture: In Figure 2 e.g. the two Linalool enantiomers indeed show more differences of activation areas in the input when compared to their output patterns (Figure 2C,D). In contrast the cis- and trans-isomers vary already in their input pattern. Interestingly, although the strength of dissimilarity seems to be maintained in the output (2E, F), the character of dissimilarity changes (different activity regions as well as emergence of inhibition as well as excitation).

Optical recording studies at of the olfactory bulb and the AL showed that odorants sharing similar molecular structure also activated similar patterns of glomeruli (Friedrich and Korsching, 1997; Rubin et al., 1999; Sachse et al., 1999; Uchida et al., 2000; Wachowiak and Cohen, 2001; Fried et al., 2002). Moreover, Guerrieri et al. (Guerrieri et al., 2005) correlated behavioral perceptual odor similarity with optophysiological studies measured at the input level of the honeybee AL (Sachse et al., 1999). Actually, the molecular communalities between odors determined by similar input activity patterns in the AL are reflected in the perceptual odor space of bees. These findings are consistent with behavioral studies in moths showing that structural characteristics such as functional group and carbon-chain length play an important role for odor learning. Both functional group and chain length seem to affect the perceived odor quality and differences in carbon number between components are reflected by reliable odor discrimination (Daly et al., 2001a & 2001b). Hence blends composed of closely related odors should reveal stronger interactions than mixtures of less similar compounds (Smith, 1998) and may explain the high levels of interactions reported in our study. However, it is also known that marginal modifications in the molecular structure can lead to substantial differences in the perceived odor quality (Laska et al., 1999) and one should keep in mind that similarity in the processing patterns and behavioral relevance may diverge substantially for specific components depending on the context as well as the physiological state of the animal.

The increased network interactions shown for PAA, Z3HA & (+) Lin could indicate the behavioral relevance of these components, which are all present in the odor bouquet of the flowers and plants on which *Manduca* feeds and oviposits (Kessler and Baldwin, 2001; Reisenman et al., 2009; Allmann and Baldwin, 2010). Future behavioral trials may clarify the correlation between compound quality and behavioral relevance. PAA, the only aromatic compound tested in the study, revealed the most distinct pattern similarity at the output level compared to the blend and also showed the most

diverse input pattern. It is conceivable that PAA is not part of the blend percept itself, but rather serves as an attention cue priming the network e.g. shown for cross-modal integration in humans (Gottfried and Dolan, 2003; Bensafi et al., 2007). Conversely, the relative similarity between input and output patterns for E2HA and (-) Lin may indicate that these odorants are processed via labeled-line pathways. Both components could trigger avoidance behavior in *Manduca* (Reisenmann et al., 2010, Allman and Baldwin, 2010). Interestingly, a similar labeled-line pathway for avoidance behavior has been suggested in other systems, e.g. CO₂ and Acid-sensing pathways in *Drosophila* (Ai et al., 2010). Taken together, our results indicate that the degree of network interactions is to a certain extent component specific.

A blend feature created by the moth AL

Our combined physiological approach indicates that the local network (LNs) modulates PN output in the moth AL to generate a unique blend feature as early in the olfactory pathway as the first processing stage, the AL. In addition to the local inhibitory (GABAergic) network, cholinergic, multiglomerular LNs have been recently described in *D. melanogaster* (Olsen et al., 2007; Root et al., 2007; Shang and Miesenböck, 2007) suggesting that cholinergic LNs could be involved in broadening the response profile of PNs (Shang and Miesenböck, 2007), presumably in a glomerulus dependent manner (Olsen et al., 2007). Furthermore excitatory, glutamatergic LNs (Chou et al., 2010) and electrical synapses between excitatory LNs and PNs can also mediate lateral excitation (Huang et al., 2010; Yaksi and Wilson, 2010). Excitatory local neurons are likely candidates to be a major player generating synergistic interactions, but have not yet been discovered in *Manduca*. Interestingly, in our study, a broadening effect of the PN profile was witnessed in two out of seven animals (e.g. Figure 3F,C, truly synergistic effects). The comparable lower levels of synergistic effects infers disinhibition effects among GABAergic LNs rather than necessitating an additional costly but rarely used excitatory network. However, as stated before, our approach was not intended to reveal glomerular connectivity across individuals and thus does not allow for conclusions concerning specific glomerulus-dependent interactions. Moreover, in contrast to honeybees (Fonta et al 1993), in *Manduca* most local neurons show a typical broad “symmetrical” arborization pattern innervating the majority of AL glomeruli (Matsumoto and Hildebrand, 1981; Reisenman et al., 2011, also compare Chapter III). Consequently, an inhibitory global network incorporating a population of neurons with glomerulus-specific connectivity for general odor blends seems unlikely in *Manduca* (but compare the *Manduca* MGC: Christensen and Hildebrand, 1997; Lei et al., 2002; Heinbockel et al., 2004).

Once blend information is separated into different input OSN channels, a subsequent regrouping of at least a part of the blend information must occur to establish the reported unique blend feature. Since there are limited mixture interactions at the input level in *Manduca*, a blend feature created by the moth AL seems logical: In contrast to the very narrowly tuned and highly sensitive pheromone receptors in moths (Kaissling et al., 1989; Kalinova et al., 2001), general odorant receptors may be both narrowly or broadly tuned (Hansson and Hallberg, 1999; Rostelien et al., 2000a & 2000b; Shields and Hildebrand, 2000; Hillier et al., 2006; Hillier et al., 2007). Single sensillum recordings recently conducted in our lab show that OSN response profiles of *Manduca* can be very broadly tuned, and in some cases as much as 30 components may induce activity in a single sensillum (Shields and Hildebrand, 2001). An olfactory system incorporating high levels of nonlinear coding, demanding broadly tuned receptors, may be advantageous to process signals from a “noisy” periphery. As a consequence, a minimum of receptors with varying selectivity could detect a huge variety of complex blends. A low number of receptor types in *Manduca* is supported by the small numbers of olfactory receptors identified (Chapter I). However, considering this “peripheral cacophony”, a presorting at the input level, which could not be confirmed in the recent study, should thus not be totally excluded (Ochieng et al., 2002; Hillier and Vickers, 2011). Moreover, when studying olfactory processing in the AL, one must also consider that downstream events (e.g. mushroom bodies, lateral horn) may significantly alter blend representations by combining different channels (Laurent, 1999; Perez-Orive et al., 2002).

Conclusions

Blend patterns in *Manduca* are highly non-linear and strong patterns of interactions, such as suppression and synergism emerged. Moreover, our results indicate that the degree of network interactions is to a certain extent component specific.

Our combined physiological approach showed that at the input level the pattern of blend representation in the moth antennal lobe (AL) is reassembled by the representation of the single components. In contrast, at the output level strong mixture interactions occurred. At the output level a resulting loss or gain of activity regions in the blend pattern as compared to single components was witnessed in 6 out of 7 animals, providing evidence for strong interglomerular inhibition (suppressive effects) and potential dis-inhibition (synergistic effects). Hence, the output odor pattern of a blend response cannot be predicted simply from its single component patterns.

Generation of a novel pattern thus establishes a unique blend feature as early as the initial olfactory processing center in the brain, the AL. Suppressive effects may enhance the contrast of blend representation (Sachse and Galizia, 2002; Vucinic et al., 2006) as well as strengthen intraglomerular synchrony (Lei et al., 2002) and therefore build a profound basis for further downstream blend processing in the insect's brain.

ACKNOWLEDGEMENTS

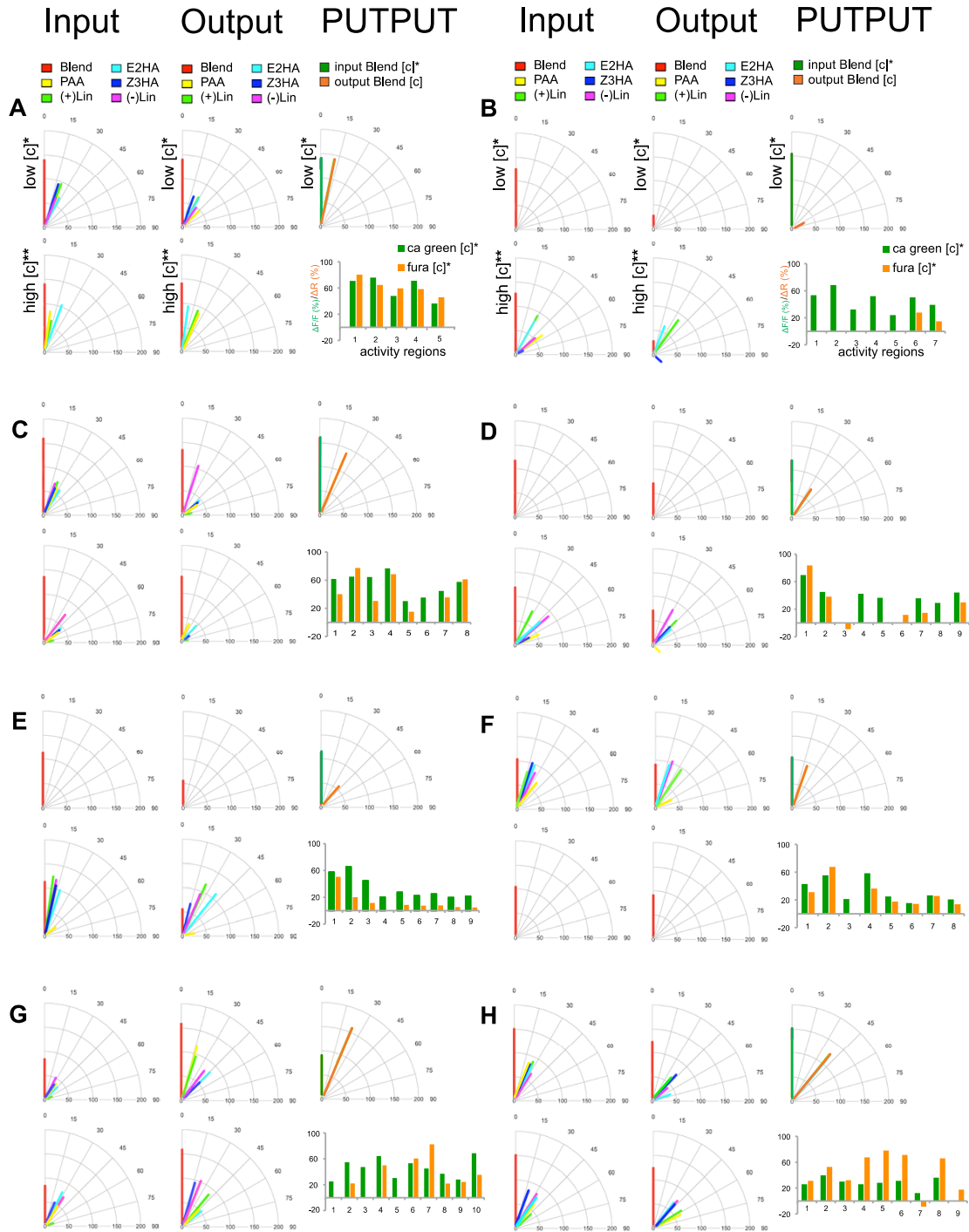
This work was supported by Ichem (6th programme of the EU) and funding from the Max Planck Society to BSH. We thank Daniel Veit for engineering the stimulus delivery system, writing the lab-view software and solving technical problems. We are grateful to Silke Sachse for support and helpful advice on Calcium Imaging. We also thank Martin Strube-Bloss and Sonja Bisch-Knaden for statistical advice. We would like to express our gratitude to the Ichem consortium for fruitful discussion.

ABBREVIATIONS

AL, antennal lobe; LN, local interneuron; OSN, olfactory sensory neuron; PN, projection neuron; MB, mushroombodies; LH, lateral horn.

Supplemental Data

Supplementary Figures



Supplemental Figure S1. AL odor representation between input and output across all tested animals (n=8). Comparison of angles for each individual as calculated in Figure 4 reveals inter-individual differences: Whereas in most cases single components in general seem to diverge from the blend and spread more in the output, there is no clear pattern visible for separate components. Only PAA (yellow vector) was found to be nearly significantly different when compared to the blend ($p = .08$, f-test). Please note that the mean angles and cosines shown in Figure 4 are calculated from all angles shown for high[c]**.

GENERAL DISCUSSION

Our world is a cacophony of scent. What we perceive as a single scent is indeed several compounds acting in concert to form an odor blend. An insect's ability to perform odor-mediated behavior (e.g. mate finding, nectar feeding, and host locating) requires the olfactory system to process and reliably identify complex volatile signals in a constantly changing background. Yet how do animals decipher these complex mixtures from a noisy background and extract a meaningful signal? Searching for the neuronal mechanisms that underlie complex odor information processing in the moth brain was the central task of this dissertation.

A blend feature established by the AL

My findings reveal that odor blends establish a unique blend feature separate from individual component identities as early as in the first olfactory processing stage, the antennal lobe. Once blend information is separated into different input OSN channels, a subsequent regrouping of at least a part of the blend information must occur to establish the reported unique blend feature. However, little is known where or how this integration occurs in the olfactory system.

Laurent in his review (Laurent, 2002) states that if we wish to understand brain operations we should alter our thinking about sensory integration by dissociating ourselves from a linear and passive point of view where stimulus A leads to a response in area B (...). Rather, we should picture sensory integration in active terms considering a response as an ongoing transformation towards some other goal. Indeed, downstream events (e.g. Mushroom bodies and/or lateral horn) significantly alter odor representations by combining information pooled across different channels (Perez-Orive et al., 2002; Laurent, 2002). Thus, retaining the complete information about each single component seems highly inefficient and a certain convergence of the vast amounts of information within the AL should be a required step.

As shown by the morphological data in Chapter III, neural circuits in *Manduca* are massively interconnected by the local neuron network and uniglomerular projection neurons innervating completely different areas in the AL still respond to the same components. The finding that uniglomerular PNs with similar response profiles revealed remarkably different innervation patterns supports that LNs are a major player in the optimization of blend processing in the AL, and strengthens the assumption that blends are represented globally across the AL network. Thus the

moth olfactory system is not based on a simple sequential scheme of elemental linear integration, but rather utilizes non-linear feature extraction to reduce dimensionality of the vast receptor input and concentrate the output signal for further processing by higher brain areas.

From a peripheral view, a unique blend feature created by the moth AL seems logical: In contrast to the very narrowly tuned and highly sensitive pheromone receptors in moths (Kaissling et al., 1989; Kalinova et al., 2001), general odorant receptors can be both narrowly or broadly tuned (Hansson and Hallberg, 1999; Rostelien et al., 2000a; Rostelien et al., 2000b; Shields and Hildebrand, 2000; Hillier et al., 2006; Hillier et al., 2007). Single sensillum recordings show that OSN response profiles of *Manduca* can be very broadly tuned and in some cases and at least 30 components may induce activity in a single neuron (Shields and Hildebrand, 2001).

An olfactory system incorporating high levels of nonlinear coding, demanding broadly tuned receptors, may be advantageous to process signals from a “noisy” periphery. As a consequence, a minimum number of receptors with varying selectivity could detect a huge variety of complex blends. This is also supported by our antennal transcriptome study, reporting a rather small number of putative antennal receptor genes (Chapter I). Moreover, our optophysiological studies (Chapter IV) revealed only limited mixture interactions at the input level in *Manduca*. A presorting of blend components at the receptor level in *Manduca* is thus implausible.

As shown in Chapter III and IV, the neurophysiological studies reveal significant non-linear coding of host-associated blends, indicating high levels of across-fiber patterning that establish a novel “blend code” separate from individual component identities. This confirms that the moth olfactory system is not simply based on a sequential scheme of linear integration where the representation of odor mixtures can be explained by their elementary compounds. Indeed, the AL utilizes feature extraction to reduce dimensionality of the vast receptor input emitted by the plethora of odors *Manduca* encounters in nature. In this process, the lateral network plays a major role in concentrating the output signal for further processing by higher brain areas.

The AL, the first olfactory neuropil in insects is thus not a simple relay station, but an indispensable early sensory circuit that optimizes input formatting.

Mechanisms of blend processing

Utilizing the novel stimulus device for our electrophysiological experiments (Chapter II), we were able to assess the cellular and spatiotemporal response kinetics of single AL neurons. In Chapter III, we show that at least 3 different cellular parameters appear to be involved in establishing the blend

response: (1.) the morphology and location of neurons within the AL, (2.) the firing rate of individual neurons (frequency and temporal pattern), and (3.) the neuronal response latency. These results indicate that each neuron utilizes a variety of parameters to produce the novel, unique signal representing the entire blend.

In particular, all neurons exhibited high levels of non-linearity for both response frequency and latency, indicating that both response rate and latency are important for coding the unique blend identity. Moreover temporal patterns revealed that across single antennal lobe neurons, inhibitory responses may signify the general presence of an odor, while excitatory and biphasic responses indicate odor concentration and identity, respectively. Sensory information incorporating both rate and spike timing, allows for processing of complex mixtures by a limited number of cells, with blends coded not only by where and how cells fire, but when.

Although both types of AL neurons analyzed were similar in terms of response patterns and types (ChapterIII), LNs exhibited significantly shorter latencies. Additionally, uniglomerular PNs with similar response profiles revealed remarkably different innervation patterns. This supports the role of LNs in the first level of blend processing in the AL and strengthens the assumption that blends are represented globally across the AL network.

Intrestingly the mechanisms of blend processing revealed on the single neuron level were maintained across the glomerular array (ChapterIV): we could show that at the input level, the pattern of blend representation in the moth antennal lobe (AL) was reassembled by the representation of the single components. In contrast, strong patterns of mixture interactions occurred at the output level, such as suppression and synergism. Thus, the cellular mechanisms discussed in ChapterIII not only alter the blend response in single AL neurons, but shape the unique global pattern of the blend across the glomerular array. In short, the output odor pattern of a blend response cannot be predicted simply from its single component patterns. As a consequence, higher order levels in the moth brain receive information containing the unique quality of a mixture, but may also lose some information about its single components.

Form follows function in the olfactory system

Odorant molecules are detected by peripheral sensory neurons (OSNs) on the antenna that relay the information about the odorant molecule from the external world to the insect brain. Each receptor encodes a seven-transmembrane domain protein that is generally expressed by only a single OSN type (Mombaerts, 1996). As a consequence, OSNs expressing the same olfactory receptor protein

converge typically onto the same glomerulus in the antennal lobe (AL) (Ressler et al., 1994; Mombaerts, 1996; Vosshall, 2000). Thus, the response of a particular glomerulus is to a certain extent determined by the odor response spectrum of a specific OSN type. But, as shown by the high levels of interaction reported in Chapter III and IV, a glomerulus is not a simple relay station and comprises more than just the averaged receptor input. Indeed, glomeruli provide a sophisticated microcircuitry among OSN input, local interneurons (LNs) and output neurons (PNs), which convey the olfactory information to higher order brain centers (reviewed by Mori and Yoshihara 1995; Shipley and Ennis 1996; Hansson and Anton 2000).

Olfactory glomeruli are present in virtually all olfactory systems and have been described as one of the most distinctive structures in the brain (Shipley and Ennis 1996). Across animal species, the number of glomeruli ranges from 43 (*Drosophila* Laissue et al., 1999), up to 1800 in mice (Zhang and Firestein, 2002). In Chapter I, we report the identification of 54 receptor fragments from the *Manduca* antennal transcriptome compared to 70±1 and 68 designated glomeruli in the female and male AL, respectively. A high number of olfactory glomeruli (typical for hymenopterans: Flanagan and Mercer, 1989; Galizia et al., 1999c; Smid et al., 2003; Kleineidam et al., 2005; Nishikawa et al., 2008; Zube et al., 2008b; Zube and Rössler, 2008; Kelber et al., 2009), is considered to reflect outstanding abilities in odor discrimination (Kleineidam et al., 2007) and could establish the basis for the sophisticated life-style of social insects, but may also suggest perceptual biases for the smaller *Manduca* AL. However, considering *Manduca* as a solitary feeding generalist, strict odor discrimination of monomolecular components may be less important than identifying a viable nectar source during variable environmental conditions. Generalizing of similar odors, e.g. reported in honeybees (Giurfa et al., 2003; Guerrieri et al., 2005) therefore should not be considered a restriction in the processing system, but an adaptation to identify behaviorally important odor mixtures in nature.

The multidimensional olfactory space

Olfactory stimuli offer multidimensional information and processing, and can be studied from many different perspectives. From a physical perspective, molecular features such as chain length, molecular weight, chirality, or stability may be reasonable anchor points, whereas a neuroethologist would rather begin from the animal's point of view. When a female moth searches for a nectar-rich flower or a suitable oviposition substrate, her olfactory system must extract information from a potpourri of components. Therefore, rather than assess the molecular composition of an odor, the

moth may reliably identify an odor blend as a unique feature in a steadily changing natural environment.

Most blend coding studies have utilized binary mixtures; (Boyle et al., 2009; Broome et al., 2006; Carlsson et al., 2007; Deisig et al., 2003; Galizia and Menzel, 2001; Brossard et al., 2007; Cashion et al., 2006; McNamara et al., 2007; Lapid et al., 2008; Fernandez et al., 2009; Frederick et al., 2009; Rospars et al., 2008) but ChapterII shows that only 15% of all recorded cells in our electrophysiological study responded to only two compounds. Indeed, most cells responded to tertiary (26%) and quaternary mixtures (41%), suggesting that investigations of blend processing involving several compounds may reflect the natural processing of host odors more accurately. But, we admit; compared to the plethora of odors *Manduca* encounters in nature, the selected compounds for this study were still extremely limited.

The complex nature of accurate stimulus presentation, and the lack of adequate devices may be the reason why mostly binary odor mixtures have been investigated: Most natural odors possess considerably different chemical and physical properties [see Dunkel et al., 2009 database “Superscent”, Charité Berlin] challenging the spatiotemporal presentation of blend stimuli for olfactory experiments. Presenting a complex, unified blend not only necessitates accurate control of the timing and homogeneity of the odor stream, but also requires adjustment of concentrations and calibration for different vapor pressures of the single components. Improper blend presentation can even alter the outcome of olfactory experiments as recently shown by Syed and Leal (2008). They discovered that DEET, the most common active ingredient in insect repellents, “masks” or inhibits the volatility of odors when they are placed together in conventional odor cartridges. For this reason, we developed a novel, multicomponent stimulus system for use in olfactory experiments to accurately assess first order blend processing in the moth brain (ChapterIII&IV). This multicomponent device, described in detail in ChapterII, is capable of presenting up to 8 different odors simultaneously or in sequence at defined concentrations and time scales to 10 Hz without leakage or contamination. All odorants are separated in individual bottles to minimize physical or chemical interactions, and stimulations are exclusively performed from a saturated headspace of the odor solution.

Methodical prospects & constrains of the combined physiological approach

Although the sharp recordings reported in ChapterIII provide high temporal resolution, only one neuron can be measured at a time. Simultaneous analysis of the entire antennal lobe network was therefore necessary to properly demonstrate the “blend representation” occurring in AL (ChapterIV). Thus, we performed optophysiological studies of the AL to monitor odor-evoked neuronal activity across the glomerular array.

In optophysiological studies, the visibility of glomeruli and assignment of activity spots to identified glomeruli is an important issue when working with non-genetically modified animals. In most Hymenoptera, the glomerular structure is clearly visible under fluorescent light (Galizia et al., 1998; Galizia et al., 1999a; Zube et al., 2008a; Dupuy et al., 2010) and identification of single glomeruli using a digital atlas of the AL is common practice (Galizia et al., 1999b; Sachse et al., 1999, Sachse, 1999 #153). ChapterI provides an example of a newly constructed 3D AI map of *Manduca* based on confocal data. Nevertheless, in many moths including *Manduca*, the glomerular organization under fluorescent light is indeterminable and the glomerular structure may be unclear. Different techniques were developed to either circumvent this problem (Hansson et al., 2003; Carlsson et al., 2002) or ameliorate it through subsequent application of additional staining methods (voltage dependent dyes Galizia et al., 1999c; Carlsson and Hansson, 2003). To make glomeruli visible, Skiri et al (Skiri et al., 2004) treated ALs after recording with proteases to digest the neurolemma in combination with membrane permeable dyes.

For the optophysiological study described in ChapterIV, two different calcium sensitive dyes were applied concurrently within one animal (Sachse and Galizia, 2003). Simultaneous measurement of OSN network input in concert with PN output enabled us to assess network processing across the glomerular array, irrespective of glomerular identity. Further elucidation of glomerular structure was not necessary for generating conclusions concerning blend processing. With this elaborate technique first shown by Sachse in honeybees (Sachse and Galizia, 2003), we were able to quantify the odor information fed into the network (OSN input) as well as the resultant output of network processing (PN output) based on Ca²⁺ signals elicited by a blend vs. its single components. In short, this tool provided us with direct information on how the cellular network of the AL shapes the representation of odor blends.

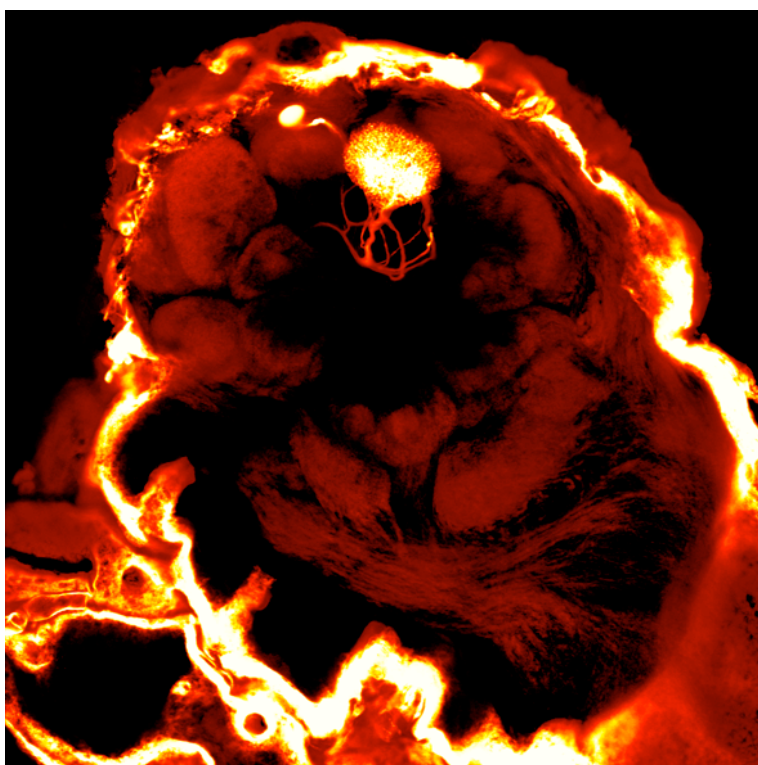
Component specificity & its behavioral impact

In ChapterI, our 3D-reconstruction of the *Manduca* AL data revealed five female-specific glomeruli correlating to five female-specific OR genes. Three receptors are expected to belong to the well-described female specific LFG complex consisting of two distinct glomeruli (King et al., 2000). Those glomeruli were recently described by Reisenmann et al. to process the two linalool enantiomers respectively (Reisenman et al., 2004). Obvious receptor candidates could be the two homologues of the Bombyx linalool-receptors BmorOR-19, MsexOR-5 and -6 (27-32). We therefore hypothesize that the detection of the two linalool enantiomers in *Manduca* is mediated by different neuron populations and receptors (most likely MsexOR-5 and -6). The missing third LFG-related receptor is probably the homolog of the Bombyx female-specific BmorOR-30: MsexOR-13. Interestingly, in our electrophysiological study (ChapterIII) 100% of all blend- responsive cells responded to (+)-linalool (both PNs & LNs), a compound suggested as particularly important for oviposition behavior in *Manduca* (Reisenman et al., 2009; Reisenman et al., 2010). Moreover, in agreement with our electrophysiological study in ChapterIII this component specificity was also maintained across the glomerular array (ChapterIV). Optophysiology revealed increased network interactions for (+) Lin, PAA and Z3HA, suggesting the behavioral relevance of these components found in the odor bouquet of the flowers and plants on which *Manduca* feeds and oviposits (Kessler and Baldwin, 2001;Reisenman et al., 2009;Allmann and Baldwin, 2010). Future behavioral trials may clarify the correlation between compound quality and behavioral relevance.

General Conclusion

The main challenge of my study was to reveal how complex odor information is processed in the insect olfactory system. I show that odor mixture processing in the moth olfactory system is a highly combinatorial, non-linear integration process. My findings reveal that odor blends establish a unique blend percept separate from individual component identities as early as the first olfactory processing stage, the antennal lobe. This indicates that the moth olfactory system is not based on a simple sequential scheme of elemental linear integration, but rather utilizes non-linear feature extraction to reduce dimensionality of the vast receptor input and concentrate the output signal for further processing by higher brain areas. An early sensory circuit that optimizes input formatting seems reasonable condensing the vast amounts of information that converge onto the AL. The local network via its mainly inhibitory connections is likely the main player in generating this novel blend feature. Combinatorial coding demanding broadly tuned receptors may be advantageous to process signals from the diverse olfactory bouquet *Manduca* encounters in nature. As a consequence, a

minimum of broadly tuned receptors would be necessary to detect a multitude of complex blends. It further suggests that a biomimetic system based on the moth brain can, with a minimum of detectors and processing power, decipher complex odor information on both temporal and spatial scales. Thus, the results of this dissertation provide a solid foundation for future studies on complex blend processing across processing levels in the olfactory system. Moreover my study gives new insights into how the brain processes multidimensional feature space. In this framework, therefore, studies of AL processing may also have long term implications on the general design of biomimetic technology such as automatic identification and data capture, product labeling, search and rescue and medical diagnostic technology.



Stained uniglomerular projection neuron in the antennal lobe of a female *Manduca sexta* moth

SUMMARY

The world is a cacophony of scent, creating a spatially and temporally dynamic olfactory environment through which animals navigate. An animal's ability to perform odor-mediated behavior (e.g. resource allocation or mate finding) requires the olfactory system to process and reliably identify complex volatile signals in a constantly changing background. Insects have the remarkable capacity to recognize and discriminate odor blends even at extremely low odor concentrations. Moths are widely utilized in the field of insect olfaction because of their highly specific and sensitive olfactory sense, as well as their extraordinarily complex chemosensory behavior. When a female moth searches for a nectar-rich flower or a suitable oviposition substrate, her olfactory system must extract information from a broad palette of components. Therefore, rather than recognize the monomolecular odors themselves, the moth may identify an odor blend as a unique feature with particular relevance. The underlying processing codes in the brain should reflect such perceptual biases.

The aim of this dissertation is to investigate the processing of complex odor blends at multiple levels in the olfactory system of the hawkmoth *Manduca sexta*. Using a novel multicomponent stimulus device (ChapterII) and combined neurophysiological techniques (ChapterIII&IV), I addressed how complex host blend information is processed in relation to its individual component identities.

In insects, the initial representation of an odor blend occurs in the first olfactory center of the brain, the antennal lobe (AL). The resultant neural representation of an odor mixture may either retain the single-odor information of blend components, or reveal non-linear interactions between the components due to processing in the AL network. The phenomenon of a non-linear response to a mixture that is not predictable from its single component responses is called a "mixture interaction". Probing single AL neurons in ChapterIII, my electrophysiological recordings revealed that the vast majority of individual *in vivo* recorded neurons showed non-linear spike frequencies in response to a host blend versus its individual compounds. Multicomponent responses exhibited an array of "mixture interactions" including suppression, hypoadditivity, and synergism.

In ChapterIV, I applied optophysiological studies in order to monitor odor evoked calcium changes across the AL network to five host volatiles and their mixture. I simultaneously measured afferent network input descending from the antenna in concert with efferent output relaying the odor

information to higher brain areas. Comparison of neuronal activity patterns and response intensities showed that the blend pattern is reassembled by the representation of its single components at the input level. In contrast, at the output level strong mixture interactions occurred. Hence, the output activity pattern of a blend response is novel and cannot be predicted simply from its single component patterns.

My findings reveal that odor blends establish a unique blend feature separate from individual component identities as early as in the first olfactory processing stage, the antennal lobe. Moreover, analysis of blend input from OSNs cannot unambiguously predict AL output on any spatial or temporal scale. Shaped by the AL network, blend coding thus involves high levels of non-linear responses by AL neurons that produce the novel, unique signal representing the entire blend. Each neuron utilizes a variety of parameters such as, (1.) the morphology and location of neurons within the AL, (2.) the firing rate of individual neurons (frequency and temporal pattern), and (3.) the neuronal response latency. This indicates that the moth olfactory system is not based on a simple sequential scheme of elemental linear integration, but rather utilizes non-linear feature extraction to reduce dimensionality of the vast receptor input and concentrate the output signal for further processing by higher brain areas.

An olfactory system incorporating high levels of nonlinear coding, demanding broadly tuned receptors, may be advantageous to process signals from the diverse olfactory bouquet *Manduca* encounters in nature. As a consequence, a minimum of receptors with varying selectivity could detect a huge variety of complex blends. This is also supported by our antennal transcriptome study, reporting a rather small number of putative antennal receptor genes (Chapter I). In short, this dissertation shows that the AL is not a simple relay station, but an indispensable early sensory circuit that optimizes input formatting. The lateral network establishes novel global representations that describe the quality of the total sensor input specifically and concisely. In this framework, my study gives new insights into how the brain processes multidimensional feature space.

ZUSAMMENFASSUNG

Insekten müssen sich in einer zeitlich und räumlich dynamischen Duftwelt orientieren. Für das Aufspüren von Ressourcen oder Partnern sind sie auf ihren Geruchssinn angewiesen. Doch Düfte sind komplexe Gemische aus einem Potpourri von hunderten verschiedenen Substanzen. Die Fähigkeit, geruchsorientiertes Verhalten aufzuzeigen setzt voraus, dass das olfaktorische System komplexe volatile Komponenten in einem variablen Dufthintergrund verlässlich erkennt und auswertet. Motten sind aufgrund ihres hochsensitiven und teilweise sehr spezifischen olfaktorischen Sinns und Dank ihres komplexen chemosensorischen Verhaltens ein beliebter Modelorganismus in der Olfaktorik. Ein Mottenweibchen auf der Suche nach einer reichhaltigen Nektarquelle oder einem geeigneten Eiablageplatz, benötigt ein olfaktorisches System das in der Lage ist, spezielle Informationen aus einer großen Bandbreite von Komponenten zuverlässig zu extrahieren. Anstatt die monomolekularen Eigenschaften der Duftmoleküle zu identifizieren, sollte ihr olfaktorisches System ein Duftbouquet als ein eigenständiges Charakteristikum erkennen können. Dadurch kann die Motte auch bei wechselnden exogenen Faktoren (z. B. klimatische Bedingungen) dem Stimulus eine bestimmte Relevanz zuordnen, und sich dementsprechend kontextabhängig verhalten. Die verantwortlichen verarbeitenden Regionen im Insektengehirn sollten folglich diese perzeptuellen Tendenzen widerspiegeln.

Das Ziel dieser Dissertation ist die Erforschung der Verarbeitungsmechanismen komplexer Geruchsmischungen auf unterschiedlichen Ebenen im ZNS des Tabakswärmers *Manduca sexta*. Mittels einer neu entwickelten Multikomponenten-Stimulus-Apparatur (Kapitel II) und kombinierten elektrophysiologischen Techniken (Kapitel III & IV) beantworte ich die Frage: Wie ist komplexe Geruchsinformation in Relation zu ihren individuellen monomolekularen Komponenten kodiert?

Die initiale Repräsentation eines Duftbouquets geschieht im Antennallobus, Riechhirn und erste Schaltstation des olfaktorischen Systems von Insekten.

Die resultierende neuronale Repräsentation eines komplexen Duftgemischs kann entweder die Information der jeweiligen Einzelkomponenten der Mischung beibehalten (lineare Integration) oder auf Grund von Netzwerkinteraktionen von der schieren Summe abweichen (nichtlineare Interaktion).

Das Phänomen, dass eine nichtlineare Antwort auf ein Duftgemisch nicht mehr durch die Einzelkomponentenantworten vorhersehbar ist, wird „Mischungsinteraktion“ genannt.

Ableitungen einzelner Nervenzellen im Antennallobus in Kapitel III zeigen, dass ein Großteil der in vivo getesteten Neuronen mit nichtlinearen Feuerfrequenzen von Aktionspotenzialen auf eine Duftmischung im Vergleich zu deren Einzelkomponenten antwortet. Die Antwortmuster sind sehr divers und enthüllen eine große Anzahl von „Mischungsinteraktionen“, einschließlich Suppression, Hypoadditivität und Synergismus.

In Kapitel IV visualisieren optophysiological Messungen duftinduzierte Kalziumaktivität des AL-Netzwerkes als Antwort auf fünf Einzelkomponenten und ihre Mischungen. Durch gleichzeitige Visualisierung des afferenten Eingangs von der Antenne in den AL und des efferenten Ausgangs zu höheren Gehirnregionen haben wir die Verarbeitung der olfaktorischen Information durch das neuronale Netzwerk analysiert. Der Vergleich neuronaler Aktivitätsmuster und Antwortintensitäten zeigt, dass im Eingang das neuronale Muster der Duftmischung durch die Repräsentation der Einzelkomponenten zusammengefügt wird. Im Gegensatz dazu erscheint im Ausgang ein völlig neues Bild: Mischungsinteraktionen modellieren die Aktivitätsmuster im Ausgang so stark, dass eine komplett neue Repräsentation der Duftmischung entsteht, welche nicht mehr durch die Aktivitätsmuster der einzelnen Komponenten vorhersagbar ist.

Die Ergebnisse der vorliegenden Arbeit zeigen, dass Duftmischungen bereits in der ersten Schaltstation des olfaktorischen Systems, dem AL, ein einzigartiges „Mischungs-Charakteristikum“ gesondert von der Identität der Einzelkomponenten etablieren. Darüber hinaus kann man über die Analyse des olfaktorischen Rezeptor neuroneneingangs keine eindeutige Aussage über den möglichen AL-Ausgang treffen, weder räumlich noch zeitlich. Die Kodierung von Duftmischungen beinhaltet ein starkes Maß an nichtlinearen Interaktionen durch AL-Nervenzellen, um ein neues eindeutiges Signal zu produzieren, welches die Duftmischung repräsentiert. Jede Nervenzelle nutzt dabei eine Vielzahl an Parametern wie z. B. (1) Morphologie und Standort einzelner Neuronen innerhalb des ALs, (2) die Feuerrate einzelner Neurone (Frequenz der Aktionspotenziale sowie zeitliche Muster) oder (3) die Latenzzeit der Antwort.

Dies impliziert, dass das olfaktorische System der Motte nicht auf einem simplen sequenziellen Verarbeitungsschema basiert, welches elementare lineare Integration betreibt. Vielmehr dient nichtlineare Merkmalsextraktion im AL der Motte dazu, die Dimensionalität der enormen Menge an olfaktorischen Rezeptoreingang zu reduzieren, und somit das Ausgangssignal für weitere Verarbeitungsschritte in den höheren Gehirnregionen zu konzentrieren. Ein olfaktorisches System welches nichtlineare Kodierung in hohem Maße integriert benötigt breitgefächerte, unspezifische Rezeptoren und könnte gerade dadurch von Vorteil sein, um die diversen Signale eines natürlichen Duftbouquets zu verarbeiten.

Folglich kann bereits ein Minimum an unterschiedlichen Rezeptoren mit variabler Selektivität eine Vielzahl an unterschiedlichen, komplexen Duftmischungen detektieren. Diese Hypothese wird auch von unseren Daten des antennalen Transkriptoms gestützt. In Manuskript I berichten wir über eine verhältnismäßig kleine Anzahl putativer antennaler Rezeptorgene.

Zusammengefasst zeigt diese Doktorarbeit, dass der AL keine einfache Verschaltungsstation ist, sondern ein unverzichtbares frühes sensorisches Netzwerk darstellt, welches die Formatierung des olfaktorischen Eingangssignals optimiert. Das AL Netzwerk etabliert dabei eine neue globale Repräsentation welche die Qualität des gesamten sensorischen Eingangs prägnant und spezifisch beschreibt. Vor diesem Hintergrund bietet die vorliegende Arbeit neue Einblicke und Ansichten darüber, wie das Gehirn multidimensionale Merkmalsräume verarbeitet.



REFERENCES

- Ai, M., Min, S., Grosjean, Y., Leblanc, C., Bell, R., Benton, R., and Suh, G.S. (2010). Acid sensing by the *Drosophila* olfactory system. *Nature* 468, 691-695.
- Akers, R.P., and Getz, W.M. (1993). Response of olfactory receptor neurons in honeybees to odorants and their binary mixtures. *J Comp Physiol A* 173, 169–185.
- Allmann, S., and Baldwin, I.T. (2010). Insects betray themselves in nature to predators by rapid isomerization of green leaf volatiles. *Science* 329, 1075-1078.
- Anderson, P., Hansson, B.S., and Löfqvist, J. (1995). Plant-odour-specific receptor neurones on the antennae of female and male *Spodoptera littoralis*. *Physiological Entomology* 20, 189-198.
- Anderson, A.R., Wanner, K.W., Trowell, S.C., Warr, C.G., Jaquin-Joly, E., Zagatti, P., Robertson, H., and Newcomb, R.D. (2009). Molecular basis of female-specific odorant responses in *Bombyx mori*. *Insect Biochem Mol Biol* 39, 189-197.
- Angeli, S., Ceron, F., Scaloni, A., Monti, M., Monteforti, G., Minnocci, A., Petacchi, R., and Pelosi, P. (1999). Purification, structural characterization, cloning and immunocytochemical localization of chemoreception proteins from *Schistocerca gregaria*. *Eur J Biochem* 262, 745-754.
- Anton, S., Lofstedt, C., and Hansson, B. (1997). Central nervous processing of sex pheromones in two strains of the European corn borer *Ostrinia nubilalis* (Lepidoptera: Pyralidae). *J Exp Biol* 200, 1073-1087.
- Ashburner, M., Ball, C.A., Blake, J.A., Botstein, D., Butler, H., Cherry, J.M., Davis, A.P., Dolinski, K., Dwight, S.S., Eppig, J.T., Harris, M.A., Hill, D.P., Issel-Tarver, L., Kasarskis, A., Lewis, S., Matese, J.C., Richardson, J.E., Ringwald, M., Rubin, G.M., and Sherlock, G. (2000). Gene Ontology: tool for the unification of biology. *Nat Genet* 25, 25-29.
- Baker, T.C. (1989). Sex-Pheromone Communication in the Lepidoptera- New research progress. *Experientia* 45, 248-262.
- Barrozo, R.B., Jarriault, D., Simeone, X., Gaertner, C., Gadenne, C., and Anton, S. (2010). Mating-induced transient inhibition of responses to sex pheromone in a male moth is not mediated by octopamine or serotonin. *J Exp Biol* 213, 1100-1106.
- Bell, R.A., and Joachim, F.A. (1976). Techniques for rearing laboratory colonies of tobacco hornworms and pink bollworms. *Annals of the Entomological Society of America* 69, 365-373.
- Benton, R., Sachse, S., Michnick, S.W., and Vosshall, L.B. (2006). Atypical membrane topology and heteromeric function of *Drosophila* odorant receptors in vivo. *PLoS Biol* 4, e20.
- Benton, R., Vannice, K.S., Gomez-Diaz, C., and Vosshall, L.B. (2009). Variant ionotropic glutamate receptors as chemosensory receptors in *Drosophila*. *Cell* 136, 149-162.
- Benton, R., Vannice, K.S., and Vosshall, L.B. (2007). An essential role for a CD36-related receptor in pheromone detection in *Drosophila*. *Nature* 450, 289-293.
- Bensafi, M., Frasnelli, J., Reden, J., and Hummel, T. (2007). The neural representation of odor is modulated by the presence of a trigeminal stimulus during odor encoding. *Clinical Neurophysiology* 118, 696-701.
- Boeckh, J., and Tolbert, L.P. (1993). Synaptic organization and development of the antennal lobe in insects. *Microsc Res Tech* 24, 260-280.
- Boyle, J.A., Djordjevic, J., Olsson, M.J., Lundstrom, J.N., and Jones-Gotman, M. (2009). The human brain distinguishes between single odorants and binary mixtures. *Cereb Cortex* 19, 66-71.
- Brockerhoff, E., and Grant, G. (1999). Correction for differences in volatility among olfactory stimuli and effect on EAG responses of *Dioryctria abietivorella* to plant volatiles. *J Chem Ecol* 25, 1353-1367.

REFERENCES

- Broome, B.M., Jayaraman, V., and Laurent, G. (2006). Encoding and Decoding of Overlapping Odor Sequences. *Neuron* 51, 467-482.
- Brossard, C., Rousseau, F., and Dumont, J.P. (2007). Perceptual interactions between characteristic notes smelled above aqueous solutions of odorant mixtures. *Chem Senses* 32, 319-327.
- Buck, L., and Axel, R. (1991). A novel multigene family may encode odorant receptors: a molecular basis for odor recognition. *Cell* 65, 175-187.
- Butenandt, A., Beckmann, R., Stamm, D. & Hecker, E. (1959) Über den Sexuallockstoff des Seidenspinners *Bombyx mori*. Reindarstellung und Konstitution. *Z. Naturforsch.*, 14b, 283–284.
- Butenandt, A., Beckmann, R.D., and Stamm, D. (1961). Über den Sexuallockstoff des Seidenspinners, II. Konstitution und Konfiguration des Bombykols. *Zeitschrift für physiologische Chemie* 324, 84-87.
- Cardé, R., Dindonis, L., Agar, B., and Foss, J. (1984). Apparency of pulsed and continuous pheromone to male gypsy moths. *Journal of Chemical Ecology* 10, 335-348.
- Carlsson, M., Knusel, P., Verschure, P., and Hansson, B. (2005). Spatio-temporal Ca²⁺ dynamics of moth olfactory projection neurones. *Eur J Neurosci* 22, 647 - 657.
- Carlsson, M.A., Chong, K.Y., Daniels, W., Hansson, B.S., and Pearce, T.C. (2007). Component information is preserved in glomerular responses to binary odor mixtures in the moth *Spodoptera littoralis*. *Chemical Senses* 32, 433-443.
- Carlsson, M.A., and Hansson, B.S. (2003). Dose-response characteristics of glomerular activity in the moth antennal lobe. *Chem Senses* 28, 269-278.
- Carlsson, M.A., Knüsel, P., Verschure, P.F.M.J., and Hansson, B.S. (2005). Spatio-temporal Ca²⁺dynamics of moth olfactory projection neurones. *European Journal of Neuroscience* 22, 647-657.
- Cashion, L., Livermore, A., and Hummel, T. (2006). Odour suppression in binary mixtures. *Biol Psychol* 73, 288-297.
- Chandra, S., and Smith, B.H. (1998). An analysis of synthetic processing of odor mixtures in the honeybee (*Apis mellifera*). *J Exp Biol* 201, 3113-3121.
- Chou, Y.H., Spletter, M.L., Yaksi, E., Leong, J.C., Wilson, R.I., and Luo, L. (2010). Diversity and wiring variability of olfactory local interneurons in the *Drosophila* antennal lobe. *Nat Neurosci* 13, 439-449.
- Christensen, T.A., Harrow, I.D., Cuzzocrea, C., Randolph, P.W., and Hildebrand, J.G. (1995). Distinct projections of two populations of olfactory receptor axons in the antennal lobe of the sphinx moth *Manduca sexta*. *Chemical Senses* 20, 313-323.
- Christensen, T.A., and Hildebrand, J.G. (1987). Male-specific, sex pheromone-selective projection neurons in the antennal lobes of the moth *Manduca sexta*. *J Comp Physiol A* 160, 553-569.
- Christensen, T.A., and Sorensen, P.W. (1996). Pheromones as tools for olfactory research. Introduction. *Chemical Senses* 21, 241-243.
- Christensen, T.A., Waldrop, B.R., Harrow, I.D., and Hildebrand, J.G. (1993). Local interneurons and information processing in the olfactory glomeruli of the moth *Manduca sexta*. *J Comp Physiol A* 173, 385-399.
- Christensen, T.A., and Hildebrand, J.G. (1997). Coincident stimulation with pheromone components improves temporal pattern resolution in central olfactory neurons. *J Neurophysiol* 77, 775-781.
- Cometto-Muniz, J., Cain, W., and Abraham, M. (2003). Quantification of chemical vapors in chemosensory research. *Chemical Senses* 28, 467-477.
- Conesa, A., Gotz, S., Garcia-Gomez, J.M., Terol, J., Talon, M., and Robles, M. (2005). Blast2GO: a universal tool for annotation, visualization and analysis in functional genomics research. *Bioinformatics* 21, 3674-3676.

REFERENCES

- Consortium., I.S.G. (2008). The genome of a lepidopteran model insect, the silkworm *Bombyx mori*. *Insect Biochem Mol Biol* 38, 1036-1045.
- Couto, A., Alenius, M., and Dickson, B.J. (2005). Molecular, Anatomical, and Functional Organization of the *Drosophila* Olfactory System. *Current Biology* 15, 1535-1547.
- Croset, V., Rytz, R., Cummins, S.F., Budd, A., Brawand, D., Kaessmann, H., Gibson, T.J., and Benton, R. (2010). Ancient protostome origin of chemosensory ionotropic glutamate receptors and the evolution of insect taste and olfaction. *PLoS Genet* 6, e1001064.
- Daly, K.C., Chandra, S., Durtschi, M.L., and Smith, B.H. (2001a). The generalization of an olfactory-based conditioned response reveals unique but overlapping odour representations in the moth *Manduca sexta*. *J Exp Biol* 204, 3085-3095.
- Daly, K.C., Durtschi, M.L., and Smith, B.H. (2001b). Olfactory-based discrimination learning in the moth, *Manduca sexta*. *Journal of Insect Physiology* 47, 375-384.
- Davison, I.G., and Katz, L.C. (2007). Sparse and selective odor coding by mitral/tufted neurons in the main olfactory bulb. *J Neurosci* 27, 2091-2101.
- De Bruyne, M., and Baker, T.C. (2008). Odor detection in insects: volatile codes. *J Chem Ecol* 34, 882-897.
- De Bruyne, M., Clyne, P.J., and Carlson, J.R. (1999). Odor coding in a model olfactory organ: the *Drosophila* maxillary palp. *J Neurosci* 19, 4520-4532.
- Deisig, N., Giurfa, M., Lachnit, H., and Sandoz, J.-C. (2006). Neural representation of olfactory mixtures in the honeybee antennal lobe. *European Journal of Neuroscience* 24, 1161-1174.
- Deisig, N., Lachnit, H., Sandoz, J.-C., Lober, K., and Giurfa, M. (2003). A modified version of the unique cue theory accounts for olfactory compound processing in honeybees. *Learn Mem* 10, 199-208.
- Ditzen, M., Evers, J.-F., and Galizia, C.G. (2003). Odor similarity does not influence the time needed for odor processing. *Chemical Senses* 28, 781-789.
- De Jong, R., and Visser, J.H. (1988). Specificity-related suppression of responses to binary mixtures in olfactory receptors of the Colorado potato beetle. *Brain Res* 447, 18-24.
- Duchamp-Viret, P., Duchamp, A., and Chaput, M.A. (2003). Single olfactory sensory neurons simultaneously integrate the components of an odour mixture. *Eur J Neurosci* 18, 2690-2696.
- Dunkel, M., Schmidt, U., Struck, S., Berger, L., Gruening, B., Hossbach, J., Jaeger, I.S., Effmert, U., Piechulla, B., Eriksson, R., Knudsen, J., and Preissner, R. (2009). SuperScent--a database of flavors and scents. *Nucleic Acids Research* 37, D291-D294.
- Dupuy, F., Josens, R., Giurfa, M., and Sandoz, J.-C. (2010). Calcium imaging in the ant *Camponotus fellah* reveals a conserved odour-similarity space in insects and mammals. *BMC Neuroscience* 11, 28.
- Durand, N., Carot-Sans, G., Chertemps, T., Bozzolan, F., Party, V., Renou, M., Debernard, S., Rosell, G., and Maibeche-Coisne, M. (2010). Characterization of an antennal carboxylesterase from the pest moth *Spodoptera littoralis* degrading a host plant odorant. *PLoS ONE* 5, e15026.
- Eisthen, H.L. (2002). Why are olfactory systems of different animals so similar? *Brain Behav Evol* 59, 273-293.
- Engsontia, P., Sanderson, A.P., Cobb, M., Walden, K.K., Robertson, H.M., and Brown, S. (2008). The red flour beetle's large nose: an expanded odorant receptor gene family in *Tribolium castaneum*. *Insect Biochem Mol Biol* 38, 387-397.
- Fernandez, P.C., Locatelli, F.F., Person-Rennell, N., Deleo, G., and Smith, B.H. (2009). Associative conditioning tunes transient dynamics of early olfactory processing. *J Neurosci* 29, 10191-10202.f
- Fishilevich, E., and Vosshall, L.B. (2005). Genetic and Functional Subdivision of the *Drosophila* Antennal Lobe. *Current Biology* 15, 1548-1553.

REFERENCES

- Firestein, S., Picco, C., and Menini, A. (1993). The relation between stimulus and response in olfactory receptor cells of the tiger salamander. *J Physiol* 468, 1-10.
- Flanagan, D., and Mercer, A.R. (1989). An atlas and 3-D reconstruction of the antennal lobes in the worker honey bee, *Apis mellifera* L. (Hymenoptera : Apidae). *International Journal of Insect Morphology and Embryology* 18, 145-159.
- Flecke, C., Dolzer, J., Krannich, S., and Stengl, M. (2006). Perfusion with cGMP analogue adapts the action potential response of pheromone-sensitive sensilla trichoidea of the hawkmoth *Manduca sexta* in a daytime-dependent manner. *J Exp Biol* 209, 3898-3912.
- Flecke, C., and Stengl, M. (2009). Octopamine and tyramine modulate pheromone-sensitive olfactory sensilla of the hawkmoth *Manduca sexta* in a time-dependent manner. *J Comp Physiol A Neuroethol Sens Neural Behav Physiol* 195, 529-545.
- Forstner, M., Gohl, T., Gondesens, I., Raming, K., Breer, H., and Krieger, J. (2008). Differential expression of SNMP-1 and SNMP-2 proteins in pheromone-sensitive hairs of moths. *Chem Senses* 33, 291-299.
- Fox, A.N., Pitts, R.J., Robertson, H.M., Carlson, J.R., and Zwiebel, L.J. (2001). Candidate odorant receptors from the malaria vector mosquito *Anopheles gambiae* and evidence of down-regulation in response to blood feeding. *Proc Natl Acad Sci U S A* 98, 14693-14697.
- Fraser, A.M., Mechaber, W.L., and Hildebrand, J.G. (2003). Electroantennographic and behavioral responses of the sphinx moth *Manduca sexta* to host plant headspace volatiles. *J Chem Ecol* 29, 1813-1833.
- Frederick, D.E., Barlas, L., Levins, A., and Kay, L.M. (2009). A critical test of the overlap hypothesis for odor mixture perception. *Behav Neurosci* 123, 430-437.
- Fried, H.U., Fuss, S.H., and Korsching, S.I. (2002). Selective imaging of presynaptic activity in the mouse olfactory bulb shows concentration and structure dependence of odor responses in identified glomeruli. *Proc Natl Acad Sci U S A* 99, 3222-3227.
- Friedrich, R., and Korsching, S. (1997). Combinatorial and chemotopic odorant coding in the zebrafish olfactory bulb visualized by optical imaging. *Neuron* 18, 737 - 752.
- Friedrich, R.W., and Korsching, S.I. (1998). Chemotopic, combinatorial, and noncombinatorial odorant representations in the olfactory bulb revealed using a voltage-sensitive axon tracer. *J Neurosci* 18, 9977-9988.
- Galizia, C.G., Joerges, J., Faber, T., Kuttner, A., Holldobler, B., and Menzel, R. (1998). Functional optical imaging of olfactory glomeruli in bees and ants. A universal code? *European Journal of Neuroscience* 10, 435-435.
- Galizia, C.G., McIlwrath, S.L., and Menzel, R. (1999b). A digital three-dimensional atlas of the honeybee antennal lobe based on optical sections acquired by confocal microscopy. *Cell and Tissue Research* 295, 383-394.
- Galizia, C.G., Menzel, R., and Holldobler, B. (1999). Optical imaging of odor-evoked glomerular activity patterns in the antennal lobes of the ant *Camponotus rufipes*. *Naturwissenschaften* 86, 533-537.
- Galizia, C., and Menzel, R. (2001). The role of glomeruli in the neural representation of odours: results from optical recording studies. *J Insect Physiol* 47, 115-130.
- Galizia, C.G., Nagler, K., Holldobler, B., and Menzel, R. (1998). Odour coding is bilaterally symmetrical in the antennal lobes of honeybees (*Apis mellifera*). *European Journal of Neuroscience* 10, 2964-2974.
- Galizia, C.G., Sachse, S., Rappert, A., and Menzel, R. (1999). The glomerular code for odor representation is species specific in the honeybee *Apis mellifera*. *Nat Neurosci* 2, 473-478.
- Giurfa, M., Schubert, M., Reisenman, C., Gerber, B., and Lachnit, H. (2003). The effect of cumulative experience on the use of elemental and configural visual discrimination strategies in honeybees. *Behavioural Brain Research* 145, 161-169.

REFERENCES

- Giraudet, P., Berthommier, F., and Chaput, M. (2002). Mitral cell temporal response patterns evoked by odor mixtures in the rat olfactory bulb. *J Neurophysiol* 88, 829-838.
- Girling, R., and Cardé, R. (2007). Analysis and manipulation of the structure of odor plumes from a piezo-electric release system and measurements of upwind flight of male almond moths, *Cadra cautella*, to pheromone plumes. *J Chem Ecol* 33, 1927-1945.
- Godfrey, P.A., Malnic, B., and Buck, L.B. (2004). The mouse olfactory receptor gene family. *Proc Natl Acad Sci U S A* 101, 2156-2161.
- Gong, D.P., Zhang, H.J., Zhao, P., Lin, Y., Xia, Q.Y., and Xiang, Z.H. (2007). Identification and expression pattern of the chemosensory protein gene family in the silkworm, *Bombyx mori*. *Insect Biochem Mol Biol* 37, 266-277.
- Grosse-Wilde, E., Kuebler, L., Bucks, S., Vogel, H., Wicher, D., Hansson, B. (2011). The antennal transcriptome of *Manduca sexta*. *PNAS* (in publication).
- Grosse-Wilde, E., Gohl, T., Bouche, E., Breer, H., and Krieger, J. (2007). Candidate pheromone receptors provide the basis for the response of distinct antennal neurons to pheromonal compounds. *European Journal of Neuroscience* 25, 2364-2373.
- Grosse-Wilde, E., Stieber, R., Forstner, M., Krieger, J., Wicher, D., and Hansson, B.S. (2010). Sex-Specific Odorant Receptors of the Tobacco Hornworm *Manduca sexta*. *Front Cell Neurosci* 4.
- Grosse-Wilde, E., Svatos, A., and Krieger, J. (2006). A Pheromone-Binding Protein Mediates the Bombykol-Induced Activation of a Pheromone Receptor In Vitro. *Chem. Senses* 31, 547-555.
- Gottfried, J.A., and Dolan, R.J. (2003). The Nose Smells What the Eye Sees: Crossmodal Visual Facilitation of Human Olfactory Perception. *Neuron* 39, 375-386.
- Gotz, S., Garcia-Gomez, J.M., Terol, J., Williams, T.D., Nagaraj, S.H., Nueda, M.J., Robles, M., Talon, M., Dopazo, J., and Conesa, A. (2008). High-throughput functional annotation and data mining with the Blast2GO suite. *Nucleic Acids Res* 36, 3420-3435.
- Guerenstein, P.G., Christensen, T.A., and Hildebrand, J.G. (2004). Sensory processing of ambient CO2 information in the brain of the moth *Manduca sexta*. *J Comp Physiol A Neuroethol Sens Neural Behav Physiol* 190, 707-725.
- Guerrieri, F., Schubert, M., Sandoz, J., and Giurfa, M. (2005). Perceptual and neural olfactory similarity in honeybees. *Plos Biology* 3, e60.
- Gyorgyi, T.K., Roby-Shemkovitz, A.J., and Lerner, M.R. (1988). Characterization and cDNA cloning of the pheromone-binding protein from the tobacco hornworm, *Manduca sexta*: a tissue-specific developmentally regulated protein. *Proc Natl Acad Sci U S A* 85, 9851-9855.
- Hallem, E., and Carlson, J. (2006). Coding of odors by a receptor repertoire. *Cell* 125, 143 - 160.
- Hallem, E.A., Ho, M.G., and Carlson, J.R. (2004). The Molecular Basis of Odor Coding in the *Drosophila* Antenna. *Cell* 117, 965-979.
- Hansson, B.S. (1995). Olfaction in Lepidoptera. *Experientia* 51, 1003-1027.
- Hansson, B.S. (2002). A bug's smell-research into insect olfaction. *Trends Neurosci* 25, 270-274.
- Hansson, B.S., and Anton, S. (2000). Function and morphology of the antennal lobe: new developments. *Annu Rev Entomol* 45, 203-231.
- Hansson, B.S., Carlsson, M.A., and Kalinová, B. (2003). Olfactory activation patterns in the antennal lobe of the sphinx moth, *Manduca sexta*. *J Comp Physiol A* 189, 301-308.
- Hansson, B.S., Christensen, T.A., and Hildebrand, J.G. (1991). Functionally distinct subdivisions of the macroglomerular complex in the antennal lobe of the male sphinx moth *Manduca sexta*. *J Comp Neurol* 312, 264-278.
- Hansson, B.S., and Hallberg, E. (1999). Introduction to insect sensory structures. *Microsc Res Tech* 47, 367.
- Hansson, B.S., Ljungberg, H., Hallberg, E., and Lofstedt, C. (1992). Functional specialization of olfactory glomeruli in a moth. *Science* 256, 1313-1315.

REFERENCES

- Hartlieb, E., Anderson, P., and Hansson, B.S. (1999). Appetitive learning of odours with different behavioural meaning in moths. *Physiol Behav* 67, 671-677.
- Heinbockel, T., and Hildebrand, J.G. (1998). Antennal receptive fields of pheromone-responsive projection neurons in the antennal lobes of the male sphinx moth *Manduca sexta*. *J Comp Physiol A* 183, 121-133.
- Heinbockel, T., Christensen, T.A., and Hildebrand, J.G. (2004). Representation of binary pheromone blends by glomerulus-specific olfactory projection neurons. *J Comp Physiol A* 190, 1023-1037.
- Hildebrand, J.G. (1995). Analysis of chemical signals by nervous systems. *Proceedings of the National Academy of Sciences of the United States of America* 92, 67-74.
- Hildebrand, J.G., and Shepherd, G.M. (1997). Mechanisms of olfactory discrimination: converging evidence for common principles across phyla. *Annu Rev Neurosci* 20, 595-631.
- Hillier, N.K., Kelly, D., and Vickers, N.J. (2007). A specific male olfactory sensillum detects behaviorally antagonistic hairpencil odorants. *J Insect Sci* 7, 4.
- Hillier, N.K., Kleineidam, C., and Vickers, N.J. (2006). Physiology and glomerular projections of olfactory receptor neurons on the antenna of female *Heliothis virescens* (Lepidoptera: Noctuidae) responsive to behaviorally relevant odors. *J Comp Physiol A Neuroethol Sens Neural Behav Physiol* 192, 199-219.
- Hillier, N.K., and Vickers, N.J. (2011). Mixture interactions in moth olfactory physiology: examining the effects of odorant mixture, concentration, distal stimulation, and antennal nerve transection on sensillar responses. *Chem Senses* 36, 93-108.
- Hölldobler, B., and Wilson, E. (1990). *The Ants*. Belknap (Harvard University Press).
- Hoballah, M.E., and Turlings, T.C.J. (2005). The role of fresh versus old leaf damage in the attraction of parasitic wasps to herbivore-induced maize volatiles. *Journal of Chemical Ecology* 31, 2003-2018.
- Homberg, U., Christensen, T.A., and Hildebrand, J.G. (1989). Structure and function of the deutocerebrum in insects. *Annu Rev Entomol* 34, 477-501.
- Homberg, U., Montague, R.A., and Hildebrand, J.G. (1988). Anatomy of antenno-cerebral pathways in the brain of the sphinx moth *Manduca sexta*. *Cell Tissue Res* 254, 255-281.
- Huetteroth, W., and Schachtner, J. (2005). Standard three-dimensional glomeruli of the *Manduca sexta* antennal lobe: a tool to study both developmental and adult neuronal plasticity. *Cell Tissue Res* 319, 513-524.
- Huang, J., Zhang, W., Qiao, W., Hu, A., and Wang, Z. (2010). Functional connectivity and selective odor responses of excitatory local interneurons in *Drosophila* antennal lobe. *Neuron* 67, 1021-1033.
- Joerges, J., Kuttner, A., Galizia, C.G., and Menzel, R. (1997). Representations of odours and odour mixtures visualized in the honeybee brain. *Nature* 387, 285-288.
- Johnson, B.A., Ong, J., and Leon, M. (2010). Glomerular activity patterns evoked by natural odor objects in the rat olfactory bulb are related to patterns evoked by major odorant components. *J. Comp. Neurol.* 518, 1542-1555.
- Jones, W.D., Cayirlioglu, P., Kadow, I.G., and Vosshall, L.B. (2007). Two chemosensory receptors together mediate carbon dioxide detection in *Drosophila*. *Nature* 445, 86-90.
- Jordan, M.D., Anderson, A., Begum, D., Carraher, C., Authier, A., Marshall, S.D., Kiely, A., Gatehouse, L.N., Greenwood, D.R., Christie, D.L., Kralicek, A.V., Trowell, S.C., and Newcomb, R.D. (2009). Odorant receptors from the light brown apple moth (*Epiphyas postvittana*) recognize important volatile compounds produced by plants. *Chem Senses* 34, 383-394.
- Kalinova, B., Hoskovec, M., Liblikas, I., Unelius, C.R., and Hansson, B.S. (2001). Detection of Sex Pheromone Components in *Manduca sexta* (L.). *Chemical Senses* 26, 1175-1186.
- Kant, I. (1917). *Anthropologie in pragmatischer Hinsicht*. Berlin: Reimer.

REFERENCES

- Karlson, P., and Luscher, M. (1959). Pheromones': a new term for a class of biologically active substances. *Nature* 183, 55-56.
- Katoh, K., Kuma, K., Toh, H., and Miyata, T. (2005). MAFFT version 5: improvement in accuracy of multiple sequence alignment. *Nucleic Acids Res* 33, 511-518.
- Kauer, J.S., and White, J. (2001). Imaging and coding in the olfactory system. *Annu Rev Neurosci* 24, 963-979.
- Kaissling, K.-E., Hildebrand, J.G., and Tumlinson, J.H. (1989). Pheromone receptor cells in the male moth *Manduca sexta*. *Archives of Insect Biochemistry and Physiology* 10, 273-279.
- Kelber, C., Rossler, W., Roces, F., and Kleineidam, C.J. (2009). The antennal lobes of fungus-growing ants (*Attini*): neuroanatomical traits and evolutionary trends. *Brain Behav Evol* 73, 273-284.
- Kent, K.S., Harrow, I.D., Quartararo, P., and Hildebrand, J.G. (1986). An accessory olfactory pathway in *Lepidoptera*: the labial pit organ and its central projections in *Manduca sexta* and certain other sphinx moths and silk moths. *Cell Tissue Res* 245, 237-245.
- Kessler, A., and Baldwin, I.T. (2001). Defensive function of herbivore-induced plant volatile emissions in nature. *Science* 291, 2141-2144.
- King, J.R., Christensen, T.A., and Hildebrand, J.G. (2000). Response characteristics of an identified, sexually dimorphic olfactory glomerulus. *J Neurosci* 20, 2391-2399.
- Kleineidam, C.J., Obermayer, M., Halbich, W., and Rossler, W. (2005). A macroglomerulus in the antennal lobe of leaf-cutting ant workers and its possible functional significance. *Chem Senses* 30, 383-392.
- Kleineidam, C.J., Rossler, W., Holldobler, B., and Roces, F. (2007). Perceptual differences in trail-following leaf-cutting ants relate to body size. *J Insect Physiol* 53, 1233-1241.
- Koch, U., Cardé, A., and Cardé, R. (2002). Calibration of an EAG system to measure airborne concentration of pheromone formulated for mating disruption of the pink bollworm moth, *Pectinophora gossypiella* (Saunders)(Lep., Gelechiidae). *Journal of Applied Entomology* 126, 431-435.
- Krieger, J., Grosse-Wilde, E., Gohl, T., and Breer, H. (2005). Candidate pheromone receptors of the silkworm *Bombyx mori*. *Eur J Neurosci* 21, 2167-2176.
- Krieger, J., Grosse-Wilde, E., Gohl, T., Dewer, Y.M., Raming, K., and Breer, H. (2004). Genes encoding candidate pheromone receptors in a moth (*Heliothis virescens*). *Proc Natl Acad Sci U S A* 101, 11845-11850.
- Krieger, J., Raming, K., Dewer, Y.M., Bette, S., Conzelmann, S., and Breer, H. (2002). A divergent gene family encoding candidate olfactory receptors of the moth *Heliothis virescens*. *Eur J Neurosci* 16, 619-628.
- Krofczik, S., Menzel, R., and Nawrot, M.P. (2008). Rapid odor processing in the honeybee antennal lobe network. *Front Comput Neurosci* 2, 9.
- Laska, M., Trolp, S., and Teubner, P. (1999). Odor Structure-Activity Relationships Compared in Human and Nonhuman Primates. *Behavioral Neuroscience* 113, 998-1007.
- Laissue, P.P., Reiter, C., Hiesinger, P.R., Halter, S., Fischbach, K.F., and Stocker, R.F. (1999). Three-dimensional reconstruction of the antennal lobe in *Drosophila melanogaster*. *J Comp Neurol* 405, 543-552.
- Laissue, P.P., and Vosshall, L.B. (2008). The olfactory sensory map in *Drosophila*. *Adv Exp Med Biol* 628, 102-114.
- Lapid, H., Harel, D., and Sobel, N. (2008). Prediction models for the pleasantness of binary mixtures in olfaction. *Chem Senses* 33, 599-609.
- Laurent, G. (1999). A systems perspective on early olfactory coding. *Science* 286, 723-728.
- Laurent, G. (2002). Olfactory network dynamics and the coding of multidimensional signals. *Nat Rev Neurosci* 3, 884-895.

REFERENCES

- Leal, W.S., Nikonova, L., and Peng, G. (1999). Disulfide structure of the pheromone binding protein from the silkworm moth, *Bombyx mori*. *FEBS Lett* 464, 85-90.
- Lee, J.K., and Strausfeld, N.J. (1990). Structure, distribution and number of surface sensilla and their receptor cells on the olfactory appendage of the male moth *Manduca sexta*. *J Neurocytol* 19, 519-538.
- Lei, H., Christensen, T.A., and Hildebrand, J.G. (2002). Local inhibition modulates odor-evoked synchronization of glomerulus-specific output neurons. *Nat Neurosci* 5, 557-565.
- Lei, H., Mooney, R., and Katz, L.C. (2006). Synaptic integration of olfactory information in mouse anterior olfactory nucleus. *J Neurosci* 26, 12023-12032.
- Lei, H., and Vickers, N. (2008). Central Processing of Natural Odor Mixtures in Insects. *J Chem Ecol* 34, 915-927.
- Lin, D.Y., Shea, S.D., and Katz, L.C. (2006). Representation of natural stimuli in the rodent main olfactory bulb. *Neuron* 50, 937-949.
- Maeda, Y., Mayanagi, T., and Amagai, A. (2009). Folic acid is a potent chemoattractant of free-living amoebae in a new and amazing species of protist, *Vahlkampfia* sp. *Zoolog Sci* 26, 179-186.
- Mcnamara, A.M., Magidson, P.D., and Linster, C. (2007). Binary mixture perception is affected by concentration of odor components. *Behav Neurosci* 121, 1132-1136.
- Malnic, B., Godfrey, P.A., and Buck, L.B. (2004). The human olfactory receptor gene family. *Proc Natl Acad Sci U S A* 101, 2584-2589.
- Mantel, N. (1967). The detection of disease clustering and a generalized regression approach *Cancer Res* 27, 209-220.
- Masse, N.Y., Turner, G.C., and Jefferis, G.S. (2009). Olfactory information processing in *Drosophila*. *Curr Biol* 19, R700-713.
- Matsumoto, S., and Hildebrand, J. (1981). Olfactory mechanisms in the moth *Manduca sexta* : response characteristics and morphology of central neurons in the antennal lobes. . *Proc R Soc Lond [Biol]*, 249-277.
- Meister, M., and Bonhoeffer, T. (2001). Tuning and topography in an odor map on the rat olfactory bulb. *J Neurosci* 21, 1351-1360.
- Miura, N., Nakagawa, T., Tatsuki, S., Touhara, K., and Ishikawa, Y. (2009). A male-specific odorant receptor conserved through the evolution of sex pheromones in *Ostrinia* moth species. *Int J Biol Sci* 5, 319-330.
- Mombaerts, P. (1996). Targeting olfaction. *Curr Opin Neurobiol* 6, 481-486.
- Moore, I. (1984). The effects of the antennal flight posture and orientation on the pheromonal stimulation patterns experienced by male *Spodoptera littoralis* (Lepidoptera: Noctuidae). *Chemical Senses* 9, 15-29.
- Mori, K., and Yoshihara, Y. (1995). Molecular recognition and olfactory processing in the mammalian olfactory system. *Prog Neurobiol* 45, 585-619.
- Mustaparta, H. (1990). Chemical information processing in the olfactory system of insects. *Physiol Rev* 70, 199-245.
- Nakagawa, T., Sakurai, T., Nishioka, T., and Touhara, K. (2005). Insect Sex-Pheromone Signals Mediated by Specific Combinations of Olfactory Receptors. *Science* 307, 1638-1642.
- Neuhaus, E.M., Gisselmann, G., Zhang, W., Dooley, R., Stortkuhl, K., and Hatt, H. (2005). Odorant receptor heterodimerization in the olfactory system of *Drosophila melanogaster*. *Nat Neurosci* 8, 15-17.
- Niessing, J., and Friedrich, R.W. (2010). Olfactory pattern classification by discrete neuronal network states. *Nature* 465, 47-52.
- Nishikawa, M., Nishino, H., Misaka, Y., Kubota, M., Tsuji, E., Satoji, Y., Ozaki, M., and Yokohari, F. (2008). Sexual dimorphism in the antennal lobe of the ant *Camponotus japonicus*. *Zoolog Sci* 25, 195-204.

REFERENCES

- Ochieng, S.A., Park, K.C., and Baker, T.C. (2002). Host plant volatiles synergize responses of sex pheromone-specific olfactory receptor neurons in male *Helicoverpa zea*. *J Comp Physiol A* 188, 325-333.
- Olivier, V., Monsempes, C., Francois, M.C., Poivet, E., and Jacquin-Joly, E. (2010). Candidate chemosensory ionotropic receptors in a Lepidoptera. *Insect Mol Biol*.
- Olsen, S.R., Bhandawat, V., and Wilson, R.I. (2007). Excitatory interactions between olfactory processing channels in the *Drosophila* antennal lobe. *Neuron* 54, 89-103.
- Olsson, S.B., Kuebler, L.S., Veit, D., Steck, K., Schmidt, A., Knaden, M., and Hansson, B.S. (2011). A novel multicomponent stimulus device for use in olfactory experiments. *J Neurosci Methods*. 195, 1-9. Epub 2010 Oct 2017.
- Olsson, S.B., Linn, C.E., Feder, J.L., Michel, A., Dambroski, H.R., Berlocher, S.H., and Roelofs, W.L. (2009). Comparing peripheral olfactory coding with host preference in the rhabdometis species complex. *Chemical Senses* 34, 37-48.
- Parker, D., Bussink, J., Grampel, H.T.V.D., Wheatley, G.W., Dorf, E.-U., Ostlinning, E., and Reinking, K. (2002). "Polymers, high temperature," in *Ullmann's encyclopedia of industrial chemistry*. 6th Edition ed (Weinheim: Wiley-VCH), 1-26.
- Patch, H.M., Velarde, R.A., Walden, K.K., and Robertson, H.M. (2009). A candidate pheromone receptor and two odorant receptors of the hawkmoth *Manduca sexta*. *Chem Senses* 34, 305-316.
- Pauchet, Y., Wilkinson, P., Vogel, H., Nelson, D.R., Reynolds, S.E., Heckel, D.G., and Ffrench-Constant, R.H. (2010). Pyrosequencing the *Manduca sexta* larval midgut transcriptome: messages for digestion, detoxification and defence. *Insect Mol Biol* 19, 61-75.
- Perez-Orive, J., Mazor, O., Turner, G.C., Cassenaer, S., Wilson, R.I., and Laurent, G. (2002). Oscillations and sparsening of odor representations in the mushroom body. *Science* 297, 359-365.
- Pinero, J.C., Giovanni Galizia, C., and Dorn, S. (2008). Synergistic behavioral responses of female oriental fruit moths (Lepidoptera: Tortricidae) to synthetic host plant-derived mixtures are mirrored by odor-evoked calcium activity in their antennal lobes. *Journal of Insect Physiology* 54, 333-343.
- Price, M.N., Dehal, P.S., and Arkin, A.P. (2010). FastTree 2--approximately maximum-likelihood trees for large alignments. *PLoS ONE* 5, e9490.
- Raguso, R.A., Leclere, A.R., and Schlumpberger, B.O. (2005). Sensory flexibility in hawkmoth foraging behavior: lessons from *Manduca sexta* and other species. *Chem Senses* 30 Suppl 1, i295-296.
- Reisenman, C.E., Christensen, T.A., Francke, W., and Hildebrand, J.G. (2004). Enantioselectivity of projection neurons innervating identified olfactory glomeruli. *J Neurosci* 24, 2602-2611.
- Reisenman, C.E., Dacks, A.M., and Hildebrand, J.G. (2011). Local interneuron diversity in the primary olfactory center of the moth *Manduca sexta*. *J Comp Physiol A Neuroethol Sens Neural Behav Physiol*.
- Reisenman, C.E., Heinbockel, T., and Hildebrand, J.G. (2008). Inhibitory interactions among olfactory glomeruli do not necessarily reflect spatial proximity. *J Neurophysiol* 100, 554-564.
- Reisenman, C.E., Riffell, J.A., and Hildebrand, J.G. (2009). Neuroethology of oviposition behavior in the moth *Manduca sexta*. *Ann N Y Acad Sci* 1170, 462-467.
- Reisenman, C.E., Riffell, J.A., Bernays, E.A., and Hildebrand, J.G. (2010). Antagonistic effects of floral scent in an insect-plant interaction. *Proceedings of the Royal Society B: Biological Sciences*, 1-9.
- Rescorla, R.A. (1972). "Configural" conditioning in discrete-trial bar pressing. *J. Comp. Physiol. Psychol* 85, 331-338.
- Ressler, K.J., Sullivan, S.L., and Buck, L.B. (1994). A molecular dissection of spatial patterning in the olfactory system. *Curr Opin Neurobiol* 4, 588-596.

REFERENCES

- Riffell, J.A., Lei, H., Christensen, T.A., and Hildebrand, J.G. (2009a). Characterization and coding of behaviorally significant odor mixtures. *Curr Biol* 19, 335-340.
- Riffell, J.A., Lei, H., and Hildebrand, J.G. (2009b). Inaugural Article: Neural correlates of behavior in the moth *Manduca sexta* in response to complex odors. *Proc Natl Acad Sci USA* 106, 19219-19226.
- Robertson, H.M., Martos, R., Sears, C.R., Todres, E.Z., Walden, K.K., and Nardi, J.B. (1999). Diversity of odourant binding proteins revealed by an expressed sequence tag project on male *Manduca sexta* moth antennae. *Insect Mol Biol* 8, 501-518.
- Robertson, H.M., and Wanner, K.W. (2006). The chemoreceptor superfamily in the honey bee, *Apis mellifera*: expansion of the odorant, but not gustatory, receptor family. *Genome Res* 16, 1395-1403.
- Robertson, H.M., Warr, C.G., and Carlson, J.R. (2003). Molecular evolution of the insect chemoreceptor gene superfamily in *Drosophila melanogaster*. *Proc Natl Acad Sci U S A* 100 Suppl 2, 14537-14542.
- Roelofs, W., Comeau, A., Hill, A., and Milicevic, G. (1971a). Sex attractant of the codling moth: characterization with electroantennogram technique. *Science* 174, 297-299.
- Roelofs, W.L. (1995). Chemistry of sex attraction. *Proc Natl Acad Sci USA* 92, 44-49.
- Roelofs, W.L., Tette, J.P., Taschenberg, E.F., and Comeau, A. (1971b). Sex pheromone of the grape berry moth: identification by classical and electroantennogram methods, and field tests. *J Insect Physiol* 17, 2235-2243.
- Rössler, W., Tolbert, L.P., and Hildebrand, J.G. (1998). Early formation of sexually dimorphic glomeruli in the developing olfactory lobe of the brain of the moth *Manduca sexta*. *J Comp Neurol* 396, 415-428.
- Rogers, M.E., Krieger, J., and Vogt, R.G. (2001). Antennal SNMPs (sensory neuron membrane proteins) of Lepidoptera define a unique family of invertebrate CD36-like proteins. *J Neurobiol* 49, 47-61.
- Root, C., Semmelhack, J., Wong, A., Flores, J., and Wang, J. (2007). Propagation of olfactory information in *Drosophila*. *Proc Natl Acad Sci USA* 104, 11826 - 11831.
- Rospars, J.P., and Hildebrand, J.G. (1992). Anatomical identification of glomeruli in the antennal lobes of the male sphinx moth *Manduca sexta*. *Cell and Tissue Research* 270, 205-227.
- Rospars, J.P., and Hildebrand, J.G. (2000). Sexually Dimorphic and Isomorphic Glomeruli in the Antennal Lobes of the Sphinx Moth *Manduca sexta*. *Chem. Senses* 25, 119-129.
- Rospars, J.P., Lansky, P., Chaput, M., and Duchamp-Viret, P. (2008). Competitive and noncompetitive odorant interactions in the early neural coding of odorant mixtures. *Journal of Neuroscience* 28, 2659-2666.
- Rostelien, T., Borg-Karlson, A.K., Faldt, J., Jacobsson, U., and Mustaparta, H. (2000a). The plant sesquiterpene germacrene D specifically activates a major type of antennal receptor neuron of the tobacco budworm moth *Heliothis virescens*. *Chem Senses* 25, 141-148.
- Rostelien, T., Borg-Karlson, A.K., and Mustaparta, H. (2000b). Selective receptor neurone responses to E-beta-ocimene, beta-myrcene, E,E-alpha-farnesene and homo-farnesene in the moth *Heliothis virescens*, identified by gas chromatography linked to electrophysiology. *J Comp Physiol A* 186, 833-847.
- Rubin, B., and Katz, L. (1999). Optical imaging of odorant representations in the mammalian olfactory bulb. *Neuron* 23, 499 - 511.
- Ruebenbauer, A., Schlyter, F., Hansson, B., and Löfstedt, C. (2008). Genetic variability and robustness of host odor preference in *Drosophila melanogaster*. *Current Biology* 18, 1438-1443.
- Rybak, J.R., Kuss, A., Hans, L., Zachow, S., Hege, H.-C., Lienhard, M., Singer, J., Neubert, K., and Menzel, R. (2010). The digital bee brain: integrating and managing neurons in a common 3D reference system. *Frontiers in Systems Neuroscience* 4, 12.

REFERENCES

- Sachse, S., and Galizia, C.G. (2002). Role of inhibition for temporal and spatial odor representation in olfactory output neurons: a calcium imaging study. *J Neurophysiol* 87, 1106-1117.
- Sachse, S., and Galizia, C.G. (2003). The coding of odour-intensity in the honeybee antennal lobe: local computation optimizes odour representation. *Eur J Neurosci* 18, 2119-2132.
- Sachse, S., Rappert, A., and Galizia, C. (1999). The spatial representation of chemical structures in the antennal lobe of honeybees: steps towards the olfactory code. *Eur J Neurosci* 11, 3970 - 3982.
- Sakurai, T., Nakagawa, T., Mitsuno, H., Mori, H., Endo, Y., Tanoue, S., Yasukochi, Y., Touhara, K., and Nishioka, T. (2004). Identification and functional characterization of a sex pheromone receptor in the silkworm *Bombyx mori*. *PNAS* 101, 16653-16658.
- Sandoz, J.C., Galizia, C.G., and Menzel, R. (2003). Side-specific olfactory conditioning leads to more specific odor representation between sides but not within sides in the honeybee antennal lobes. *Neuroscience* 120, 1137-1148.
- Sasner, J.M., and Houten, J.L.V. (1989). Evidence for a *Paramecium* folate chemoreceptor. *Chemical Senses* 14, 587-595.
- Sato, K., Pellegrino, M., Nakagawa, T., Vosshall, L.B., and Touhara, K. (2008). Insect olfactory receptors are heteromeric ligand-gated ion channels. *Nature* 452, 1002-1006.
- Scaloni, A., Monti, M., Angeli, S., and Pelosi, P. (1999). Structural analysis and disulfide-bridge pairing of two odorant-binding proteins from *Bombyx mori*. *Biochem Biophys Res Commun* 266, 386-391.
- Schneider, D. (1962). Electrophysiological Investigation on the olfactory specificity of sexual attracting substances in different species in moths. *Journal of Insect Physiology* 8, 15-30.
- Schuckel, J., Siwicki, K.K., and Stengl, M. (2007). Putative circadian pacemaker cells in the antenna of the hawkmoth *Manduca sexta*. *Cell Tissue Res* 330, 271-278.
- Scott, K., Brady, R., Jr., Cravchik, A., Morozov, P., Rzhetsky, A., Zuker, C., and Axel, R. (2001). A chemosensory gene family encoding candidate gustatory and olfactory receptors in *Drosophila*. *Cell* 104, 661-673.
- Semmelhack, J.L., and Wang, J.W. (2009). Select *Drosophila* glomeruli mediate innate olfactory attraction and aversion. *Nature* 459, 218-223.
- Shang, Y., and Miesenböck, G. (2007). Excitatory Local Circuits and Their Implications for Olfactory Processing in the Fly Antennal Lobe. *Cell* 128, 601-612.
- Shepherd, G.M. (1972). Synaptic organization of the mammalian olfactory bulb. *Physiol Rev* 52, 864-917.
- Shields, V.D., and Hildebrand, J.G. (2000). Responses of a population of antennal olfactory receptor cells in the female moth *Manduca sexta* to plant-associated volatile organic compounds. *J Comp Physiol A* 186, 1135-1151.
- Shipley, M.T., and Ennis, M. (1996). Functional organization of olfactory system. *J Neurobiol* 30, 123-176.
- Silbering, A.F., and Galizia, C.G. (2007). Processing of odor mixtures in the *Drosophila* antennal lobe reveals both global inhibition and glomerulus-specific interactions. *J Neurosci* 27, 11966-11977.
- Silbering, A., Okada, R., Ito, K., and Galizia, C. (2008). Olfactory information processing in the *Drosophila* antennal lobe: anything goes? *J Neurosci* 28, 13075 - 13087.
- Skiri, H., Galizia, C., and Mustaparta, H. (2004). Representation of primary plant odorants in the antennal lobe of the moth *Heliothis virescens* using calcium imaging. *Chem Senses* 29, 253 - 267.
- Smid, H.M., Bleeker, M.A., Van Loon, J.J., and Vet, L.E. (2003). Three-dimensional organization of the glomeruli in the antennal lobe of the parasitoid wasps *Cotesia glomerata* and *C. rubecula*. *Cell Tissue Res* 312, 237-248.

REFERENCES

- Smith, B.H. (1998). Analysis of interaction in binary odorant mixtures. *Physiol Behav* 65, 397-407.
- Stocker, R.F. (1994). The organization of the chemosensory system in *Drosophila melanogaster*: a review. *Cell Tissue Res* 275, 3-26.
- Stocker, R.F., Singh, R.N., Schorderet, M., and Siddiqi, O. (1983). Projection patterns of different types of antennal sensilla in the antennal glomeruli of *Drosophila melanogaster*. *Cell Tissue Res* 232, 237-248.
- Stopfer, M., and Laurent, G. (1999). Short-term memory in olfactory network dynamics. *Nature* 402, 664-668.
- Stopfer, M., Jayaraman, V., and Laurent, G. (2003). Intensity versus identity coding in an olfactory system. *Neuron* 39, 991-1004.
- Syed, Z., and Leal, W. (2008). Mosquitoes smell and avoid the insect repellent DEET. *Proceedings of the National Academy of Sciences* 105, 13598-13603.
- Tabor, R., Yaksi, E., Weislogel, J.-M., and Friedrich, R.W. (2004). Processing of odor mixtures in the zebrafish olfactory bulb. *J Neurosci* 24, 6611-6620.
- Tamura, K., Dudley, J., Nei, M., and Kumar, S. (2007). MEGA4: Molecular Evolutionary Genetics Analysis (MEGA) software version 4.0. *Mol Biol Evol* 24, 1596-1599.
- Tanaka, K., Uda, Y., Ono, Y., Nakagawa, T., Suwa, M., Yamaoka, R., and Touhara, K. (2009). Highly selective tuning of a silkworm olfactory receptor to a key mulberry leaf volatile. *Curr Biol* 19, 881-890.
- Tolbert, L.P., Matsumoto, S.G., and Hildebrand, J.G. (1983). Development of synapses in the antennal lobes of the moth *Manduca sexta* during metamorphosis. *J Neurosci* 3, 1158-1175.
- Touhara, K. (2007). Deorphanizing vertebrate olfactory receptors: recent advances in odorant-response assays. *Neurochem Int* 51, 132-139.
- Tunstall, N.E., Sirey, T., Newcomb, R.D., and Warr, C.G. (2007). Selective pressures on *Drosophila* chemosensory receptor genes. *J Mol Evol* 64, 628-636.
- Uchida, N., Takahashi, Y.K., Tanifuji, M., and Mori, K. (2000). Odor maps in the mammalian olfactory bulb: domain organization and odorant structural features. *Nat Neurosci* 3, 1035-1043.
- Vareschi, E. (1971). Duftunterscheidung bei der Honigbiene — Einzelzell-Ableitungen und Verhaltensreaktionen. *Journal of Comparative Physiology A: Neuroethology, Sensory, Neural, and Behavioral Physiology* 75, 143-173.
- Vetter, R.S., Sage, A.E., Justus, K.A., Carde, R.T., and Galizia, G.C. (2006). Temporal integrity of an airborne odor stimulus is greatly affected by physical aspects of the odor delivery system. *Chemical Senses* 31, 359-369.
- Vogel, H., Heidel, A.J., Heckel, D.G., and Groot, A.T. (2010). Transcriptome analysis of the sex pheromone gland of the noctuid moth *Heliothis virescens*. *BMC Genomics* 11, 29.
- Vogt, R.G. (2003). "Biochemical diversity of odor detection: OBPs, ODEs and SNMPs," in *Insect Pheromone Biochemistry and Molecular Biology*, eds. B. Gary & V. Richard. (San Diego: Academic Press), 391-445.
- Vogt, R.G., and Riddiford, L.M. (1981). Pheromone binding and inactivation by moth antennae. *Nature* 293, 161-163.
- Vogt, R.G., Rogers, M.E., Franco, M.D., and Sun, M. (2002). A comparative study of odorant binding protein genes: differential expression of the PBP1-GOBP2 gene cluster in *Manduca sexta* (Lepidoptera) and the organization of OBP genes in *Drosophila melanogaster* (Diptera). *J Exp Biol* 205, 719-744.
- Vogt, R.G., Rybczynski, R., and Lerner, M.R. (1991). Molecular cloning and sequencing of general odorant-binding proteins GOBP1 and GOBP2 from the tobacco hawk moth *Manduca sexta*: comparisons with other insect OBPs and their signal peptides. *J Neurosci* 11, 2972-2984.
- Vosshall, L.B. (2000). Olfaction in *Drosophila*. *Curr Opin Neurobiol* 10, 498-503.

REFERENCES

- Vosshall, L.B., Amrein, H., Morozov, P.S., Rzhetsky, A., and Axel, R. (1999). A spatial map of olfactory receptor expression in the *Drosophila* antenna. *Cell* 96, 725-736.
- Vosshall, L.B., and Stocker, R.F. (2007). Molecular architecture of smell and taste in *Drosophila*. *Annu Rev Neurosci* 30, 505-533.
- Vucinic, D., Cohen, L.B., and Kosmidis, E.K. (2006). Interglomerular center-surround inhibition shapes odorant-evoked input to the mouse olfactory bulb in vivo. *J Neurophysiol* 95, 1881-1887.
- Wachowiak, M., and Cohen, L. (2001). Representation of odorants by receptor neuron input to the mouse olfactory bulb. *Neuron* 32, 723 - 735.
- Wang, J.W., Wong, A.M., Flores, J., Vosshall, L.B., and Axel, R. (2003). Two-Photon Calcium Imaging Reveals an Odor-Evoked Map of Activity in the Fly Brain. *Cell* 112, 271-282.
- Wanner, K.W., Anderson, A.R., Trowell, S.C., Theilmann, D.A., Robertson, H.M., and Newcomb, R.D. (2007a). Female-biased expression of odourant receptor genes in the adult antennae of the silkworm, *Bombyx mori*. *Insect Molecular Biology* 16, 107-119.
- Wanner, K.W., Nichols, A.S., Allen, J.E., Bungler, P.L., Garczynski, S.F., Linn, C.E., Robertson, H.M., and Luetje, C.W. (2010). Sex pheromone receptor specificity in the European corn borer moth, *Ostrinia nubilalis*. *PLoS ONE* 5, e8685.
- Wanner, K.W., Nichols, A.S., Walden, K.K.O., Brockmann, A., Luetje, C.W., and Robertson, H.M. (2007b). A honey bee odorant receptor for the queen substance 9-oxo-2-decenoic acid. *Proceedings of the National Academy of Sciences* 104, 14383-14388.
- Wicher, D., Schafer, R., Bauernfeind, R., Stensmyr, M.C., Heller, R., Heinemann, S.H., and Hansson, B.S. (2008). *Drosophila* odorant receptors are both ligand-gated and cyclic-nucleotide-activated cation channels. *Nature* 452, 1007-1011.
- Wilson, R.I., and Mainen, Z.F. (2006). Early events in olfactory processing. *Annu Rev Neurosci* 29, 163-201.
- Wright, G.A., Thomson, M.G.A., and Smith, B.H. (2005). Odour concentration affects odour identity in honeybees. *Proceedings of the Royal Society B-Biological Sciences* 272, 2417-2422.
- Wu, W., Anton, S., Löfstedt, C., and Hansson, B.S. (1996). Discrimination among pheromone component blends by interneurons in male antennal lobes of two populations of the turnip moth, *Agrotis segetum*. *Proc Natl Acad Sci USA* 93, 8022-8027.
- Yaksi, E., and Wilson, R.I. (2010). Electrical Coupling between Olfactory Glomeruli. *Neuron* 67, 1034-1047.
- Zhao, H., and Firestein, S. (1999). Vertebrate odorant receptors. *Cell Mol Life Sci* 56, 647-659.
- Zhang, X., and Firestein, S. (2002). The olfactory receptor gene superfamily of the mouse. *Nat Neurosci* 5, 124-133.
- Zhulidov, P.A., Bogdanova, E.A., Shcheglov, A.S., Vagner, L.L., Khaspekov, G.L., Kozhemyako, V.B., Matz, M.V., Meleshkevitch, E., Moroz, L.L., Lukyanov, S.A., and Shagin, D.A. (2004). Simple cDNA normalization using kamchatka crab duplex-specific nuclease. *Nucleic Acids Res* 32, e37.
- Zube, C., Kleineidam, C., Kirschner, S., Neef, J., and Rössler, W. (2008a). Organization of the olfactory pathway and odor processing in the antennal lobe of the ant *Camponotus floridanus*. *J Comp Neurol* 506, 425 - 441..
- Zube, C., and Rössler, W. (2008b). Caste- and sex-specific adaptations within the olfactory pathway in the brain of the ant *Camponotus floridanus*. *Arthropod Struct Dev* 37, 469-479.

Declaration of Independent Assignment

I declare in accordance with the conferral of the degree of doctor from the School of Biology and Pharmacy of Friedrich Schiller University Jena that the submitted thesis was written only with the assistance and literature cited in the text.

People who assisted in the experiments, data analysis and writing of the manuscripts are listed as coauthors of the respective manuscripts. I was not assisted by a consultant for doctorate theses.

The thesis has not been previously submitted whether to the Friedrich-Schiller-University, Jena or to any other university.

Jena, March 31, 2011



.....
Linda Sara Kübler

ACKNOWLEDGEMENTS

Four years is a long time and a single page can't express my gratitude. This goes out to all the people who encouraged my scientific development and this includes far more people than listed here.

I am deeply thankful to Bill while during a poster session in Vienna - directly whisked me away to Jena, a place I have never heard of before. Thanks for giving me the opportunity to work on this exciting project, supervising and encouraging my work and watching my scientific development. I am very proud to be part of the Hansson's. There is no better place to do a PhD.

Der Weg ist das Ziel-Tack så mycket!

My biggest „Dankeschön“ goes to Shannon who is not only an outstanding scientist, but a beautiful person inside and outside. This little paragraph can never justify her contribution: This work would have not been possible without her outstanding scientific expertise and hard work. Thank you so much for supporting our „Happy Place“. You have got the „Beaver Fever“!

Ein großer Dank gilt Christoph, der mich während meinen Anfängen in der Wissenschaft begleitete und mich für die Elektrophysiologie begeisterte. Ohne seinen großen Enthusiasmus und die Freude an der Neuroethologie wäre ich Heute wohl Barfrau bei Harry in Würzburg (oder Rockstar).

Ich danke Jürgen der mir auch noch nach 8 Jahren Zusammenarbeit immer noch neue Amira Tricks zeigen kann.

Ich Danke Daniel für die zahllosen Überstunden programmieren, bauen und testen und für das Buch „Einführung in Labview“, das ich aber leider nie gelesen habe.

Einen sehr herzlichen Dank an meine Leidensgenossen Anna und Antonia, die mir anschaulich zeigten: „schlimmer geht immer“ und immer ein offenes Ohr für mich hatten,- egal ob wissenschaftlich oder privat. I love Ost!

Danke an Ewald für die wundervolle Paperpartnerschaft und andere kulinarische Highlights: Es war mir ein Vergnügen!

I thank Marco for his contribution to Chapter IV and as Shannon would put it: The sexiest Imager alive!

ACKNOWLEDGEMENTS

I am deeply grateful to the whole Ichem gang and our Lovebots, teaching me to think outside of the box!

I thank Anna-Sara for guiding me through my very short but fundamental Leopard Phase.

Ein kurzfristiges Dankeschön an Diana, die mir trotz IMac in letzter Minute noch beim Formatieren der Arbeit half und mich somit rettete.

Danke an Silke für Ihre Tipps bei den Imaging Experimenten, scientific Rat & Tat und wundervolle Wochenenden in Berlin, und, und...

Thanks to Kirk for his support back than in Utah and during our short get-together in Jena, for helping me to put up this wonderful Rig (also an indirect thanks to NPI buildig „my baby“).

I thank all the Hansson's for the tremendously inspiring, encouraging and happy environment. Just wanna say: Excellent!

Ich danke der Max Planck Gesellschaft für das Stipendium welches mir die Durchführung meiner Studien ermöglichte.

Einen Dank an meine Mitbewohner Dave und Lenny die trotz streckenweiser Mangelernährung durchhielten, und mich stets zum Lachen bringen.

Einen großen Kuß an meine beste Freundin Ina aus Hamburg, die mich dank Handy Flatrate immer moralisch unterstützt, Texte professionell editiert und sehr stolz auf mich ist.

Mille Grazie an Markus, bester Freund und hochtalentierter Journalist für das ständige und stets sehr kurzfristige Korrekturlesen. Du bist die ungeschlagene „Prinzessin“ der Kommata und der Rächer des Dativs. Vielen Dank!

Der persönlichste Dank gebührt wohl meiner Mama, die zwar nie genau weiß was ich mache, aber mir dennoch seit unzähligen Jahren geduldig finanziell unter die Arme greift. Sie ermöglichte es mir diesen Weg zu gehen und dabei stets meinen Magen und meinen Schuhschrank zu füllen. Dafür ein dickes allgäuer Bussi.